

NASA Technical Paper 1664

NASA  
TP  
1664  
c.1

LOAN COPY: RET  
AFWL TECHNICAL  
KIRTLAND AFB, TX

0067671



TECH LIBRARY KAFB, NM

# Simulation Development and Evaluation of an Improved Longitudinal Velocity- Vector Control-Wheel Steering Mode and Electronic Display Format

George G. Steinmetz

AUGUST 1980

**NASA**



NASA Technical Paper 1664

Simulation Development and Evaluation  
of an Improved Longitudinal Velocity-  
Vector Control-Wheel Steering Mode  
and Electronic Display Format

George G. Steinmetz  
*Langley Research Center*  
*Hampton, Virginia*



National Aeronautics  
and Space Administration

**Scientific and Technical  
Information Branch**

1980





## SUMMARY

A simulation project was conducted which involved the development and testing of an improved longitudinal velocity-vector control-wheel steering mode and an improved electronic display format for an advanced avionics flight system. Guidelines for the development phase were provided by test-pilot critique summaries of the previous system. The results include performances from computer-generated step-column inputs across the full airplane speed and configuration envelope, as well as piloted performance results taken from a reference-line tracking task and an approach-to-landing task conducted under various environmental conditions. The analysis of the results for the reference-line tracking and approach-to-landing tasks indicates clearly detectable improvement in pilot-tracking accuracy with a reduction in physical workload.

The original objectives of upgrading the longitudinal axis of the velocity-vector control-wheel steering mode were successfully met when measured against the test-pilot critique summaries and the original purposes outlined for this type of augmented control mode.

## INTRODUCTION

The Langley Research Center has several long-range research efforts focusing on conventional take-off and landing aircraft. The NASA Terminal Configured Vehicle (TCV) program represents one such research effort. Its chief objectives are to address the improvement of airborne equipment and procedures in future high-density terminal areas. This is principally focused on advanced avionics flight systems in a futuristic cockpit arrangement (ref. 1). As one of its research tools, the TCV project operates the TCV Boeing 737 airplane, which was highly modified to include a research cockpit located in the aft portion of the airplane. This cockpit (aft cab) incorporates electronic displays and all-digital flight-control computers. The advanced navigation, guidance, and control features are implemented in a fly-by-wire concept. The electronic displays contain situation information in both an electronic attitude indicator (EADI) format and an electronic horizontal situation indicator (EHSI) arrangement (refs. 2 to 5).

As tasks relating to the overall objectives of the TCV program, certain work elements consist of analysis, piloted simulation, testing, and flight testing of advanced controls and displays. The focus of one such effort was the further improvement of a computer-augmented manual-control mode, control-wheel steering (CWS) within the advanced guidance and control system aboard the airplane. The CWS concept allows the pilot to input rate commands linearly proportional to wheel and/or column input; a zero-rate hold feature is also employed.

Velocity control-wheel steering (VCWS) allows the pilot to manage the orientation of the airplane's velocity vector as defined in an inertial axis. Vertical flight-path angle  $\gamma$  and track angle  $\psi$  are the principal orientations

being controlled with a bank-angle hold mode for bank angles exceeding 5°. The electronic displays provide the pilot with the status of these quantities.

The upgrading of this particular control mode, VCWS, was deemed necessary by observing piloted performances and collating debriefing comments by the NASA test pilots involved in the TCV program. The goal of the VCWS was to reduce pilot workload while increasing piloted tracking performance. This goal was being partially fulfilled but not to the extent expected by the test engineers and test pilots involved. As a first step, an improved longitudinal-axis control and display system was sought. The lateral-axis system was not treated at this point.

This paper discusses, for the longitudinal axis, the deficiencies of the original control and display system, including pilot summaries, and the development of a replacement control and display system. Participation by the chief TCV test pilot in the refinement of the advanced control system as implemented on the real-time simulation complex is outlined. A preliminary evaluation (a tracking task) as well as the main evaluation experiment (an approach-to-landing task) are described. Statistical analysis of root-mean-square (rms) measures representing physical workload and tracking performance is presented in the section entitled "Results and Discussion."

This work was performed by engineers from both NASA and The Boeing Commercial Airplane Company, and much of the redesign of the control system was done by A. A. Lambregts of the Boeing TCV project group.

Use of trade names or names of manufacturers in this report does not constitute an official endorsement of such products or manufacturers, either expressed or implied, by the National Aeronautics and Space Administration.

## SYMBOLS AND ABBREVIATIONS

### Symbols

g	acceleration due to gravity
h	altitude
$\dot{h}$	rate of change of altitude rate
K_ _ _	constant
q	pitch rate
S	Laplace variable
s	statistical standard deviation
(T - R)	target flight-path angle minus reference flight-path angle

$V_g$	ground velocity
$x$	inertial axis along runway heading
$\bar{x}$	statistical mean
$\gamma$	inertial flight-path angle
$\dot{\gamma}$	inertial flight-path rate
$\gamma_R$	reference flight-path angle
$\dot{\gamma}_R$	rate of change of reference flight path angle
$\gamma_T$	target flight-path angle
$\gamma_E$	$= \gamma - \gamma_R$
$\delta_{PMC}$	longitudinal input of panel-mounted controller
$\delta_e$	elevator position
$\delta_{ec}$	commanded elevator position
$\theta$	pitch angle
$\Delta\theta$	change in pitch angle
$\tau$	time constant
$\psi$	inertial track angle

#### Abbreviations

ACSL	Advanced Continuous Simulation Language
AGCS	advanced guidance and control system
ANOVA	analysis of variance test
CAS	calibrated airspeed
CWS	control-wheel steering
DME	distance measuring equipment
EADI	electronic attitude direction indicator
EHSI	electronic horizontal situation indicator
GSE	glide-slope error

ILS            instrument landing system  
 INS            inertial navigation system  
 IVSI          instantaneous vertical-speed indicator  
 MLS            microwave landing system  
 NCDU          navigation computer display unit  
 PMC            panel-mounted controller  
 rms            root mean square  
 TCV            Terminal Configured Vehicle  
 VCWS          velocity control-wheel steering  
 VOR            very-high-frequency radio-direction system

#### SIMULATION FACILITY

The TCV program employs a variety of research tools to reach its objectives. One such tool is the real-time simulation facility. The NASA TCV B-737-100 airplane and its aft research cockpit (shown in figs. 1 and 2) are represented in a real-time simulation with a near duplication of the aft cockpit hardware (fig. 3) and its functional operations. The TCV B-737-100 airplane is represented by a six-degree-of-freedom set of nonlinear equations of motion. Functional aspects of the advanced flight-control configuration of the airplane (fig. 4) are also represented in the simulation including nonlinear models of servo actuators. The processing of the equations are performed on a Control Data CYBER 175 digital computer at 32 samples per second. Verification and validation of the simulation had been conducted prior to this experiment by comparisons with flight data and test-pilot evaluations.

The electronic displays (figs. 5 and 6) supplied to the pilot and copilot stations in the aft-deck simulation were mimicked on an Adage AGT 130 graphics computer. The graphics computer was linked via a digital buffer to the CYBER 175. All cathode-ray-tube presentations were monochromatic and contained no raster features. The simulation cockpit was fixed base and contained audio cues for engine sounds. The panel-mounted controllers used in the simulation were spring loaded as they were in the actual aft deck of the airplane. Break-out forces and gradients have been matched to the flight-vehicle characteristics.

A linear representation of the nonlinear equations of motion for the B-737-100 airplane was available for non-real-time portions of this research. The linear model was derived from the nonlinear real-time simulation model. This process is described in reference 6. The data for the linear representation of the airplane are contained in the appendix.

## ORIGINAL SYSTEM AND ITS DEFICIENCIES

After some description of the original control and display system, the deficiencies identified from pilot commentary will be discussed.

A block diagram representing the longitudinal axis of the original velocity-vector CWS system is shown in figure 7. In simple terms, the pilot input is fed along two paths, one providing a "direct" route to the elevator and the other providing a rate to the flight-path-angle reference integrator. The output of the reference integrator is combined with airplane flight-path angle to form an error signal which also drives the elevator command. Damping or rate feedback is provided the system through pitch rate. The only variable displayed to the pilot out of this diagram is the airplane flight-path angle.

The complete display information set is shown in figure 8 for the original display configuration. Basic flight-stability information, such as roll angle, pitch angle, flight-path angle, speed error, and flight-path-angle acceleration, is provided in this display format. Note that with the cathode-ray-tube size of 17.8 by 12.7 cm, the resolution of variables against the pitch grid shown is quite high compared to standard-attitude director indicators. This higher resolution allows the pilot to detect quite small differences or perturbations which in some situations can turn into a disadvantage. For example, the high resolution when matched with poor damping and transient response amplified the oscillatory nature, thus making steady-state estimates hard to determine. Turbulence would further aggravate this problem under certain conditions.

Pilot commentaries identifying the longitudinal deficiencies of the original system were gathered over a period of time involving both real-time simulation sessions and actual TCV B-737-100 flight testing. These comments pertain mainly to the low-speed flight envelope. The following summaries were extracted from the pilot commentary:

(1) The responsiveness to pilot input PMC at approach speeds was too low, thus forcing the pilot to use unnecessarily large input deflections in some cases. At the high-speed region of 250 knots or greater, the pilots were somewhat satisfied with the input sensitivity.

(2) The initial response of the flight-path angle  $\gamma$  on the EADI display lagged considerably behind the originating input. This also often resulted in more input by the pilot than desired. Precise pilot flight-path-angle control was quite frustrating because of the lag between displayed flight-path angle and pilot input.

(3) For certain discrete pilot inputs, the flight-path-angle response exhibited a considerable overshoot of the steady-state value of flight-path angle. In precision-control tasks, this overshoot caused the pilot to apply input reversals which are undesirable. Also interrelated with this characteristic was the poor damping of flight-path angle which made difficult the quick assessment of the steady-state flight-path-angle value. If these characteristics were combined with turbulence, the task difficulty was further increased,

and the pilot was drawn into the control loop more frequently than necessary, often with undesirable results.

Each of the aforementioned characteristics except turbulence effects can be readily seen in the response of the original control system to a fixed-duration step input. The standard input was 1.27 cm for a 5-sec duration. The block diagram of the original control system is shown in figure 7. Gains and time constants are presented in table I. The response of flight-path angle  $\gamma$  and computer-reference flight-path angle  $\gamma_R$  to the column step input is shown in figure 9. The reference flight-path angle  $\gamma_R$  responds to the input signal immediately, but note the lag between  $\gamma_R$  and the actual flight-path angle  $\gamma$ . Note that the actual flight-path angle  $\gamma$  is the displayed information to the pilot. Notice the different rates at which  $\gamma_R$  and  $\gamma$  respond. A crossover occurs approximately midway in the step-input interval. This provides a condition such that  $\gamma$  leads  $\gamma_R$  which will cause an overshoot when the step input terminates and a hold condition exists within the control system. The overshoot is evident in the response tracing after 5 sec when the step input is removed. The damping of  $\gamma$  to the  $\gamma_R$  level is clearly poor with the system as defined. The response of  $\gamma_R$  to the input level can be determined in figure 9 and from KCOLI in table I to be approximately 0.31 deg/sec/cm. In the unaugmented forward deck of the airplane, better than twice this response is available when flying at approach speeds.

Aside from the obvious difficulties in the control-system response, there are certain recognizable defects in the display format as shown in figure 9. Note that  $\gamma$  is presented but  $\gamma_R$ , the value being directly controlled by the pilot input, must be estimated. Historically, this situation developed because various control systems have evolved over a course of time and some of the early control systems established a  $\gamma_R$  based on the current value of  $\gamma$ . While the control system had been modified, the display format had not been coordinated with these developments.

#### IMPROVED SYSTEM APPROACH AND PRELIMINARY DEVELOPMENT

The deficiencies noted by the pilot comments and analysis of the original control display system served as a general improvement guideline for the qualities desirable in an improved system. The improved system was expected to be a combination of control system and display-information advancements. The integration of displays and controls was a desired requirement in this development. Thus, the extreme positions that the deficiencies of the current system could be solved to the pilot's satisfaction by either a control-system improvement alone or a display change alone were avoided and a dual or integrated approach was planned. However, in most of the tests and evaluations, separate effects of control and display improvements are examined, but the major focus should be on the effect obtained when these improvements are used in combination.

#### CONTROL-SYSTEM IMPROVEMENTS

The approach toward resolving some of the control-system deficiencies began in a non-real-time computing program. A linearized set of equations describing

the longitudinal axis was programmed on the Langley digital computer complex using the Advanced Continuous Simulation Language program (ACSL). The equations, flight configuration, and elevator dynamic description are contained in the appendix along with a block diagram of the simulation program. The original control system was inserted into this program and served as a benchmark upon which to gauge progress. No attempts were made to optimize the original system. The original-control-system schematic as implemented and the corresponding response to a step input are presented in figures 7 and 9, respectively.

The improved control system began as a modification of the original system. The modified features planned were: (1) a lead circuit in the direct column to the elevator path to quicken the airplane response to pilot inputs, (2) a flight-path-angle-rate ( $\dot{\gamma}$ ) feedback loop to provide better damping characteristics, and (3) an increased pilot input to reference flight-path-angle integrator gain (KCOL1) to match the increased sensitivity obtainable in the basic airplane. However, with this third modification it was recognized that a modulation of this KCOL1 gain might be necessary; otherwise, a solution to the approach speed region might be avoided at the sacrifice of the somewhat satisfactory system in the higher speed regions. Thus, a decision to make this gain a function of speed was made early and is shown in the block diagrams. Only upon placement of the control system in the nonlinear real-time simulation was this theory examined. For the ACSL work the ratio of 202.7 KCOL1 divided by  $V_g$  was equal to KCOL1. Improvements in the control-system response were made in an iterative manner across several computer sessions. The computer setup included a graphic-display output upon which pitch, flight-path angle (reference and actual), elevator, and PMC input were displayed and available for hard-copy records. Redesign and matching of gains were accomplished empirically on the computer and supported by some root locus work. The resulting improved-system diagram containing the proposed modification features is shown in figure 10. The gains and time constants are contained in table II.

The response of the improved system to an input of 1.27 cm with a 5-sec duration is shown in figure 11. The response clearly illustrates that the damping has been vastly improved, the overshoot has been virtually eliminated, and the rate of actual flight-path angle has been closely matched to the rate of reference flight-path angle. Also notice that the response of reference flight-path angle per pilot input level has been increased by a factor of roughly  $2 \frac{1}{2}$ .

The lag between initial input and actual flight-path-angle response has been slightly reduced but still should be apparent to the pilot. The solution to alleviating this pilot complaint was solved with the displayed information to the pilot and will be discussed in the display improvement and integration section. The lead modification had only a small impact on reducing the lag and was causing approximately a 20-percent increase in the elevator spike. Removal of the lead filter ( $\tau_{LE} = 0$  in fig. 10) produced the results shown in figure 12. A slight overshoot did occur between reference and actual flight-path angle; thus, a decision was made to include provisions for incorporation of the lead circuit in the system when installed into the real-time simulation. The final decision on whether to retain this feature in the real-time simulation version was made by the chief TCV test pilot.

The next step was to incorporate the candidate-improved control system within the full-envelope nonlinear real-time simulation system. The control system (herein labeled A) was tuned on the nonlinear simulation to compensate for such items as speed variation, engine pitch moments, and nonlinear elevator characteristics. The corresponding response and the gains used are presented in figure 13 and table III, respectively. The response contains nearly all of the characteristics of the precursor development on the ACSL simulation. The basic block diagram (fig. 10) remained intact.

### Display Improvement and Integration

The information set of the original display concept as shown in figure 8 had proven to be highly useful and well received by the NASA test pilots. Previous studies have documented the value of this particular display in both simulation and flight studies (refs. 2 and 7). The most notable subjective deficiency was the stability of the actual flight-path information during turbulence or rough-air conditions and the delay in response of the actual flight-path-angle information for a control input. A solution was to present the pilot the reference-value information on the display which would give the pilot an immediate reading of input consequence and one which would remain steady during turbulence.

This added more information to the display since the actual flight-path angle remained desirable information for the pilot to receive. The reference flight-path angle was placed on the display with a set of dashed-line wedges in the same manner as the actual flight-path-angle symbol. Since these information sets would be coincidental or nearly so much of the time, it was deemed prudent to clip off the points of the actual flight-path-angle symbol such that the dashed reference flight-path angle could be determined easily at all times. A drawing of this display format as implemented in the real-time simulation is shown in figure 14.

### Pilot Refinement and Preliminary Evaluation

After flying the improved system (control system A and the new display format), the chief TCV NASA test pilot participated in the further development of two alternate control systems (herein labeled systems B and C). System B was developed mainly through further gain tuning and feedback path matching of system A to create a system which retained the characteristics of system A without the abruptness in pitch upon the release of the pilot input. System C was developed basically through gain adjustments of system B to produce a pitch rate nearly identical to reference flight-path-angle rate. The two systems B and C differ from each other only in gain settings which are given in tables IV and V, respectively. The common block diagram is presented in figure 15.

Figure 16 illustrates that system B retains the characteristics of A without the objectionable abruptness. Figure 17 illustrates that C yields a pitch

rate matched to reference flight-path angle but does so at the expense of increased lag.

Two major design changes have occurred between the block diagrams of system A and systems B and C: (1) the lead circuit in the "direct" pilot-input path was dropped after agreement among engineers and chief test pilot as to its minimal contributions, and (2) a lag filter was included in front of the reference flight-path-angle integrator. This second change was included to satisfy the chief test pilot's desire to eliminate the abruptness in the starting and stopping of reference flight-path-angle information. The change was examined as shown in the diagram and by placing the same lag circuit only in the path of the reference flight-path-angle valve being fed to the display (hence, not part of the control system). The inclusion of the circuit within the control system, rather than in just the displayed value, was preferred by the chief test pilot.

### Evaluation

The three control systems (two tailored by the chief TCV pilot, labeled B and C, and the tuned ACSL real-time control system, labeled A) were screened by gathering the subjective opinions of three NASA test pilots. Each pilot flew the simulator for approximately an hour total by using each candidate with the capability for recalling any candidate as desired. The unanimous choice was control system B.

The participating test pilots also flew control system B throughout the entire speed envelope and found the characteristics to be quite satisfactory. The response of control system B for fixed-duration step inputs at various airspeeds and airplane configurations is shown in figure 18. Note the uniformity of the response characteristics as the speed and airplane configuration are varied. The lag decreases slightly as airplane speed is increased, and the reference flight-path-angle response to the step input is diminished as speed increases to meet a constant stick force per "g" type of criteria.

### Experiments and Test Procedure

The objective of the experiments was to create situations, under controlled environments, in which pilot-vehicle performance could be readily evaluated. The experiments were conducted in two phases, a preliminary tracking task and an approach-to-landing task.

In all experiments the original control mode and display presentation served as a baseline upon which to gauge progress. The principal comparison in all experiments was between the advanced control system combined with the improved display and the baseline system. In most of the experiments some additional combinations of controls and displays were included in the testing, thus providing some insight into the separate effect of control and display modification.

## Preliminary Tracking Task

The tracking task was considered a preliminary experiment to be conducted by using only a single NASA test pilot and completed in the span of a single 3-hr simulation session. All four combinations of control and display configurations were tested. The task required the pilot to make step-type changes in flight-path angle ranging from small ( $1.5^\circ$ ) to medium ( $3.0^\circ$ ) to large ( $5.0^\circ$ ) and were conducted in both calm air and with turbulence levels having standard deviations of 0.3 m/sec in each axis.

The tracking task was presented to the pilot in the form of a target reference line  $\gamma_T$  on the EADI. The pitch reference line shown in figures 8 and 14 was driven by the target-reference-line values as a function of time. The time function is shown in figure 19. Occurrences of the three step sizes are mixed in order and direction. (Both pitch-up and pitch-down are required.) For data-analysis purposes the pitch-up and pitch-down steps were treated as equivalents, thus counting as a replicate. As shown in figure 19, the basic sequence of steps was implemented three times to constitute a single run. Thus, in a given run, each step size is required six times when assuming that pitch-up and pitch-down requirements are equivalent. A run took approximately 3 min.

A single NASA test pilot flew the tracking task for each of the four possible control-display configurations. This procedure was conducted for both turbulence and calm conditions, thus requiring a total of eight runs. The sequence of the eight runs was chosen randomly to spread any learning bias. In addition, the pilot, who had over 200 prior hours in the simulator, was given a brief practice period before data runs were conducted.

The data for this experiment were gathered across 10-sec intervals for each step function in the tracking profile. The beginning of each data block was 1 sec prior to the step being initiated and ended 9 sec after the step commencement. Data were sampled 32 times per sec. A typical data recording segment for an example step size is shown in figure 19. The data measured were the rms of difference between target reference value  $\gamma_T$  and reference flight-path angle  $\gamma_R$ : that is,  $\gamma_T - \gamma_R$ .

The reference flight-path angle  $\gamma_R$  used in this measure,  $\text{rms}(\gamma_T - \gamma_R)$ , was not visible to the pilot in two of the four control-display configurations. However, the pilot was advised of the measure to be used and was requested to be aware of the fact that reference flight-path angle and actual flight-path angle do not coincide at various times. Thus, the pilot had to estimate the state of the reference flight-path angle for these control-display configurations. Strip-chart recordings were made during each of the test runs and are presented in the section entitled "Results and Discussion."

## Approach-to-Landing Task

The second and more thorough experiment was an approach-to-landing task which involved a level flight portion, an intercept of a  $3^\circ$  glide slope, and the tracking of glide slope to flare and touchdown. (See fig. 20.) No lateral off-

set was provided since the control-display modifications were in the longitudinal axis; however, the lateral axis was fully operational during the tests for realistic workload purposes.

Four different atmospheric conditions (calm, turbulence, wind shear, and a combination of turbulence and wind shear) were used in conjunction with the approach-to-landing task. The turbulence model was fed into all three axes and was set for a standard deviation of 0.98 m/sec, which was increased after experience with the tracking task. A wind shear was represented by a rotating, altitude-dependent wind condition. This wind profile (see fig. 21) presents a continuous shear and contains a brief (approximately 10 sec) downdraft of 2.4 m/sec at approximately 85 m. The direction of the downdraft was such as to lessen the shear effect and, thus, to cause the shear to be considered mild.

During this experiment, the displays, both the original and improved versions, contain relative track information and a perspective runway image. More complete information concerning these features is contained in reference 2. The runway image and track information, as shown with the improved display format, was shown in figure 14.

Data were collected in two segments of the approach-to-landing tasks. These zones are shown and defined in figure 22. The higher altitude zone represented a region where the initial pitch over had been settled, and glide-slope tracking was accomplished by using principally the pitch reference line and glide-slope error indicator. Therefore, the second zone began at approximately the point where the perspective runway and its markings became dominant in the chief pilot's opinion. The second zone was terminated before the flare began. Glide-slope error (in distance) and longitudinal pilot input (panel-mounted controller activity in distance units) were gathered in rms format in each zone. Strip-chart recordings were taken during all runs of the approach-to-landing task.

Again, the main comparison sought was that of the baseline configuration with the fully improved configuration (both control and display). However, in three of the four atmospheric conditions, additional combinations of control and display improvements were included in the testing. The matrix in table VI shows the test conditions for each control, display, and atmosphere condition. Three NASA test pilots served as subjects for this experiment. Two of the pilots performed a replication of the test conditions. The third pilot performed only the 12 test runs of table VI, and the third pilot-input activity was obtained only for the shear-and-turbulence-condition runs. To minimize learning-curve effects in the data, the three pilots were each allowed sufficient practice time, and a randomization of test conditions was made.

## RESULTS AND DISCUSSION

This section treats the preliminary tracking task first, followed by the approach-to-landing task. In each of these two experiments, statistical tests are used in presenting and interpreting results. The methodology employed follows loosely that contained in reference 8 (pp. 24-37). Graphs of means and

standard deviations are presented to aid in the interpretation of the statistical testing. Representative (not the best or worst cases) strip-chart recordings for each of the tests are also presented under appropriate sections.

The statistical examinations of data involved various types of testing. These techniques included homogeneity of variance, analysis of variance (ANOVA), and the Newman-Keuls method. In all of the tasks, ANOVA was employed with either step-input sizes or recording zones as one factor and a combination of controls and displays serving as the other one or two factors, depending on whether all combinations of controls and displays were included in the testing. If all combinations of controls and displays were within the testing, a direct indication of secondary interest as to whether controls or display effects alone were significant was given by the ANOVA, and the primary interest of baseline against full advanced controls and displays was determined through t-tests or the Newman-Keuls method. Whenever possible, the effects of all other factors were averaged when a comparison was being determined. This method produces unbiased evaluations. For example, if display-configuration comparisons are being determined, each display configuration was summed across all segments and control systems, thus averaging the effects of segments and control systems. In some conditions when determining control and display effects separately, this averaging was not possible. For example, under the shear condition only three combinations of controls and displays were run. This meant that the Newman-Keuls method was required to make comparisons of control and display effects. To compare display-format effects, the control system was held constant in the advanced configuration; and to compare control-system effects, the display format was held constant in the baseline configuration. Just the opposite was true for the three combinations of controls and displays under the shear and turbulence condition. The turbulence condition was a full factorial design in that all combinations of the factors were used and, hence, ANOVA was used in the determination of separate control and display effects.

#### Reference-Line Tracking Task

Selected variables from strip-chart recordings created during the reference-line tracking are presented in figures 23 to 30. The chosen variables were PMC,  $\gamma_R$ , and  $\gamma$ . From figure to figure, as the experiment conditions are changed, differences can be visually noted in each of the variables. The rms means and standard deviations per step size for each control-display configuration are shown in figure 31 for the calm conditions and in figure 32 for the turbulence conditions. These figures show very similar results for both the calm and turbulence conditions. However, on the less important side, it should be noted that in some of the cases the smaller standard deviations occur under turbulence conditions which is a reversal of expectation. No satisfactory explanation has been found as yet for this reversal trend.

As mentioned in the preceding section, the comparison of primary interest was between the baseline system and the advanced system (improved display and control). In figures 31 and 32 a comparison of mean performance measure for the baseline and advanced systems per step size yields reductions for the advanced

system ranging from 10 to 30 percent. A similar comparison of performance-measure standard deviations shows reductions ranging from 60 to 80 percent in favor of the advanced system. Each of these reductions with the exception of the medium-step-size category under calm conditions was determined to be statistically significant (discernable difference) at or above the 95-percent confidence level. When the performance measure was averaged across the step-size category, the overall reduction in mean and standard deviation for the advanced system was 20 and 35 percent, respectively, for the calm conditions and 25 and 35 percent, respectively, for the turbulence conditions.

Of secondary interest, the separate effects of improved control system and improved display format were determined by an analysis of variance tests (ANOVA) on the performance measure combining the data for all control-display configurations. This procedure was applied separately to the calm and turbulence conditions. The results are presented in table VII. There were discernable differences with reasonable confidence levels in controls and displays for both conditions. The performance-measure mean and standard deviation of the improved display format when averaged between controls and across step-size categories was reduced by 14 and 22 percent, respectively, for the calm conditions and 16 and 22 percent, respectively, for the turbulence conditions. Under the same averaging conditions, a reduction of 8 and 22 percent, respectively, for calm conditions and 12 and 22 percent, respectively, for turbulence was found in the performance-measure means and standard deviations associated with the improved control system.

It is interesting to note the significant higher order effects, such as AC, BC, and ABC, in the ANOVA testing of the calm conditions (table VII). The significance of second-order terms, such as controls A and step sizes C, implies that differences occurred in controls as step size was changed. This can be seen in the graphs of figure 31. Similar effects can be seen for other significant higher order terms. The significant third-order term ABC means that the effect of controls-step size AC varies as displays B changes, or, alternately, the effect of display-step size BC varies as controls are changed. These effects can also be seen by carefully examining the graphs of figures 31 and 32.

The time histories substantiate the results of the statistical analysis as well as point out the better physical workload of the advanced systems. The general comparison of PMC and  $\gamma_R$  time histories (figs. 24, 26, 28, and 30 against figs. 23, 25, 27, and 29) indicates lower physical activity of the test subject and better establishment of the system reference for steady-state tracking when using the advanced format. These trends highlight the expected benefits of the improved display. A comparison of the  $\gamma$  time histories presented in figures 25, 26, 29, and 30 with those in figures 23, 24, 27, and 28, substantiates the results of improving the control system. The comparison of traces in figures 26 and 30 with those in figures 23 and 27 clearly illustrates the gains made in the advanced system over the baseline system.

In summary, the results of this preliminary task indicated that real improvements in tracking and pilot physical workload can be attributed to both the control-system alteration and the additional display information. However,

combining the control-display improvements indicated a much better gain in performance than either improvement alone.

### Approach-to-Landing Task

For the approach-to-landing task, the examination of results shall be performed for each of the four environmental conditions. The portion of the approach being examined (zones 1 and 2 as defined in fig. 22) required that the pilot maintain a steady flight-path angle with modulation to satisfy his error thresholds. The measures examined were rms of glide-slope error (GSE) and rms of panel-mounted controller (PMC) movement. Through these measurements, results concerning tracking accuracy and pilot-control activity were examined.

The data groups used in the following paragraphs were created by summing across the test subjects and replicates. For the rms (GSE) data grouping, five runs (two runs each by two pilots and one run by a third pilot) were combined under each environmental condition. The rms (PMC) data grouping was compiled in a similar manner except that due to an abnormality in PMC data collection during one run, which had to be discarded, four runs per environmental condition were used. The order of presentation was chosen in accord with assumed difficulty of the task under the particular condition. Turbulence was considered a more demanding task than shear due to the mildness of the shear used in this study. Example time histories of selected parameters are presented for each environmental condition.

Calm-air cases.- Two control-display cases, the baseline configuration and the full advanced concept, form the groupings under the calm-air conditions. The relevant means and standard deviations are presented in table VIII for each recording zone for both rms (GSE) and rms (PMC). Example time histories of PMC,  $\gamma_R$ ,  $\gamma$ ,  $\theta$ , GSE, and h are contained in figure 33 for the baseline case and in figure 34 for the full-advanced-concept case.

An ANOVA was performed on the rms (GSE) data and the results are presented in table IX. With regard to glide-slope tracking there was no support to separation of control-display configurations for differences in mean rms values. There was an indication, with significant differences at a 95-percent or greater confidence level, that the glide-slope tracking performance was different in the two recording segments. Better mean performance occurred in the lower altitude zone. This was expected since the glide-slope beam narrows as the range to runway decreases. Tests (homogeneity of variance) on the standard deviations to determine consistency trends between the control-display configurations showed significant differences above the 95-percent confidence level for the glide-slope tracking performance. Better consistency, 67-percent reduction over baseline configuration, was obtained with the advanced configuration.

In a similar manner, an ANOVA test was applied to a rms (PMC) data group, and the results of this examination are presented in table X. The recording zones did not contain detectable significant differences, but the control-display configurations under this measure were deemed to contain significant differences with a confidence factor of 99 percent. The overall means (averaged across zones) indicate that less column activity, 58-percent reduction, occurred

when the advanced control-display configuration was employed. Tests for consistency of rms (PMC) standard deviations did not show any significant differences.

Shear cases.- Three combinations of control-display configurations were tested in the shear environment. These combinations were (1) baseline control system with baseline display, (2) advanced control system with baseline display, and (3) advanced control system with advanced display. Means and standard deviations for rms (GSE) for each recording zone are presented in table XI. Example time-history recordings for each configuration are contained in figures 35 to 37. Time-history tracing of the head to tail, left to right, and of vertical components of the wind profile are shown in figure 38.

An ANOVA test was conducted on the rms (GSE) data, and the results are presented in table XII. The analysis indicated a significant difference with 95-percent or greater confidence levels only among the control-display configurations. This result was further broken down by use of a Newman-Keuls test (ref. 8). The advanced configuration was significantly different with a 95-percent or greater confidence level from the baseline configuration.

Comparing the advanced and baseline configurations showed reductions of 63 and 27 percent in the means for each zone. The overall means (averaged across zones) indicated that the reduction was 48 percent in mean glide-slope performance. Tests on the overall standard deviations indicated a significant difference, with a confidence of greater than 95 percent, for the advanced against baseline configuration for the glide-slope-error measure.

Further tests using the Newman-Keuls testing did not indicate any significant difference among separate mean comparisons of either controls or displays. However, tests on overall standard deviations (averaged across zones) between the two configurations involving a display change (an advanced control system in both compared configurations) indicated a significant difference, 99-percent confidence. The better consistency, 57-percent reduction, was associated with the advanced display format.

The data grouping of rms (PMC) was subjected to the same type of statistical analysis process. Means and standard deviations per recording segment are in table XI. The results of the ANOVA tests are presented in table XIII. Both control-display configurations plus recording zones showed significant differences within their levels. The recording zones showed an across-the-board increase in the pilot's control activity for the latter stages of the approach. This was an expected result since the vertical portion of the shear input occurred in the latter portion of the approach and no detectable difference was noted in glide-slope tracking performance per recording segment (table XII). A reasonable explanation seems that more work was applied to maintain nearly the same tracking performance.

The control-display configuration factor also showed significant differences between the combinations used, and further examination by Newman-Keul testing was performed. The comparison of advanced and baseline configurations showed a significant difference with confidence level better than 95 percent. The overall reduction in the mean rms (PMC) measure was 56 percent. In the separate recording zones, the mean performance reduction attributed to the

advanced system was 75 and 53 percent. The overall comparison of standard deviation between the two configurations was also significant, greater than the 95-percent confidence level, and this difference represented approximately a 50-percent reduction.

For the rms (GSE) measure the separate effects of either controls or displays were not found to contain discernable differences at a confidence level of 95 percent or greater. However, with the rms (PMC) measure, the display effect was significant at a confidence level greater than 95 percent. The improved display format caused a reduction in the overall mean performance of 53 percent. Note that this comparison was made by using the improved control system for both display configurations. The control systems were not found to contain discernable differences with a reasonable confidence level for this measure. Also note that this comparison had to be drawn by using the baseline display (not averaged across both display formats).

Turbulence cases.- Four combinations of controls and displays were tested under the turbulence conditions. Each of the two control systems were combined with each of the two display formats. This allows the separation of control and display factors within the ANOVA tests. Example time-history tracings of a run for each of the four control-display configurations are presented in figures 39 to 42. The means and standard deviations per recording segment for rms (GSE) and rms (PMC) are presented in table XIV.

A statistical comparison of advanced and baseline systems means indicated that significant differences existed at confidence levels of 99 percent for both rms (GSE) and rms (PMC) measures. The advanced system showed a reduction in overall mean performance (averaged across zones) of 46 percent for the glide-slope measure and 59 percent for the PMC measure. The overall comparison of standard deviations indicated a significant difference at the 95-percent level for the glide-slope measure but not for the PMC measure. The improvement for the advanced system in glide-slope consistency was a reduction of 66 percent over the baseline system.

ANOVA test results on rms (GSE) data are shown in table XV. The results indicate significant differences at or above the 95-percent confidence level for the control-system factor and the recording-zone factor. No significant differences were detected among the display formats for a reasonable confidence level. The differences detected in the two recording zones were expected, as the glide-slope beam width decreases as a function of range from runway threshold.

The advanced control system produced a better overall mean performance (averaged across display and zone factors) in glide-slope tracking. The reduction represented a 37-percent change from the baseline control system. Tests on overall standard deviations (averaged over the other two factors) showed significant differences, at or above 95-percent confidence levels, for both control-system and display-format comparisons. Both the advanced control system and the advanced display format produced an improvement of 66 and 35 percent, respectively, in overall consistency from the baseline control and display format.

Table XVI contains the results of ANOVA tests on the rms (PMC) data grouping. This analysis indicated a significant difference, with a confidence level of 95 percent or greater, only in the display-format factor. The advanced display format resulted in a mean performance (averaged across zones and controls) of approximately one-half (50-percent reduction) as much control input as did the baseline format. Comparison of overall standard deviations for controls and displays indicated that significant differences existed only for the display factor. The advanced display format showed better consistency, a 37-percent reduction, in input activity.

Shear and turbulence cases.- Three combinations of controls and displays were examined under the shear and turbulence conditions. These combinations were (1) baseline control system with baseline display, (2) baseline control system with advanced display, and (3) advanced control system with advanced display. The means and standard deviations of rms (GSE) and rms (PMC) for these data groupings are presented in table XVII. Example time-history tracings for each configuration are shown in figures 43 to 45. The ANOVA test results for rms (GSE) data are shown in table XVIII. The significant differences determined were among both the control-display configurations and the recording zones. The recording-zones factor showed significant differences at a 95-percent confidence level. The reduction in the rms glide-slope-error measure can be attributed to a narrowing of the glide-slope beam as the range to threshold decreases and to increased pilot activity as seen in the plots of figure 40. The suddenness of the vertical component of the shear when coupled with turbulence increases the demands of this task in the lower altitude recording zone.

The significant difference found among the control-display configurations was further examined by Newman-Keuls testing. The principle comparison of baseline system with advanced system was shown to contain a significant difference with a confidence level greater than 95 percent. The overall mean rms (GSE) measure (averaged across zones) of the advanced system was reduced by 54 percent. The standard deviations associated with the overall means were not found to be significant at a reasonable confidence level.

By using the Newman-Keuls testing procedure, a comparison of display formats (both formats were used with the baseline control scheme) showed a significant difference at a confidence level greater than 95 percent. The reduction in the overall mean performance measure for the advanced display format was 41 percent. A comparison of control-system effects was made, by holding the display fixed at the improved version level, and differences among control systems could not be supported by the results of the testing. Overall standard deviations were not significant among the three configurations, but both configurations involving the improved display format contained significant differences from the baseline configuration in the lower altitude recording zone.

Table XIX contains the ANOVA test results of rms (PMC) data. These tests indicated that both control-display configurations and recording zones contained significant differences. The recording zones indicated, at a 95 percent or greater confidence level, that increased activity across all configurations

occurred as the altitude decreased. When considering the zone effect for the glide-slope-deviation data, it seems that extra activity was provided to decrease the glide-slope deviations as the approach phase neared the ground.

The control-display configurations were examined via Newman-Keuls tests. Comparisons of advanced and baseline configurations indicated significant differences, 95 percent or greater confidence levels, for both the overall means and standard deviations (averaged across zones). The overall advanced-system mean and standard deviation showed improvements of 66 and 60 percent, respectively.

A comparison of display formats, using a common baseline control system, indicated significant differences, 95-percent confidence levels, in both overall means and standard deviations. The improvements in the overall mean and standard deviation of the rms (PMC) measure were reductions of 55 and 50 percent, respectively. No significant differences were found for the control-system comparison (using a common improved display format).

#### Approach-Task Summary

Table XX shows a summary chart of all the approach-task statistical significant difference findings. Each of the groupings per measure contain the findings for both means and standard deviations. The broadest comparison, baseline against advanced configuration, is shown; and then a breakdown, where possible, into control-system and display-system effects is also indicated in a subgrouping.

For the glide-slope measure rms (GSE), the means associated with the comparisons of advanced and baseline configurations showed a significant difference in three of the four conditions. All of these differences resulted in a better performance for the advanced configuration. The improvements ranged from 46 to 54 percent. Likewise, the analysis of standard deviations indicated, in three of the four conditions, a significant difference in favor of the advanced configuration, 43 to 67 percent.

With the input activity measure rms (PMC), all of the comparisons of advanced and baseline configurations contained significant differences in the means. Each of these findings showed less activity for the advanced configuration, 56 to 66 percent. The standard-deviation findings were significantly different in two of the four conditions; and again where these differences were detected, less activity, 50 and 60 percent, was present under the advanced configuration.

With the glide-slope measure both means and standard deviations indicated significant differences for both separate control and display effects. The control systems contained significant differences in both means and standard deviations under the turbulence conditions. All differences showed better performance, 37 and 66 percent, with the advanced control system. The display format was responsible for detectable differences (in means, 41-percent improve-

ment) for the shear and turbulence conditions. Recall that the comparison was made under the baseline control system for the shear and turbulence conditions. Among the standard deviations, the display-format results were significantly different under two conditions. In all cases the advanced display format produced the best performance, 57- and 35-percent improvements.

With the input activity measure, only display formats of the separate examinations produced detectable significant differences among the means and standard deviations. Each of the separable conditions showed a significant difference for displays among the means, ranging from 50 to 55 percent under the advanced display format.

### CONCLUSIONS

A simulation project was conducted which involved the development and testing of an improved longitudinal velocity-vector control-wheel steering mode and an improved electronic display format for an advanced avionics flight system. From this project the following conclusions are presented:

1. The results of the preliminary tracking task clearly demonstrated real improvements over the baseline or original system for the improved control system, the improved display format, and the combination of improved control and display system. When averaged across step sizes of the tracking task, the mean performance and associated variability percentage improvements were best for the fully improved system; this was followed in magnitude by the improved display format alone which was slightly better than an improved control system alone. Definite improvements in pilot-input activity with the improved or advanced systems were noted in the time-history recordings.

The approach-to-landing task represented a more realistic task in terms of real-world requirements. Both tracking and physical workload measures were examined for this task.

2. With regard to the tracking measure, the advanced system demonstrated more discernable differences from the baseline system and larger improvements than either the improved control or display alone for the four conditions examined. This was true for the overall mean tracking and its consistency. The advanced-system improvements represented roughly 50-percent reductions over the baseline-system performances.

3. The overall mean results of the pilot-input activity or physical workload measure also demonstrated the advanced system to be roughly a 50-percent improvement from the baseline system. The consistency was improved for two of the four conditions examined. With regard to separate control or display improvements, only the improved display format produced any discernable differences in this measure, and these were lesser improvements than for the fully advanced system.

4. The original objectives of upgrading the velocity-vector control-wheel steering mode have been successfully met when measured against the test-pilot

critique summaries and the original purposes outlined for this type of augmented control mode. Certainly, evidence of reduced physical workload with better accuracy of performance has been demonstrated in the results of the simulation analysis.

Langley Research Center  
National Aeronautics and Space Administration  
Hampton, VA 23665  
June 23, 1980

## APPENDIX

### NON-REAL-TIME SIMULATION MODEL

The equations presented in this appendix were implemented as shown in figure A1.

#### Symbols

$q$	pitch angle, deg
$\Delta q$	pitch rate, deg/sec
$\dot{\Delta q}$	pitch acceleration, deg/sec <sup>2</sup>
$t$	time, sec
$\Delta \alpha$	angle-of-attack perturbation from trim, deg
$\dot{\Delta \alpha}$	rate of change of angle of attack, deg/sec
$\Delta \gamma$	flight-path-angle perturbation from trim, deg
$\dot{\Delta \gamma}$	derivative of flight-path angle, deg/sec
$\delta_{PMC}$	longitudinal input of panel-mounted controller, cm
$\delta_e$	elevator-angle perturbation from trim, deg
$\dot{\delta}_e$	rate of change of elevator-angle perturbation, deg/sec
$\delta_{ec}$	elevator command as computed by the automatic control system, deg
$\Delta \theta$	pitch-angle perturbation from trim, deg

#### Equations Representing Airplane Flight Dynamics

The airplane flight dynamics were represented by the short-period approximation of the linearized, longitudinal equations of motion. The linearization was derived around a steady-state solution at the following flight conditions:

Level flight  
Airspeed, 120.0 knots  
Altitude, 457.2 m  
Flaps deflected 40.0°  
Landing gear down  
Center of gravity, 0.3

## APPENDIX

The short-period approximation was derived by forcing the airspeed to remain at its trim value. The approximate model of the airplane flight dynamics was expected to mimic an airplane with a perfect automatic throttle for speed control.

The resulting equations were as follows:

$$\Delta \dot{\alpha} = -0.628 \Delta \alpha + 1.002 \Delta q - 0.039076 \delta_e$$

$$\Delta \dot{q} = -0.7289 \Delta \alpha - 0.4q \Delta q - 1.0853 \delta_e$$

$$\Delta \alpha = \int_0^t \Delta \dot{\alpha} dt$$

$$\Delta q = \int_0^t \Delta \dot{q} dt$$

$$\Delta \theta = \int_0^t \Delta q dt$$

$$\Delta \gamma = \Delta \theta - \Delta \alpha$$

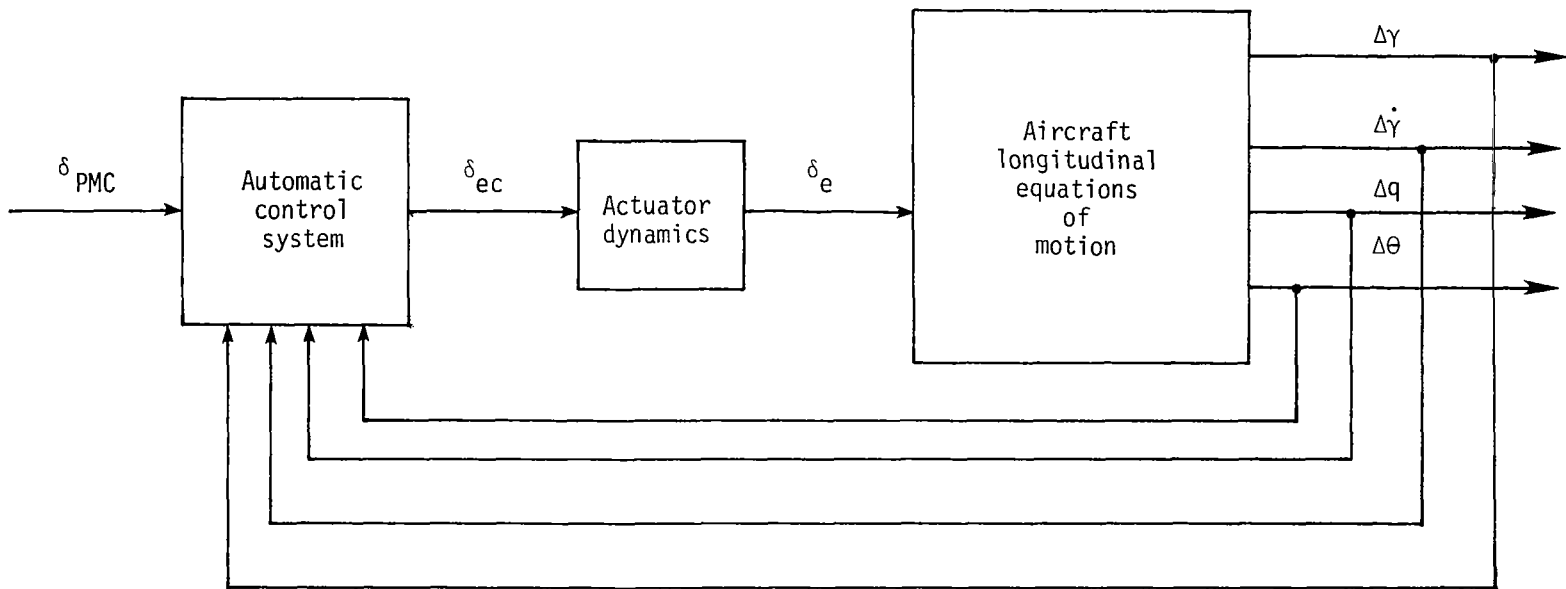
$$\Delta \dot{\gamma} = \Delta q - \Delta \dot{\alpha}$$

### Elevator Servo Dynamics

The elevator servo dynamics were represented by a rate-limited, first-order lag. The equations were as follows:

$$\dot{\delta}_e = 14.0 \left[ 1.43 (\delta_{ec} - \delta_e) \right] \quad (\text{Limited to } \pm 1.5 \text{ deg/sec})$$

$$\delta_e = \int_0^t \dot{\delta}_e dt$$



APPENDIX

Figure A1.- Simulation block diagram of linearized batch program.

## REFERENCES

1. Reeder, John P.; Schmitz, Robert A.; and Clark, Leonard V.: Operational Benefits From the Terminal Configured Vehicle. NASA TM-80046, 1979.
2. Steinmetz, George G.; Morello, Samuel A.; Knox, Charles E.; and Person, Lee H., Jr.: A Piloted-Simulation Evaluation of Two Electronic Display Formats for Approach and Landing. NASA TN D-8183, 1976.
3. Morello, Samuel A.; and Person, Lee H., Jr.: Terminal-Area Flight Experience With the NASA Terminal Configured Vehicle. NASA paper presented at the Flight Safety Foundation 23rd Annual Corporate Aviation Safety Seminar (Washington, D.C.), Apr. 9-12, 1978.
4. Dieudonne, James E.; Grove, Randall D.; and Steinmetz, George G.: A Simulation Study of Curved, Descending, Decelerating, Landing Approaches for Transport Aircraft. NASA TN D-8190, 1976.
5. Steinmetz, George G.: A Simulation Investigation of Cockpit Display of Aircraft Traffic During Curved, Descending, Decelerating Approaches. NASA TM-80098, 1979.
6. Dieudonne, James E.: Description of a Computer Program and Numerical Technique for Developing Linear Perturbation Models From Nonlinear Systems Simulations. NASA TM-78710, 1978.
7. Morello, Samuel A.; Knox, Charles E.; and Steinmetz, George G.: Flight-Test Evaluation of Two Electronic Display Formats for Approach to Landing Under Instrument Conditions. NASA TP-1085, 1977.
8. Hicks, Charles R.: Fundamental Concepts in the Design of Experiments. Second ed. Holt, Rinehart and Winston, Inc., c.1973.

TABLE I.- GAINS AND TIME CONSTANTS FOR  
ORIGINAL CONTROL SYSTEM

Time constants	Gains
$\tau_{COL} = 0.093$ $\tau_Q = 16.0$	KCOL2 = 0.760 KCOL1 = 0.774 KI = 0.100 KT = 4.320 KQ = 2.160 Deadzone = 0.254 cm KV = 1.0 at 120 knots

TABLE II.- GAINS AND TIME CONSTANTS FOR  
MODIFIED CONTROL SYSTEM

Time constants	Gains
$\tau_Q = 16$ $\tau_{COL} = 0.093$ $\tau_{LE} = 1.0$	KCOL1 = 1.88 KCOL2 = 1.85 KGE1 = 1.0 KGE2 = 0.15 KGD1 = 1.15 KGD2 = 0.15 KT = 4.32 KQ = 2.16 KV = 1.0 at 120 knots Deadzone = 0.254 cm

TABLE III.- GAINS AND TIME CONSTANTS FOR  
REAL-TIME SIMULATION (SYSTEM A)

Time constants	Gains
$\tau_{LE} = 1.0$	KCOL1 = 1.88
$\tau_{COL} = 0.093$	KCOL2 = 2.75
$\tau_Q = 16.0$	KGE1 = 1.5
$\tau_l = 16.0$	KGE2 = 0.15
	KGD1 = 1.15
	KGD2 = 0.20
	KQ = 4.32
	KT = 4.32
	KV = 1.0 at 120 knots
	Deadzone = 0.254 cm

TABLE IV.- GAINS AND TIME CONSTANTS FOR MODIFIED REAL-TIME  
SIMULATION CONTROL SYSTEM (SYSTEM B)

Time constants	Gains
$\tau_{COL} = 0.1$	KCOL1 = 1.88
$\tau_{KC} = 0.2$	KCOL2 = 2.75
$\tau_{KG} = 0.1$	KGE1 = 1.3
	KGE2 = 0.15
	KGD2 = 0.30
	KGD1 = 1.15
	KQ = 4.32
	KT = 4.32
	KV = 1.0 at 120 knots
	Deadzone = 0.254 cm

TABLE V.- GAINS AND TIME CONSTANTS FOR MODIFIED REAL-TIME  
SIMULATION CONTROL SYSTEM (SYSTEM C)

Time constants	Gains
$\tau_{COL} = 0.1$ $\tau_{KC} = 0.2$ $\tau_{KG} = 0.1$	KCOL1 = 1.88 KCOL2 = 1.85 KGE1 = 1.0 KGE2 = 0.15 KGD2 = 0.4 KGD1 = 1.15 KQ = 4.32 KT = 4.32 KV = 1.0 at 120 knots Deadzone = 0.254 cm

TABLE VI.- APPROACH-TASK TEST-CONDITION MATRIX

Display	Control	Calm	Turbulence	Wind shear	Turbulence wind shear
Baseline	Baseline	X	X	X	X
	Advanced		X	X	
Advanced	Baseline		X		X
	Advanced	X	X	X	X

TABLE VII.- TRACKING-TASK ANOVA TESTS

Treatments	Degrees of freedom	Sum of squares, deg <sup>2</sup>	Mean squares, deg <sup>2</sup>	F-value
Calm-condition data				
Control, A . . .	1	0.247	0.247	7.72**
Display, B . . .	1	0.751	0.751	23.48**
Step-input size:				
C . . . . .	2	36.446	18.223	569.76**
AB . . . . .	1	0.048	0.048	1.49
AC . . . . .	2	0.441	0.221	6.90**
BC . . . . .	2	0.562	0.281	8.79**
ABC . . . . .	2	0.366	0.183	5.73**
Error . . . . .	60	1.919	0.032	
Total . . . . .	71	40.780		
Turbulence-condition data				
Control, A . . .	1	0.546	0.546	31.94**
Display, B . . .	1	1.093	1.093	64.98**
Step-input size:				
C . . . . .	2	36.528	18.264	1068.64**
AB . . . . .	1	0.058	0.058	3.38*
AC . . . . .	2	0.754	0.377	22.05**
BC . . . . .	2	0.643	0.321	18.80**
ABC . . . . .	2	0.290	0.145	8.48**
Error . . . . .	60	1.025	0.017	
Total . . . . .	71	40.937		

\*Implies 95-percent confidence level.

\*\*Implies 99-percent confidence level.

TABLE VIII.- DATA AT CALM CONDITIONS

(a) rms (GSE) data (units are given in meters)

Control . . . . . Display . . . . .		Baseline Baseline	Advance Advance
Zone 1	{ $\bar{x}$	4.97	2.40
	{ s	3.97	1.03
Zone 2	{ $\bar{x}$	1.63	0.98
	{ s	1.34	.56
Average across zones	{ $\bar{x}$	3.30	1.70
	{ s	3.30	1.08

(b) rms (PMC) data (units are given in centimeters)

Control . . . . . Display . . . . .		Baseline Baseline	Advance Advance
Zone 1	{ $\bar{x}$	0.2766	0.0772
	{ s	.1168	.0589
Zone 2	{ $\bar{x}$	0.2459	0.1369
	{ s	.1130	.0573
Average across zones	{ $\bar{x}$	0.2614	0.1069
	{ s	.1077	.0658

TABLE IX.- rms (GSE) DATA FROM APPROACH-TASK

ANOVA TEST AT CALM CONDITIONS

Treatments	Degrees of freedom	Sum of squares, m <sup>2</sup>	Mean squares, m <sup>2</sup>	F-value
Control-display configuration, A . . .	1	13.02	13.02	2.76
Zones:				
B . . . . .	1	28.19	28.19	5.97*
AB . . . . .	1	4.57	4.57	0.97
Error . . . . .	16	75.59	4.72	
Total . . . . .	19	121.37		

\*Implies 95-percent confidence level.

TABLE X.- rms (PMC) DATA FROM APPROACH-TASK

ANOVA TEST AT CALM CONDITIONS

Treatments	Degrees of freedom	Sum of squares, cm <sup>2</sup>	Mean squares, cm <sup>2</sup>	F-value
Control-display configuration, A . . .	1	0.0952	0.0952	11.2**
Zones:				
B . . . . .	1	0.0008	0.0008	----
AB . . . . .	1	0.0081	0.0081	1.0
Error . . . . .	12	0.1024	0.0085	
Total . . . . .	15	0.2065		

\*\*Implies 99-percent confidence level.

TABLE XI.- DATA FOR SHEAR CONDITIONS

(a) rms (GSE) data (units are given in meters)

Control . . . . .		Baseline	Advance	Advance
Display . . . . .		Baseline	Baseline	Advance
Zone 1	$\bar{x}$	3.20	2.95	1.17
	s	1.17	1.80	.53
Zone 2	$\bar{x}$	2.34	1.72	1.70
	s	1.01	.93	.69
Average across zones	$\bar{x}$	2.77	2.33	1.44
	s	1.13	1.50	.65

(b) rms (PMC) data (units are given in centimeters)

Control . . . . .		Baseline	Advance	Advance
Display . . . . .		Baseline	Baseline	Advance
Zone 1	$\bar{x}$	0.2134	0.1600	0.0528
	s	.0668	.0157	.0206
Zone 2	$\bar{x}$	0.3556	0.2466	0.1669
	s	.1631	.1057	.0406
Average across zones	$\bar{x}$	0.2845	0.2035	0.1100
	s	.1382	.0838	.0678

TABLE XII.- rms (GSE) DATA FROM APPROACH-TASK

ANOVA TEST FOR SHEAR CONDITIONS

Treatments	Degrees of freedom	Sum of squares, m <sup>2</sup>	Mean squares, m <sup>2</sup>	F-value
Control-display configuration, A . . .	2	9.22	4.61	3.81*
Zones:				
B . . . . .	1	2.05	2.05	1.7
AB . . . . .	2	4.32	2.17	1.78
Error . . . . .	24	1.21		
Total . . . . .	29	16.80		

\*Implies 95-percent confidence level.

TABLE XIII.- rms (PMC) DATA FROM APPROACH-TASK ANOVA

TEST FOR SHEAR CONDITIONS

Treatments	Degrees of freedom	Sum of squares, cm <sup>2</sup>	Mean squares, cm <sup>2</sup>	F-value
Control-display configuration, A . . .	2	0.0971	0.0485	6.55**
Zones:				
B . . . . .	1	0.0784	0.0784	10.57**
AB . . . . .	2	0.0282	0.0141	1.9
Error . . . . .	18	0.1424	0.0074	
Total . . . . .	23	0.3371		

\*\*Implies 99-percent confidence level.

TABLE XIV.- DATA FOR TURBULENCE CONDITIONS

(a) rms (GSE) data (units are given in meters)

Control . . . . .		Baseline Baseline	Baseline Advance	Advance Baseline	Advance Advance
Zone 1	{ $\bar{x}$ s	6.94 2.62	4.38 1.75	2.66 .68	3.44 .87
Zone 2	{ $\bar{x}$ s	2.68 2.31	2.52 2.02	2.64 .96	1.72 .32
Average across zones	{ $\bar{x}$ s	4.13 3.23			2.58 1.10

Note 1	{ $\bar{x}$ s	4.13 2.72		2.62 .93	
Note 2	{ $\bar{x}$ s	3.73 2.54			3.01 1.65

(b) rms (PMC) data (units are given in centimeters)

Control . . . . .		Baseline Baseline	Baseline Advance	Advance Baseline	Advance Advance
Zone 1	{ $\bar{x}$ s	0.4242 .1560	0.1712 .1148	0.2868 .1529	0.1105 .0241
Zone 2	{ $\bar{x}$ s	0.3602 .1214	0.2423 .0386	0.3020 .1016	0.2103 .0823
Average across zones	{ $\bar{x}$ s	0.3922 .1339			

Note 1	{ $\bar{x}$ s	0.2995 .1453		0.2273 .1199	
Note 2	{ $\bar{x}$ s	0.3434 .1328			0.1836 .0836

Note 1: Controls averaged across displays and zones.  
 Note 2: Displays averaged across controls and zones.

TABLE XV.- rms (GSE) DATA FROM APPROACH-TASK

ANOVA TEST FOR TURBULENCE CONDITIONS

Treatments	Degrees of freedom	Sum of squares, m <sup>2</sup>	Mean squares, m <sup>2</sup>	F-value
Control, A . . . . .	1	22.92	22.92	8.5**
Display, B . . . . .	1	5.15	5.15	1.91
Zones:				
C . . . . .	1	38.64	38.64	14.32**
AB . . . . .	1	4.11	4.11	1.52
AC . . . . .	1	12.04	12.04	4.46*
BC . . . . .	1	0.31	0.31	0.11
ABC . . . . .	1	10.45	10.45	3.88
Error . . . . .	32	86.33	2.70	
Total . . . . .	39	179.98		

\*Implies 95-percent confidence level.  
 \*\*Implies 99-percent confidence level.

TABLE XVI.- rms (PMC) DATA FROM APPROACH-TASK

ANOVA TEST FOR TURBULENCE CONDITIONS

Treatments	Degrees of freedom	Sum of squares, cm <sup>2</sup>	Mean squares, cm <sup>2</sup>	F-value
Control, A . . . . .	1	0.0415	0.0415	3.5
Display, B . . . . .	1	0.2043	0.2043	17.23**
Zones:				
C . . . . .	1	0.0075	0.0075	0.6
AB . . . . .	1	0.0053	0.0053	0.4
AC . . . . .	1	0.0058	0.0058	0.5
BC . . . . .	1	0.0241	0.0241	2.0
ABC . . . . .	1	0.0012	0.0012	0.1
Error . . . . .	24	0.2846	0.0119	
Total . . . . .	31	0.5743		

\*\*Implies 99-percent confidence level.

TABLE XVII.- DATA FOR SHEAR AND TURBULENCE CONDITIONS

(a) rms (GSE) data (units are given in meters)

Control . . . . .		Baseline	Baseline	Advance
Display . . . . .		Baseline	Advance	Advance
Zone 1	$\bar{x}$	6.25	4.87	3.73
	s	2.36	3.44	2.18
Zone 2	$\bar{x}$	5.64	2.10	1.73
	s	2.61	.62	.67
Average across zones	$\bar{x}$	5.95	3.49	2.73
	s	2.37	2.75	1.85

(b) rms (PMC) data (units are given in centimeters)

Control . . . . .		Baseline	Baseline	Advance
Display . . . . .		Baseline	Advance	Advance
Zone 1	$\bar{x}$	0.3023	0.1153	0.0879
	s	.1384	.0589	.0589
Zone 2	$\bar{x}$	0.5268	0.2606	0.1928
	s	.2631	.1161	.0958
Average across zones	$\bar{x}$	0.4145	0.1880	0.1405
	s	.2286	.1153	.0925

TABLE XVIII.- rms (GSE) DATA FROM APPROACH-TASK ANOVA

TEST FOR SHEAR AND TURBULENCE CONDITIONS

Treatments	Degrees of freedom	Sum of squares, m <sup>2</sup>	Mean squares, m <sup>2</sup>	F-value
Control-display configuration, A . . . .	2	56.80	28.40	5.71**
Zones:				
B . . . . .	1	24.16	24.16	4.85*
AB . . . . .	2	6.02	3.01	0.6
Error . . . . .	24	119.43	4.98	
Total . . . . .	29	206.40		

\*Implies 95-percent confidence level.  
 \*\*Implies 99-percent confidence level.

TABLE XIX.- rms (PMC) DATA FROM APPROACH-TASK ANOVA

TEST FOR SHEAR AND TURBULENCE CONDITIONS

Treatments	Degrees of freedom	Sum of squares, cm <sup>2</sup>	Mean squares, cm <sup>2</sup>	F-value
Control-display configuration, A . . . .	2	0.3433	0.1717	8.7**
Zones:				
B . . . . .	1	0.1502	0.1502	7.6*
AB . . . . .	2	0.0148	0.0074	0.4
Error . . . . .	24	0.3535		
Total . . . . .	29	0.8619		

\*Implies 95-percent confidence level.  
 \*\*Implies 99-percent confidence level.

TABLE XX.- SUMMARY OF STATISTICAL SIGNIFICANT DIFFERENCE FINDINGS  
 FOR APPROACH TASK FOR OVERALL MEANS AND STANDARD DEVIATIONS

[Overall implies averaged over recording zones and control systems or display formats where applicable]

(a) Glide-slope measure for rms (GSE) data

Result	Conditions			
	Calm	Shear	Turbulence	Shear and turbulence
Means				
<u>Baseline against advanced</u>	None	*	**	•
Control system	Nonseparable	None	**	None
Display format	Nonseparable	None	None	•
Standard deviations				
<u>Baseline against advanced</u>	**	•	**	None
Control system	Nonseparable	None	**	None
Display format	Nonseparable	*	*	None

(b) Input activity measure for rms (PMC) data

Result	Conditions			
	Calm	Shear	Turbulence	Shear and turbulence
Means				
<u>Baseline against advanced</u>	**	*	**	*
Control system	Nonseparable	None	None	None
Display format	Nonseparable	*	*	*
Standard deviations				
<u>Baseline against advanced</u>	None	*	None	*
Control system	Nonseparable	None	None	None
Display format	Nonseparable	None	*	*

\*Implies significant difference at 95-percent confidence level.  
 \*\*Implies significant difference at 99-percent confidence level.



L-73-6283

Figure 1.- NASA TCV B-737-100 research airplane.

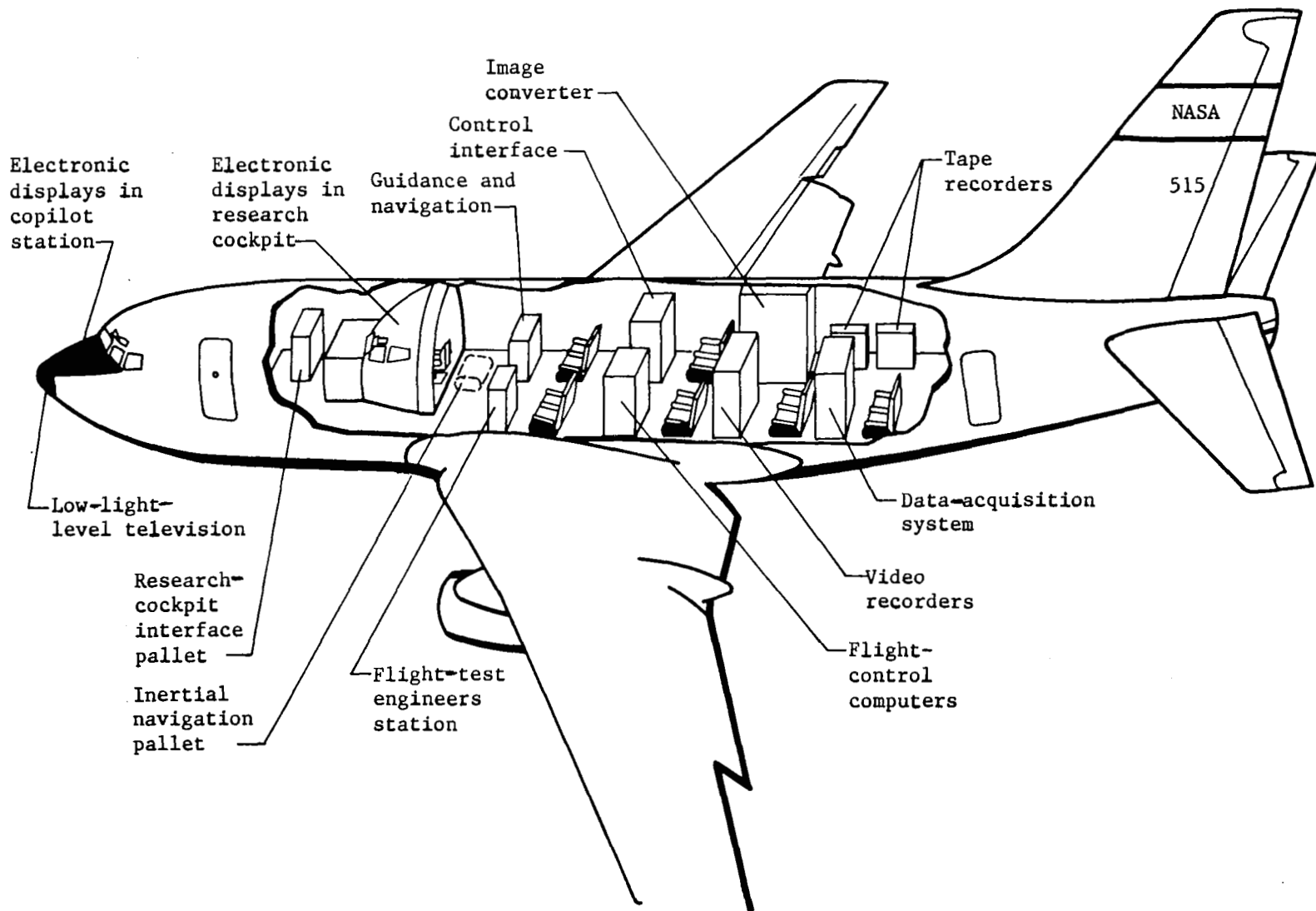


Figure 2.- Internal arrangement of NASA TCV B-737-100 research airplane.

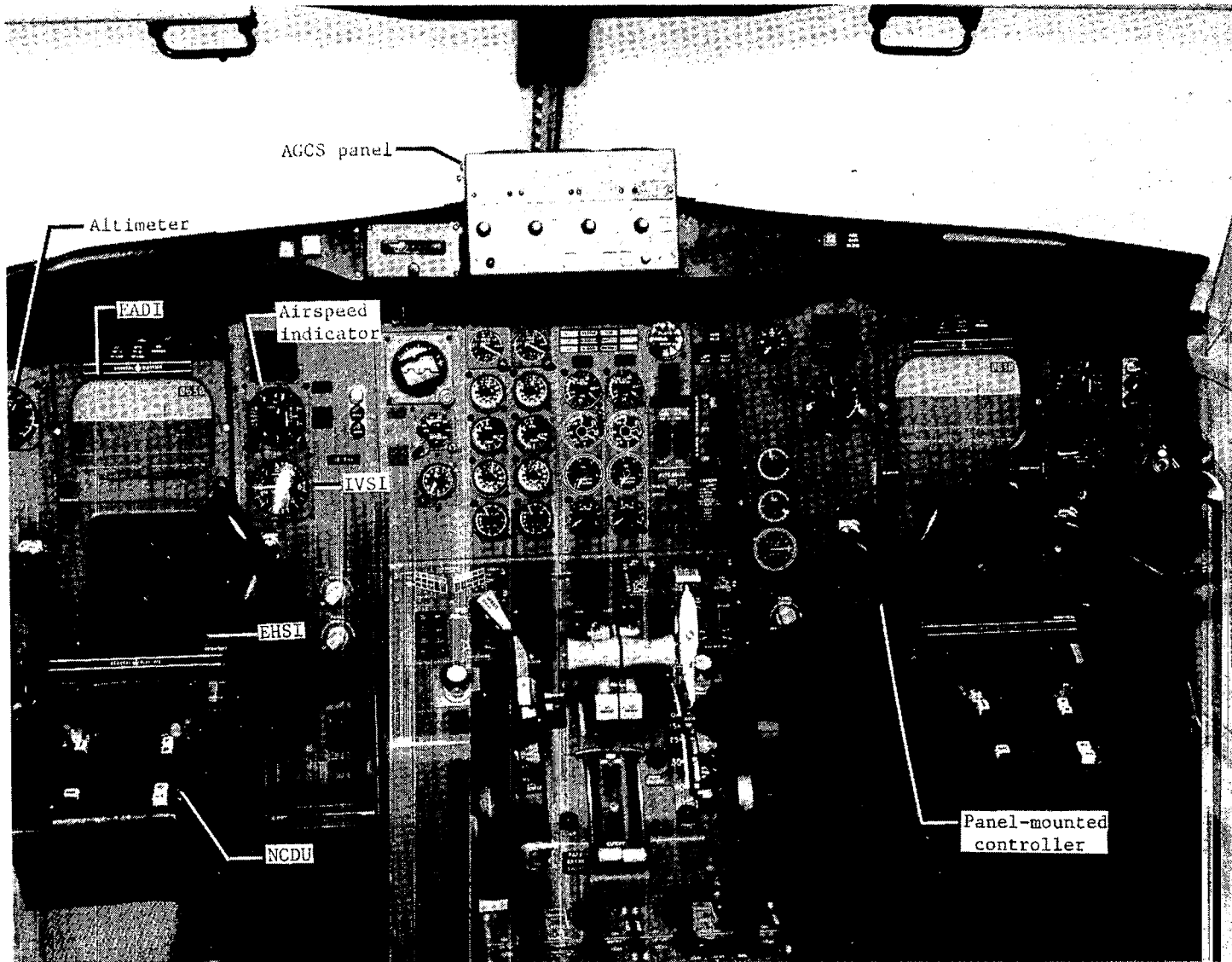


Figure 3.- Aft-flight-deck display arrangement.

L-74-5183.1

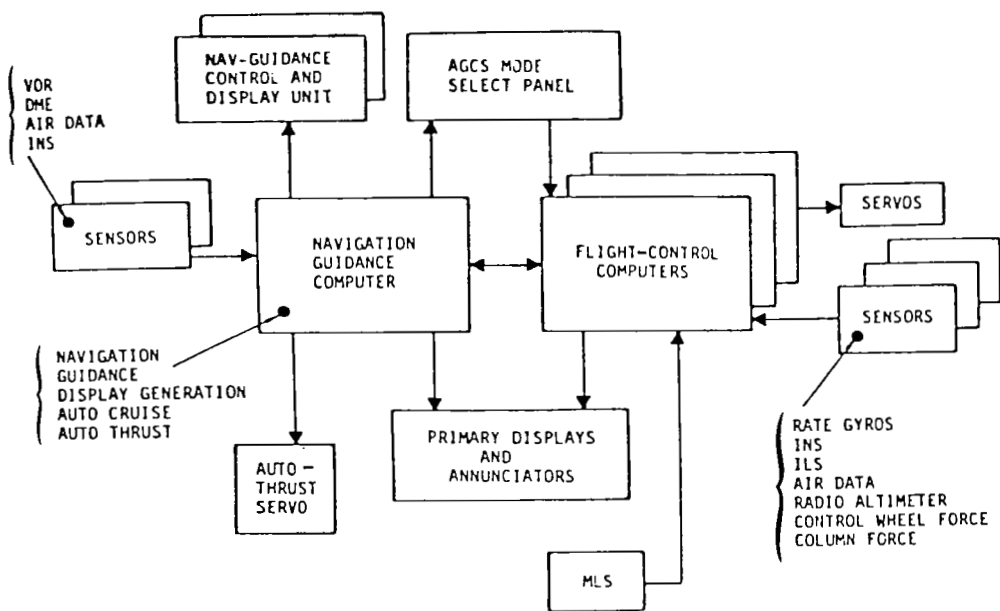
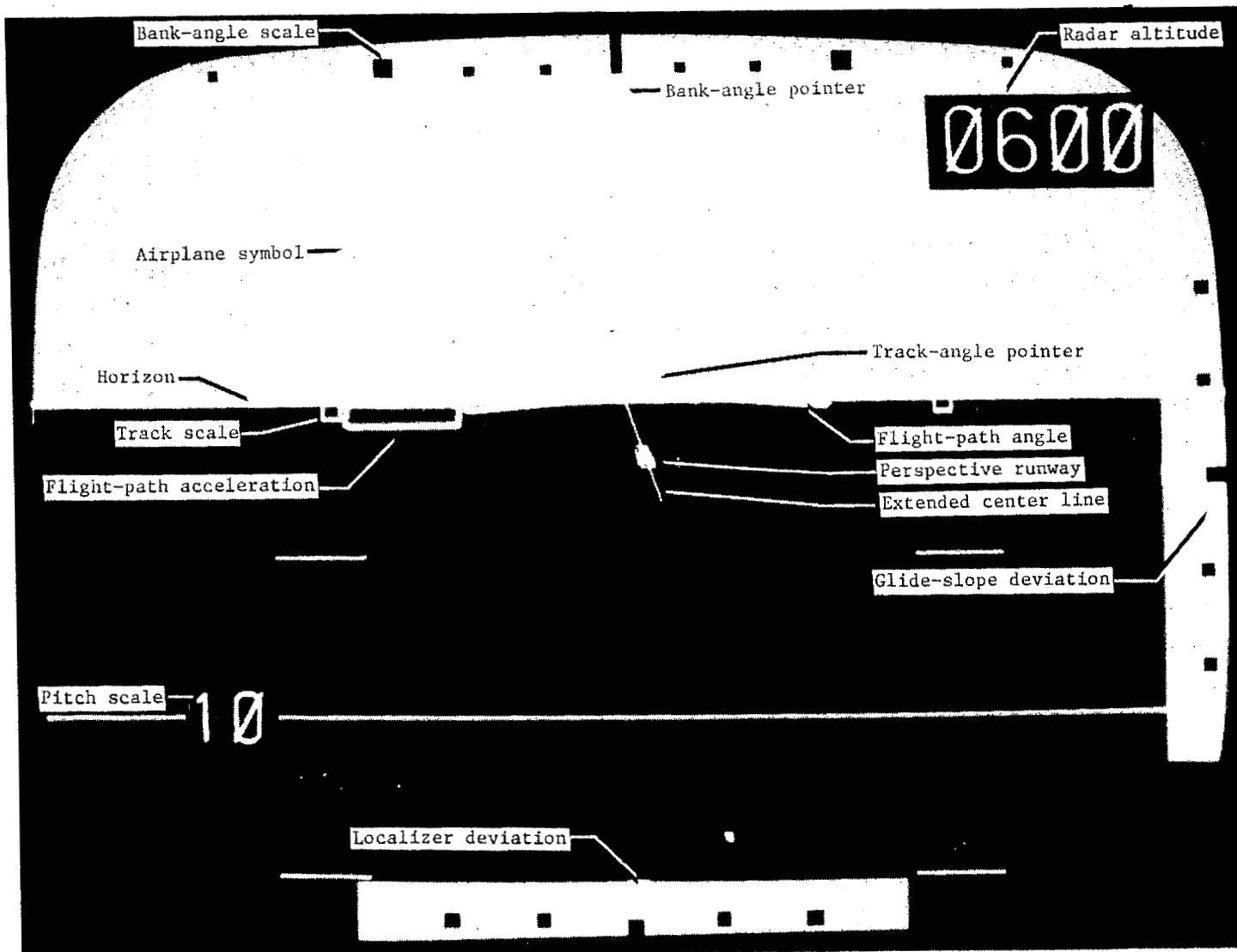


Figure 4.- NASA TCV B-737-100 flight-control configuration.



L-77-5645.1

Figure 5.- EADI display symbology.

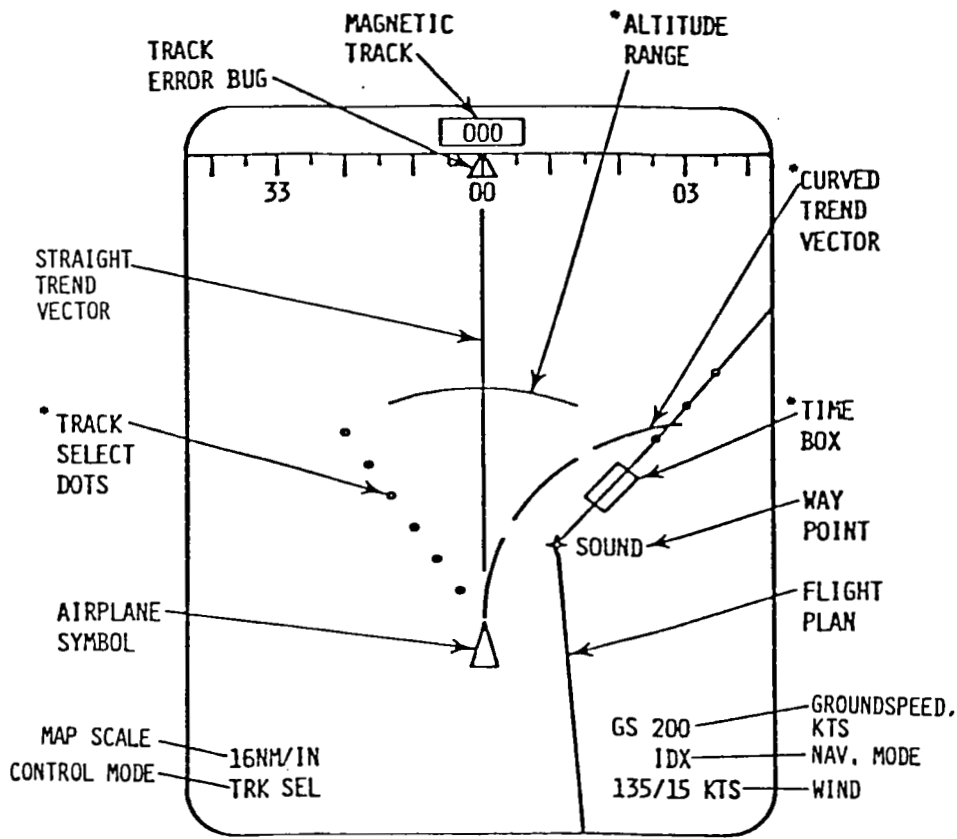


Figure 6.- EHSI display symbology.  
 16 n.mi./in. = 6.3 n.mi./cm.

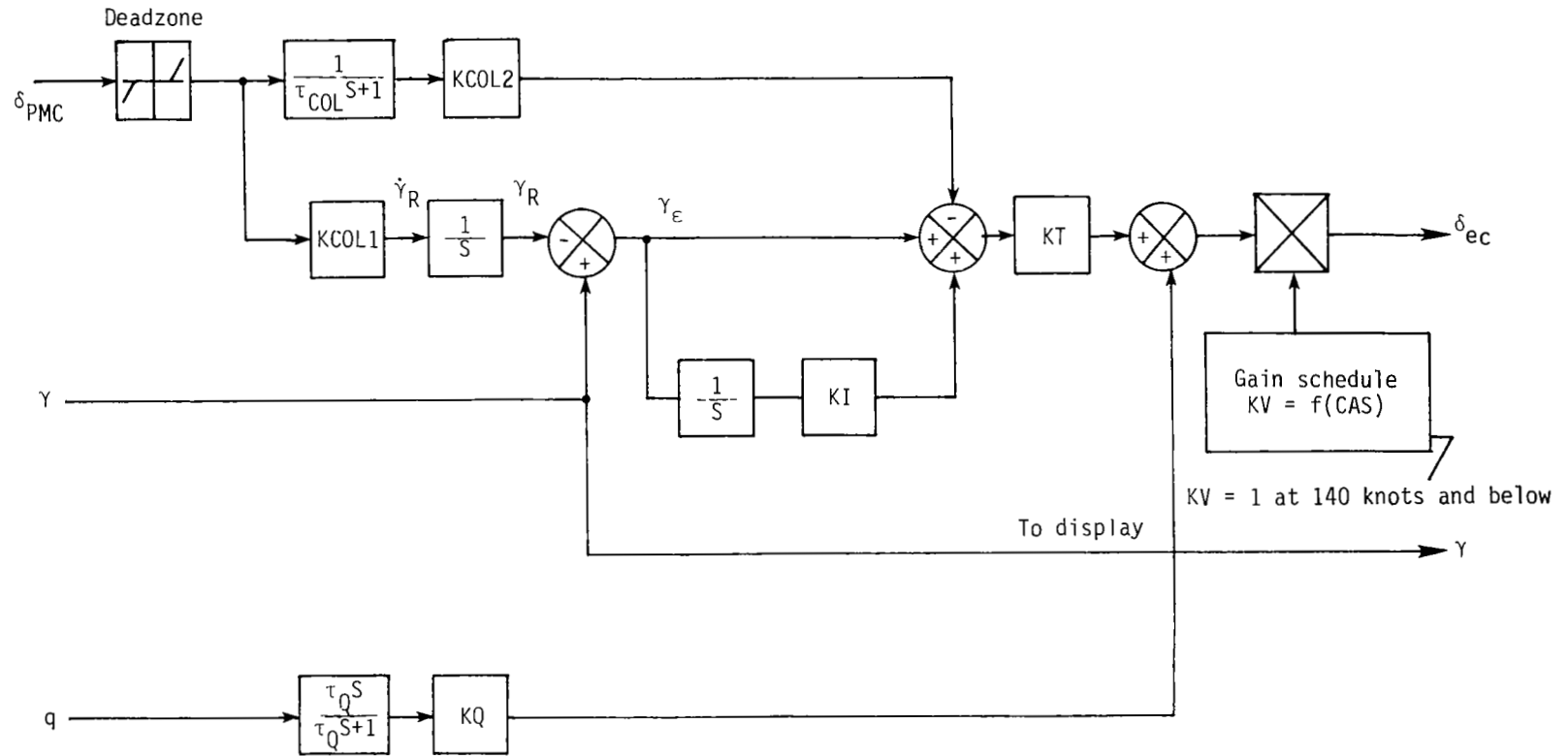


Figure 7.- Control-wheel steering-block diagram of original velocity vector system.

- |                               |                             |
|-------------------------------|-----------------------------|
| ① Roll pointer                | ⑧ Localizer error indicator |
| ② Roll scale                  | ⑨ Runway symbol             |
| ③ Pitch grid                  | ⑩ Track pointer             |
| ④ Radar altitude              | ⑪ Pitch reference line      |
| ⑤ Airplane reference symbol   | ⑫ Flight-path acceleration  |
| ⑥ Speed error indicator       | ⑬ Flight-path angle         |
| ⑦ Glide-slope error indicator |                             |

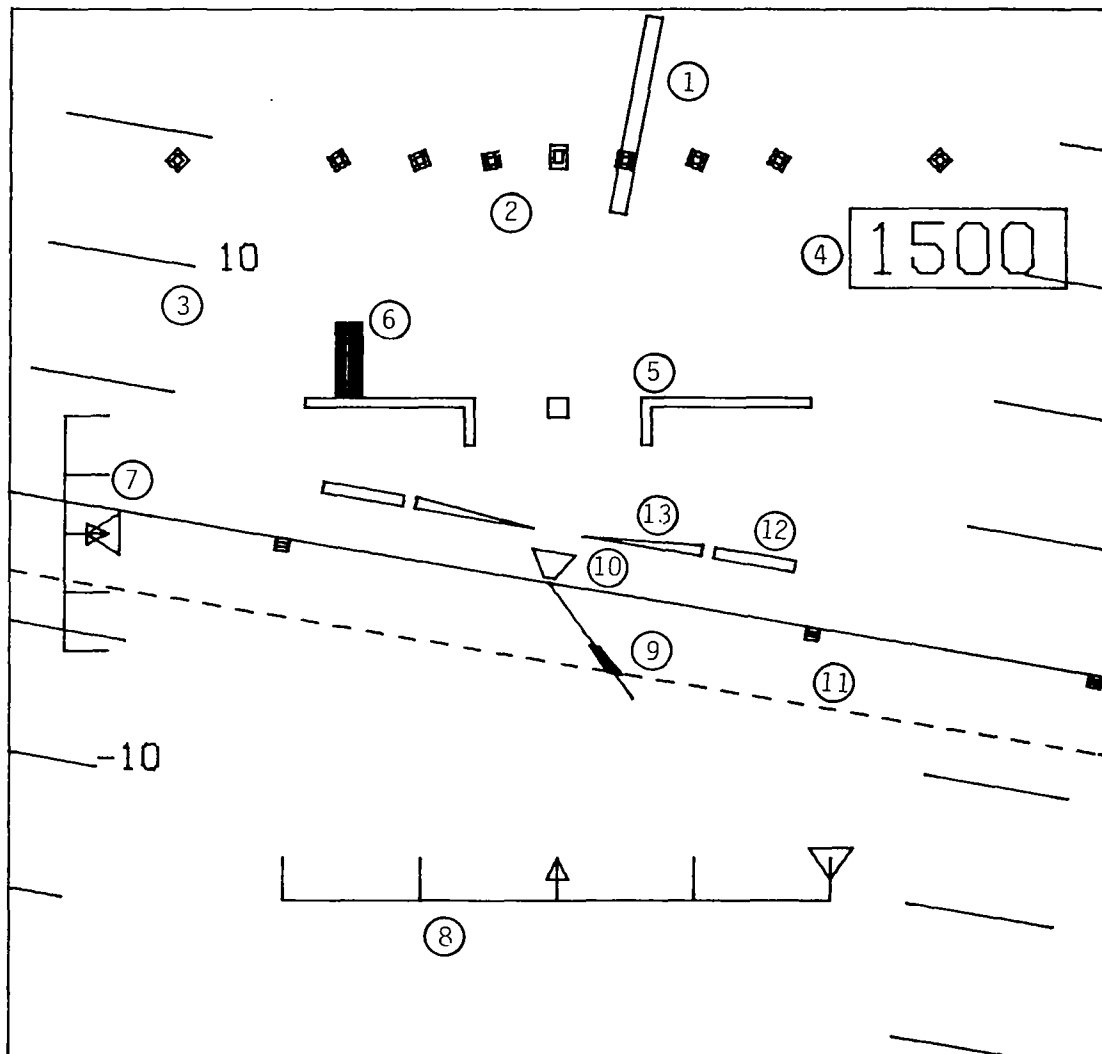


Figure 8.- Original display system of electronic attitude direction indicator (EADI).

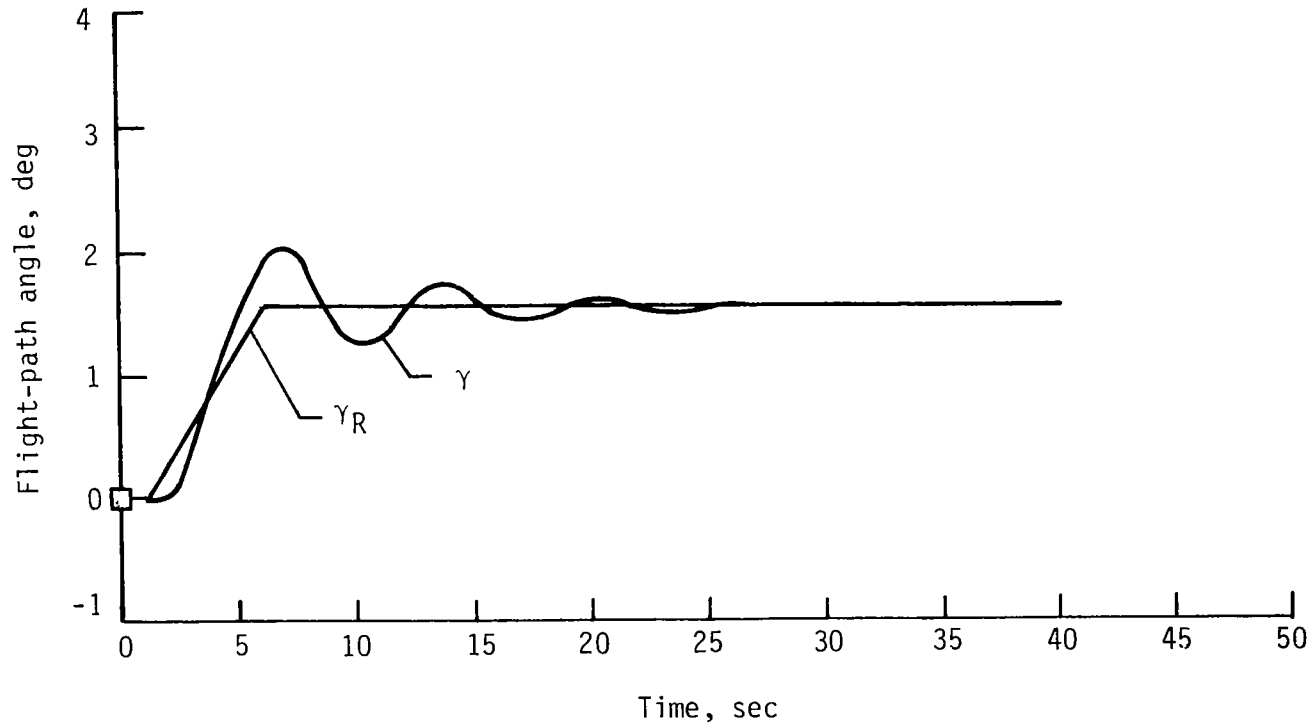


Figure 9.- Original control-system response to a step input. Step-column input of 1.27 cm with 5-sec duration. Airspeed, 120 knots.



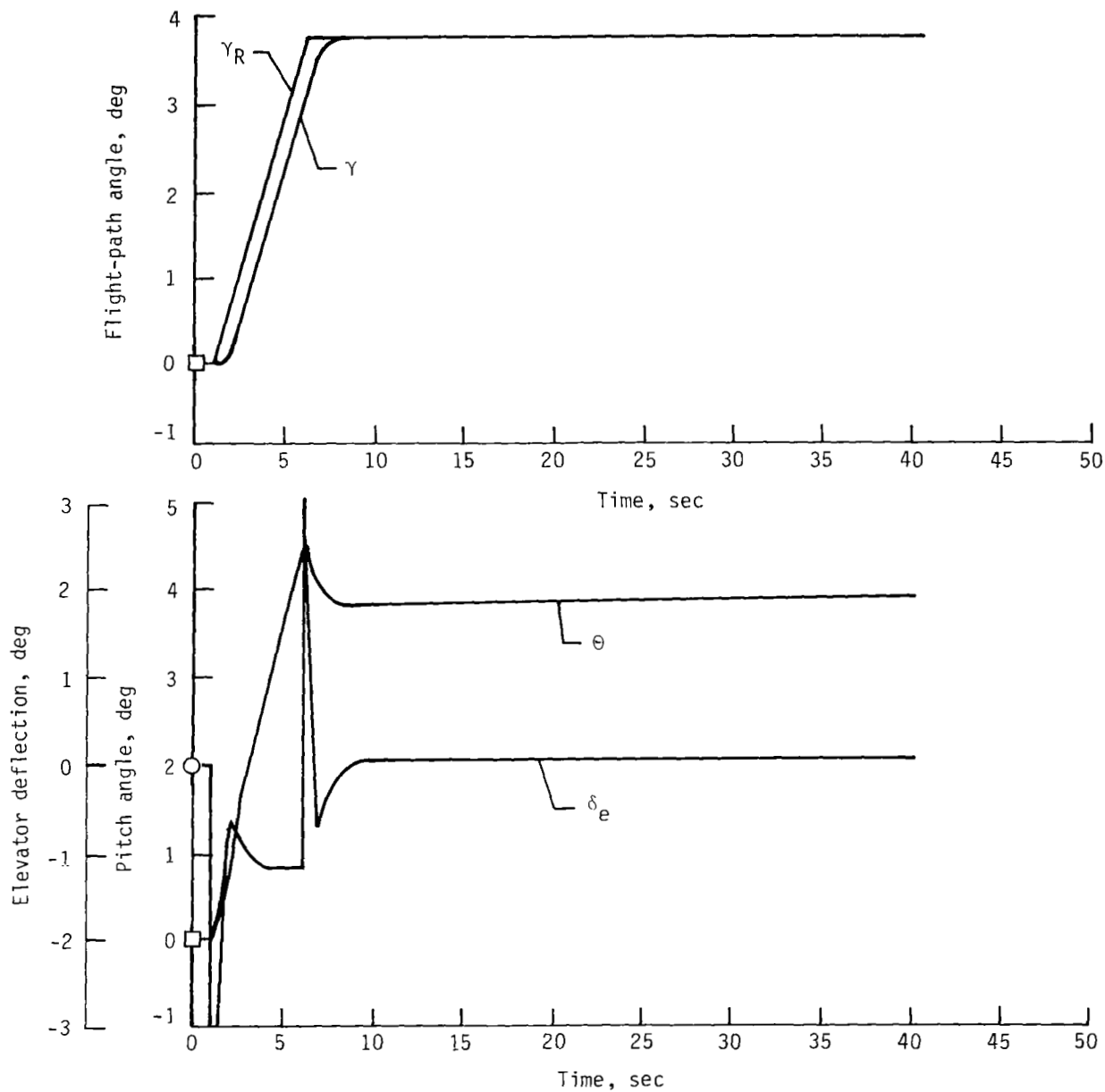


Figure 11.- Response of modified control system to step input. Step-column input of 1.27 cm with 5-sec duration.

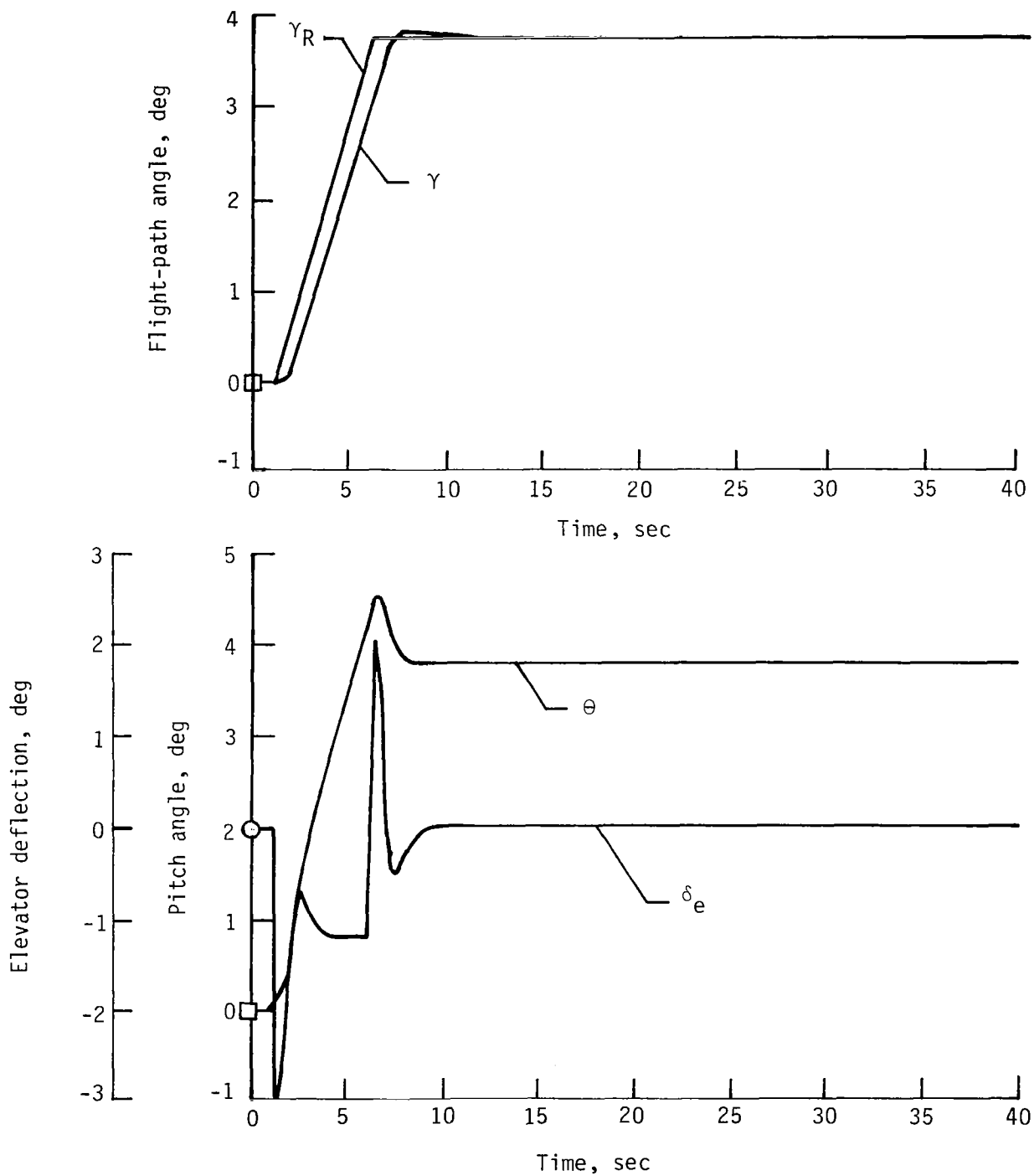


Figure 12.- Non-real-time response of modified control system to step input without lead circuit. Step-column input of 1.27 cm with 5-sec duration.

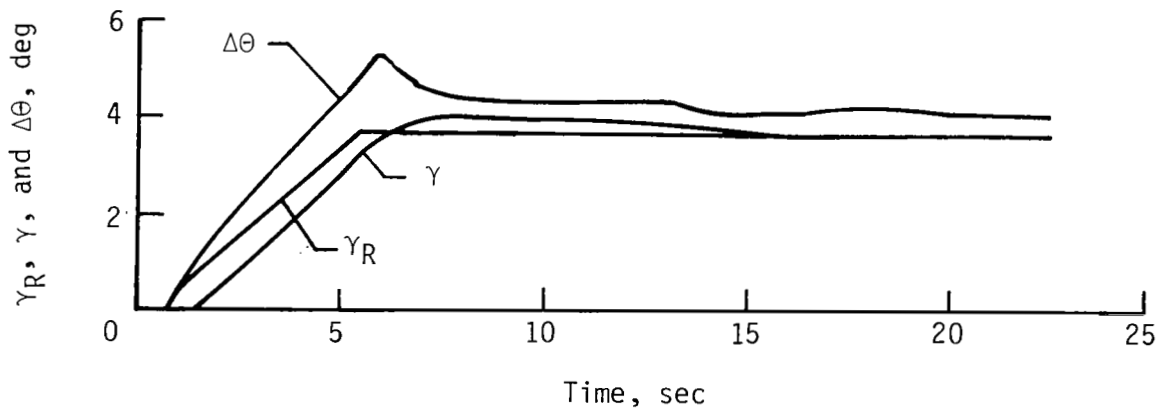


Figure 13.- Response of tuned control system on real-time simulation (system A).  
 Step-column input of 1.27 cm with 5-sec duration.

- |                               |                               |
|-------------------------------|-------------------------------|
| ① Roll pointer                | ⑧ Localizer error indicator   |
| ② Roll scale                  | ⑨ Runway symbol               |
| ③ Pitch grid                  | ⑩ Track pointer               |
| ④ Radar altitude              | ⑪ Pitch reference line        |
| ⑤ Airplane reference symbol   | ⑫ Flight-path acceleration    |
| ⑥ Speed error indicator       | ⑬ Flight-path angle           |
| ⑦ Glide-slope error indicator | ⑭ Reference flight-path angle |

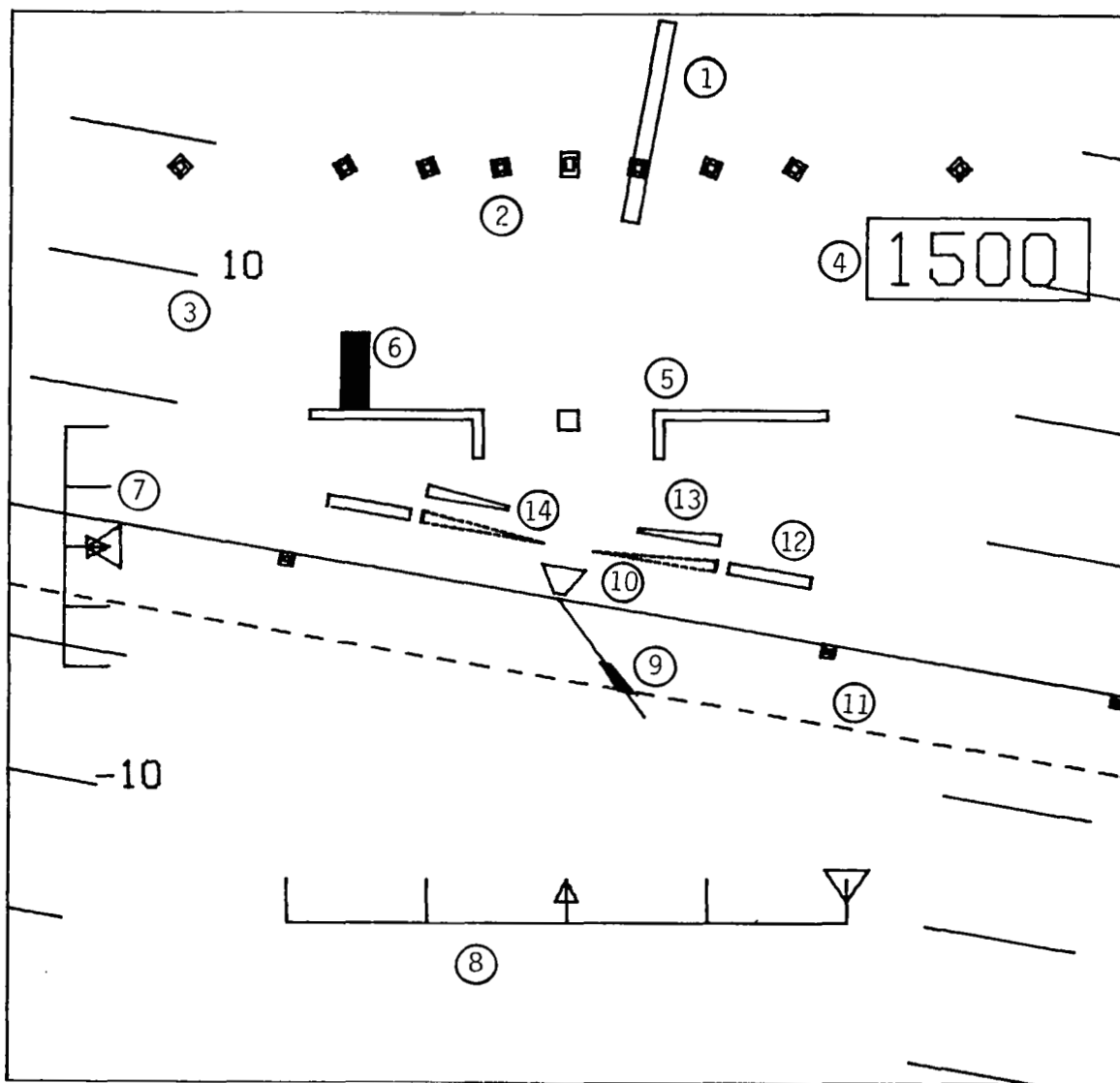


Figure 14.- Improved display system.

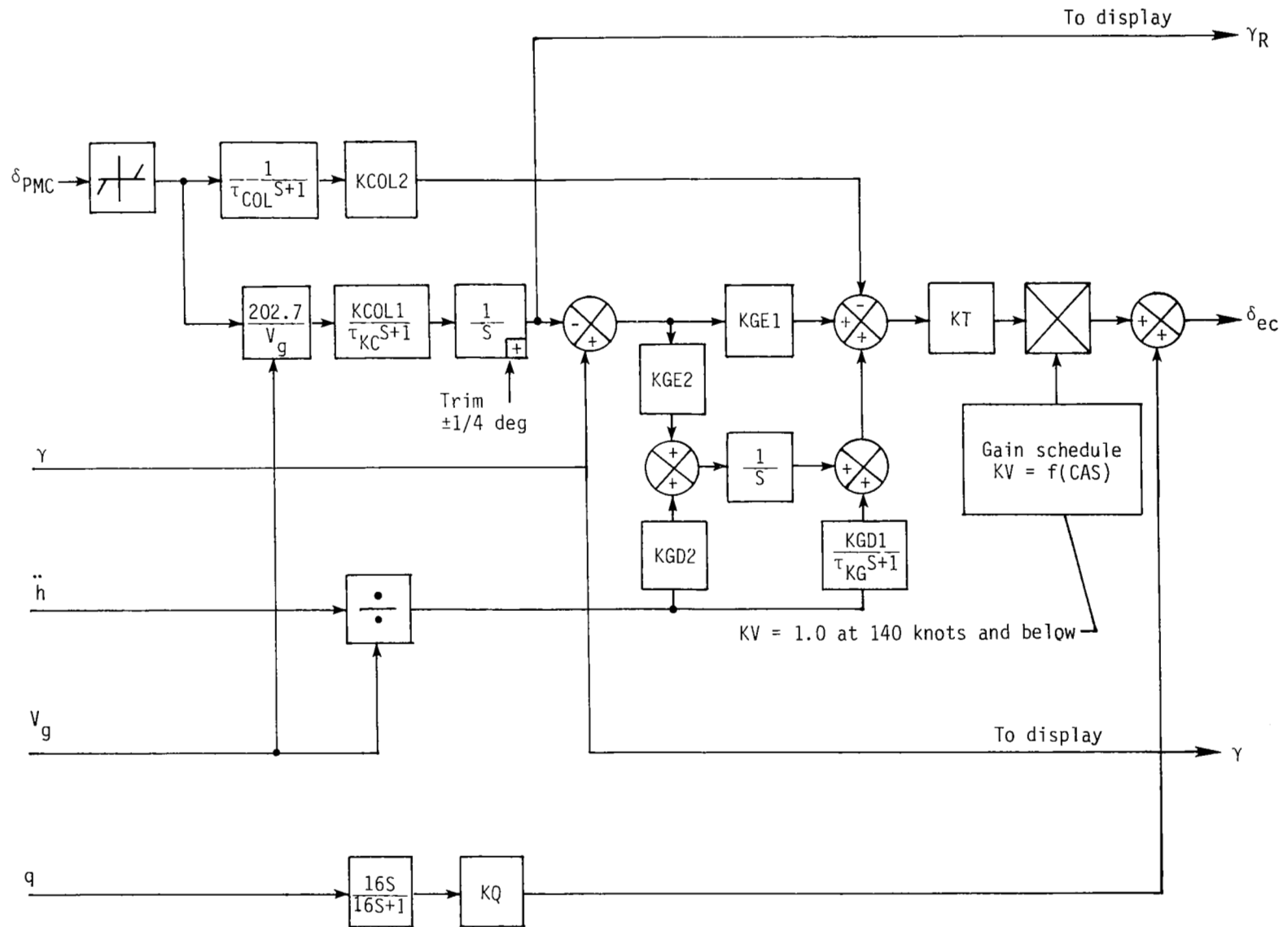


Figure 15.- Block diagram of modified real-time simulation control system (systems B and C).

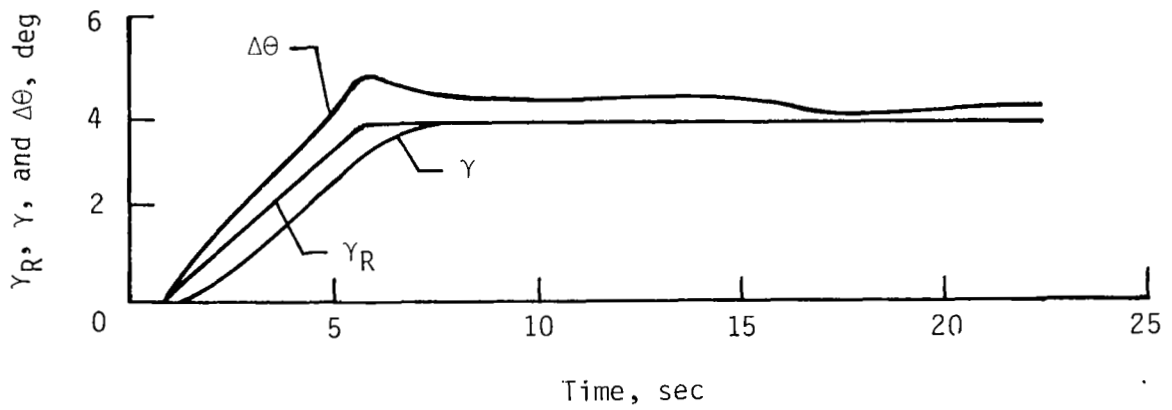


Figure 16.- Response of modified real-time simulation control system (system B).  
Step-column input of 1.27 cm with 5-sec duration.

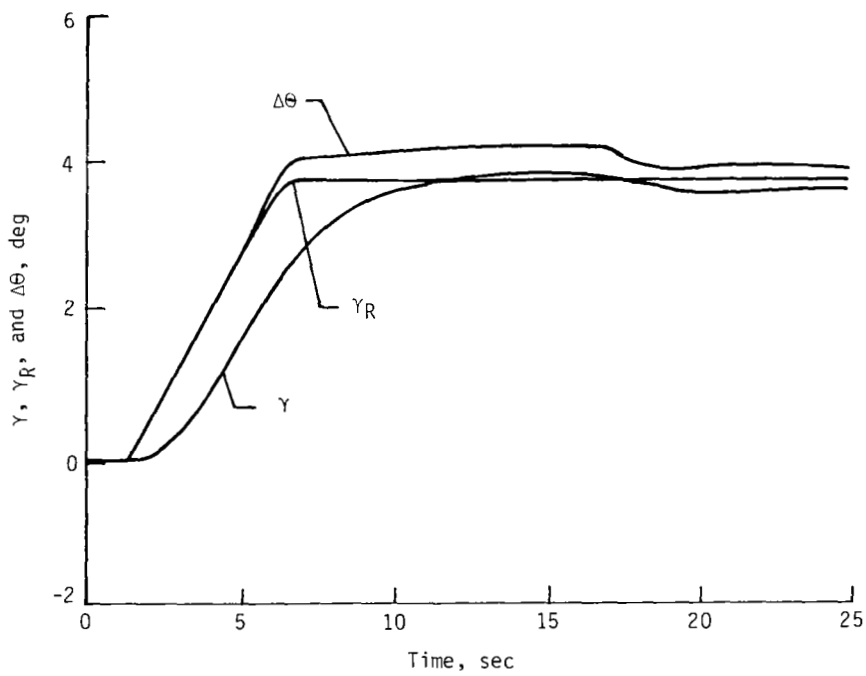


Figure 17.- Response of modified real-time simulation control system (system C). Step-column input of 1.27 cm with 5-sec duration.

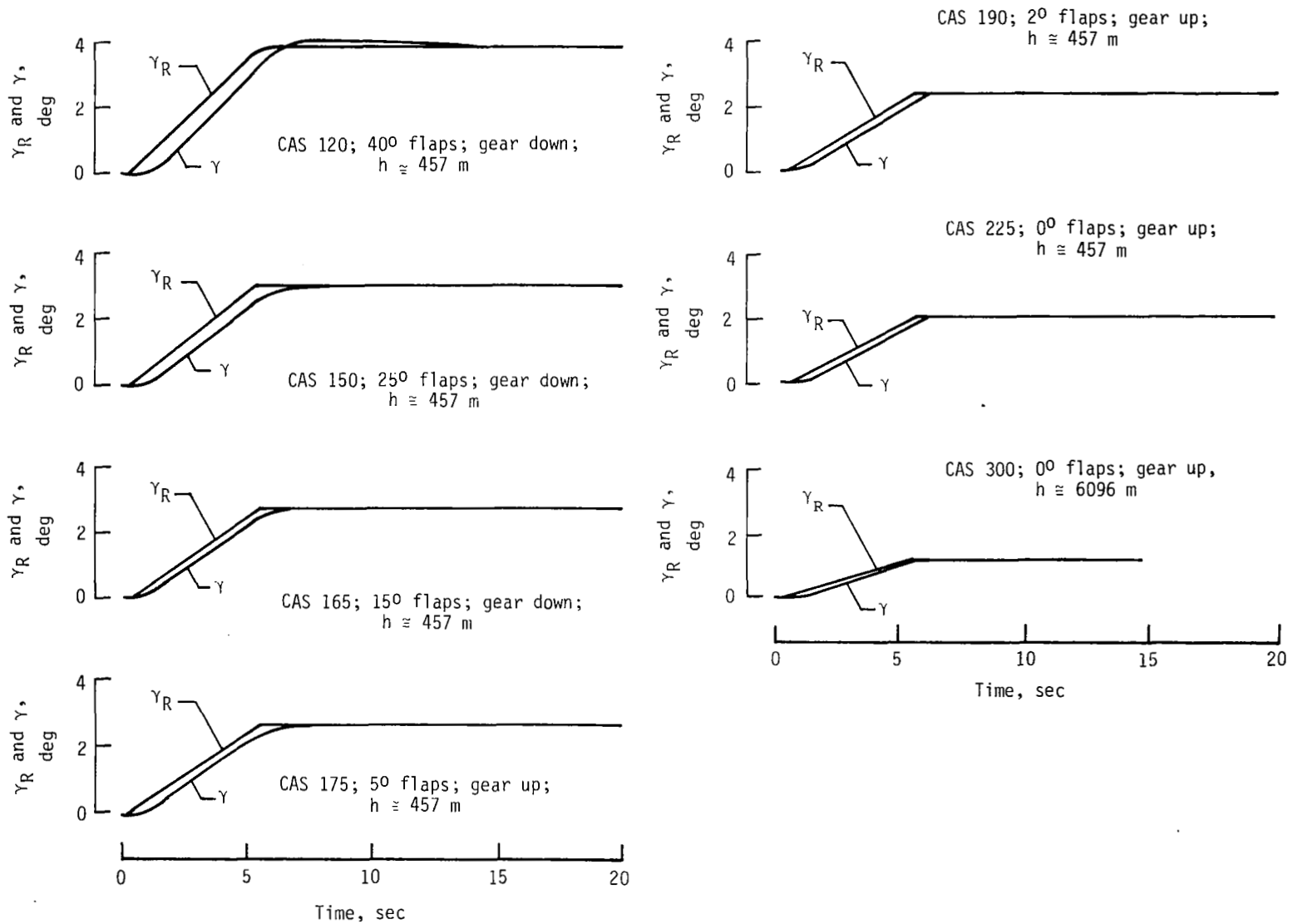


Figure 18.- Responses of selected control system (system B) for step inputs at selected points in speed envelope. Autothrottle was on in all cases; step-column input was 1.27 cm with 5-sec duration.

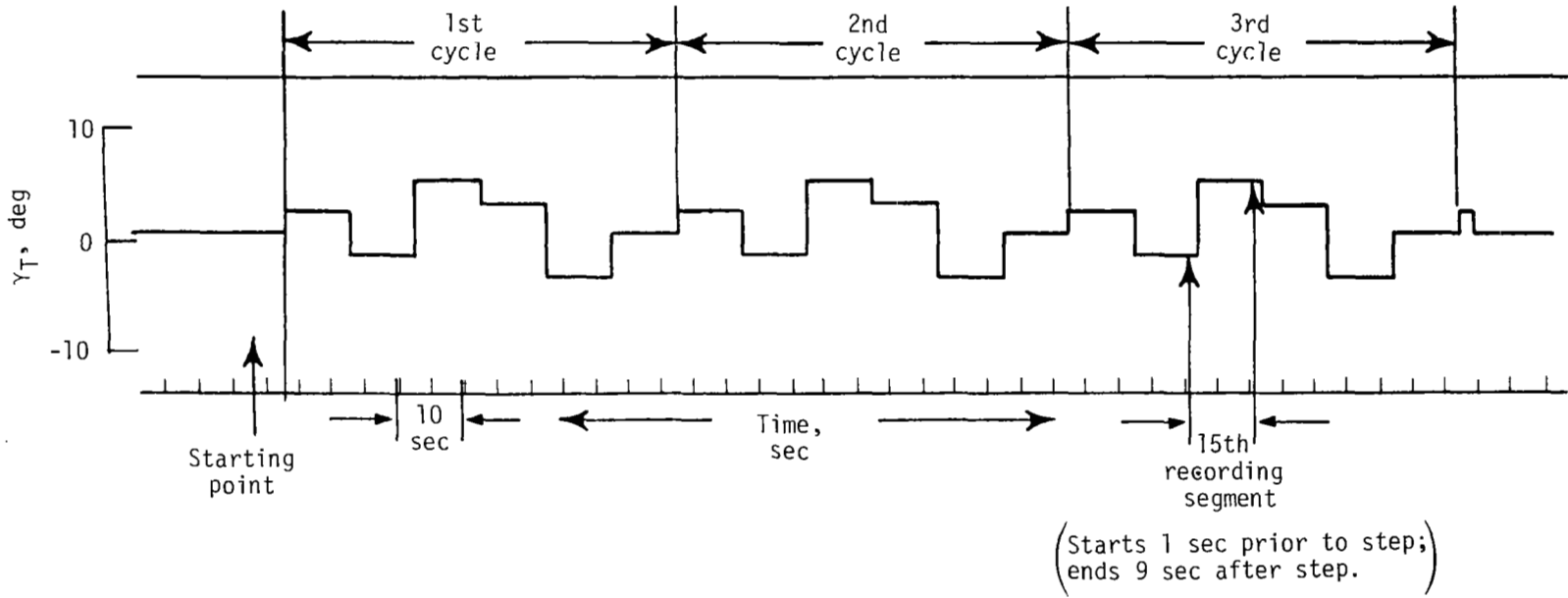


Figure 19.- Tracking-task profile and recording segments.

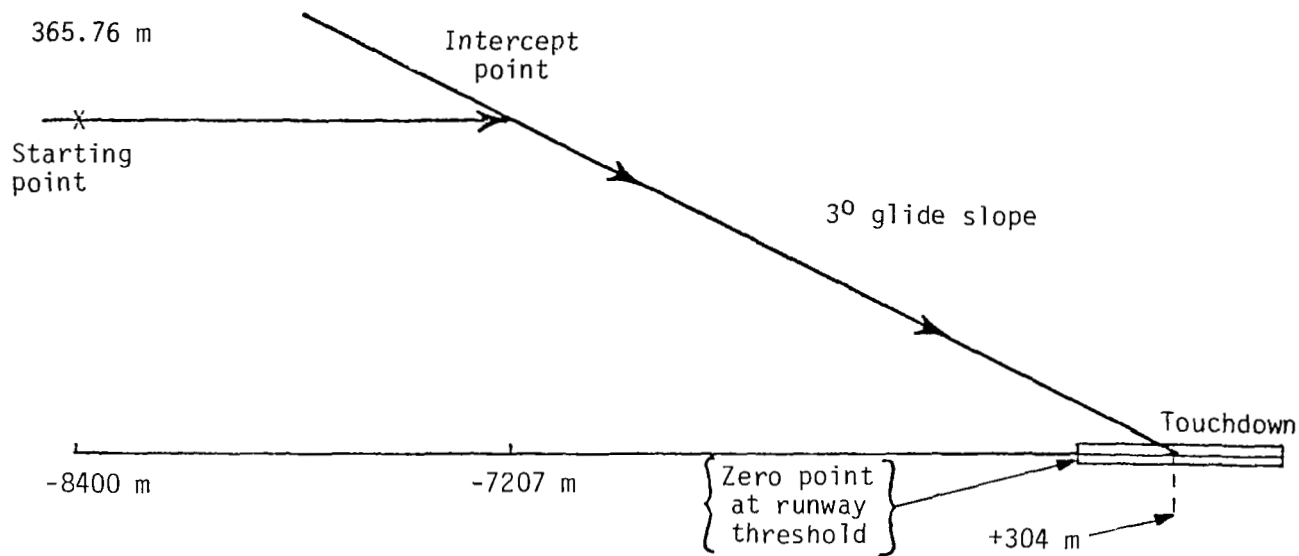


Figure 20.- Approach-task profile.

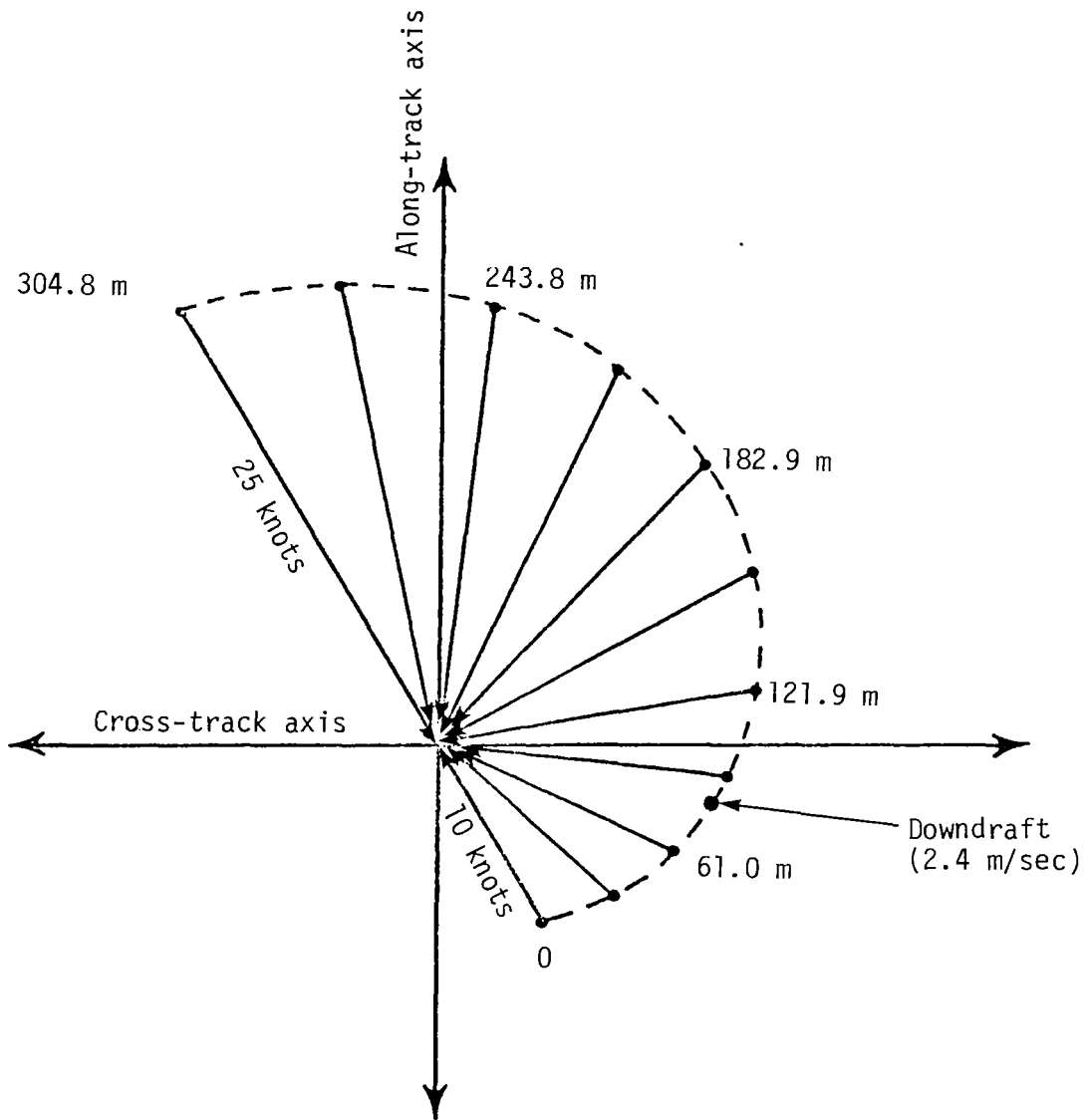
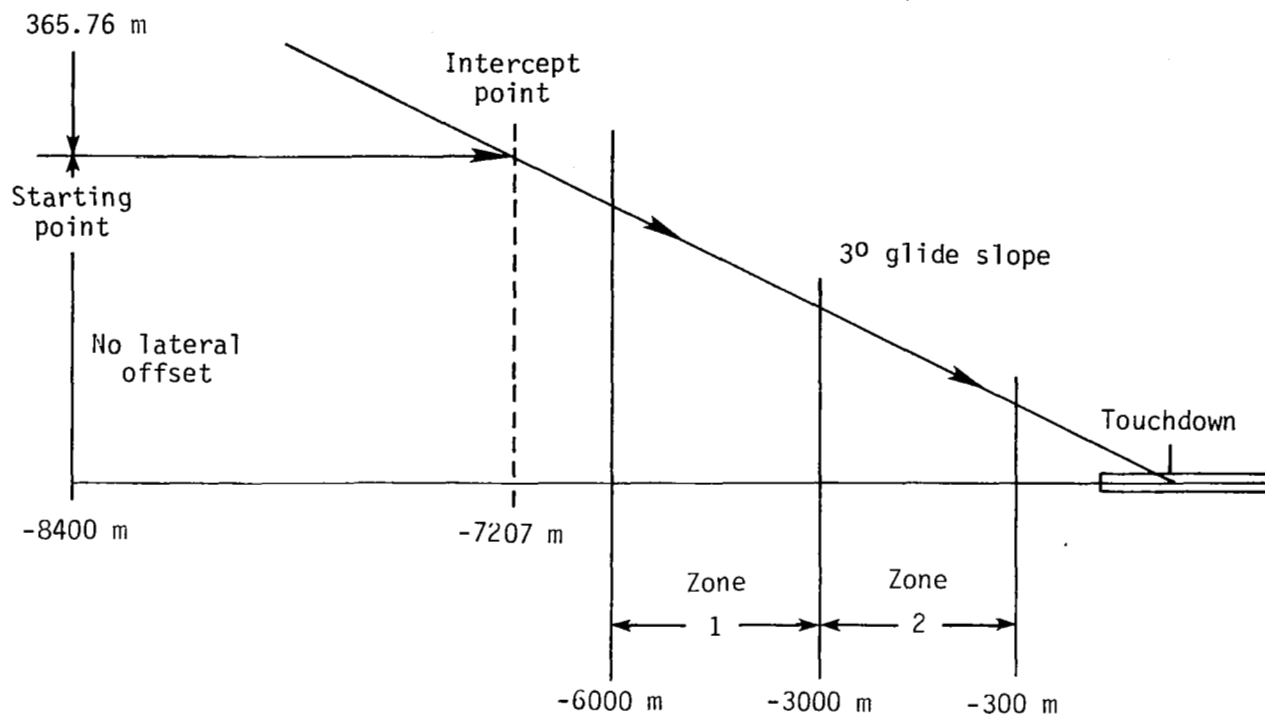


Figure 21.- Wind-shear direction and magnitude.



Recording-zone number	Starting point	End
1	$x = -6000$ m $h = 330.42$ m	$x = -3000$ m $h = 173.2$ m
2	$x = -3000$ m $h = 173.2$ m	$x = -300$ m $h = 31.7$ m

Figure 22.- Recording-segment definitions in approach task.

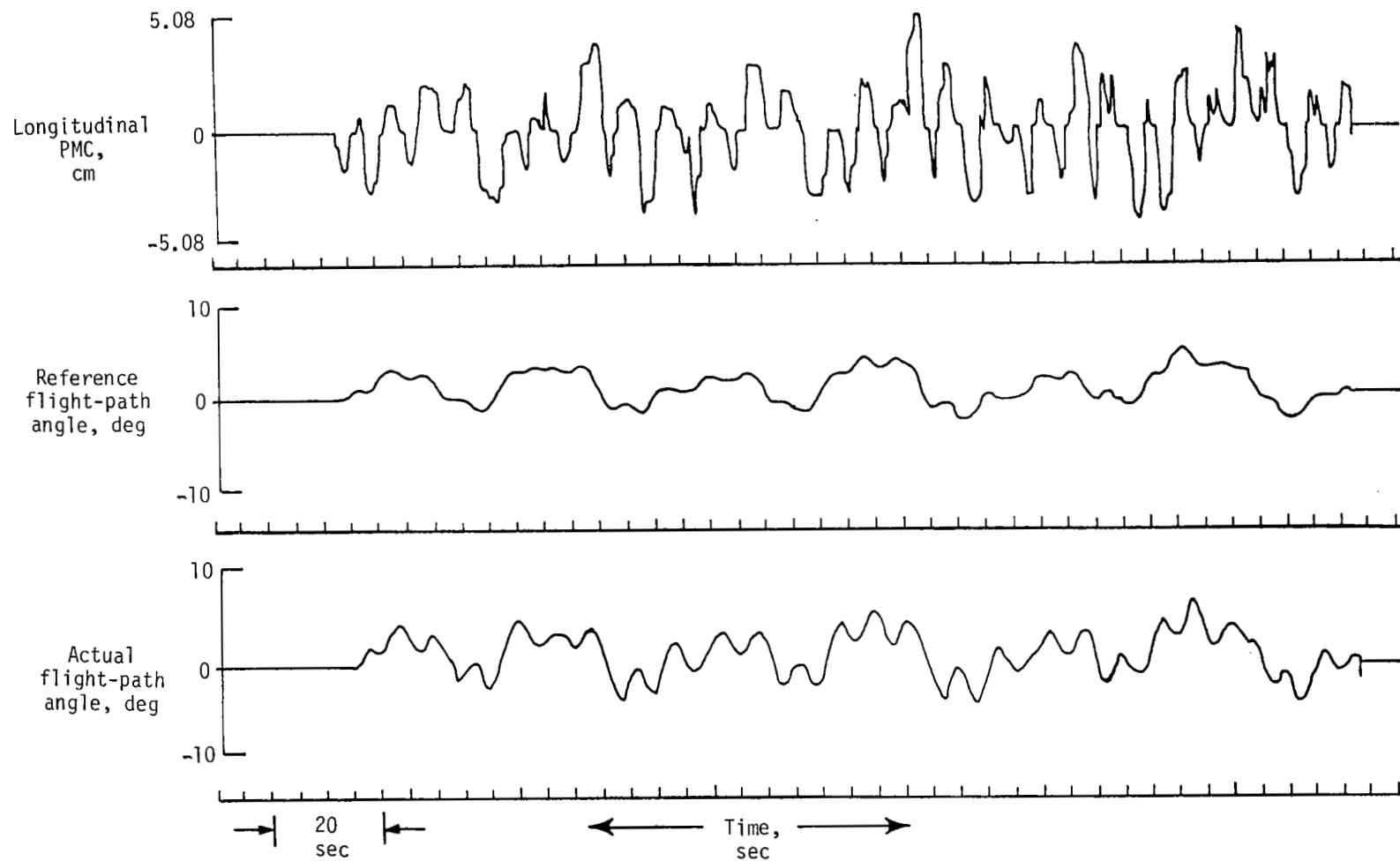


Figure 23.- Baseline system in calm conditions.

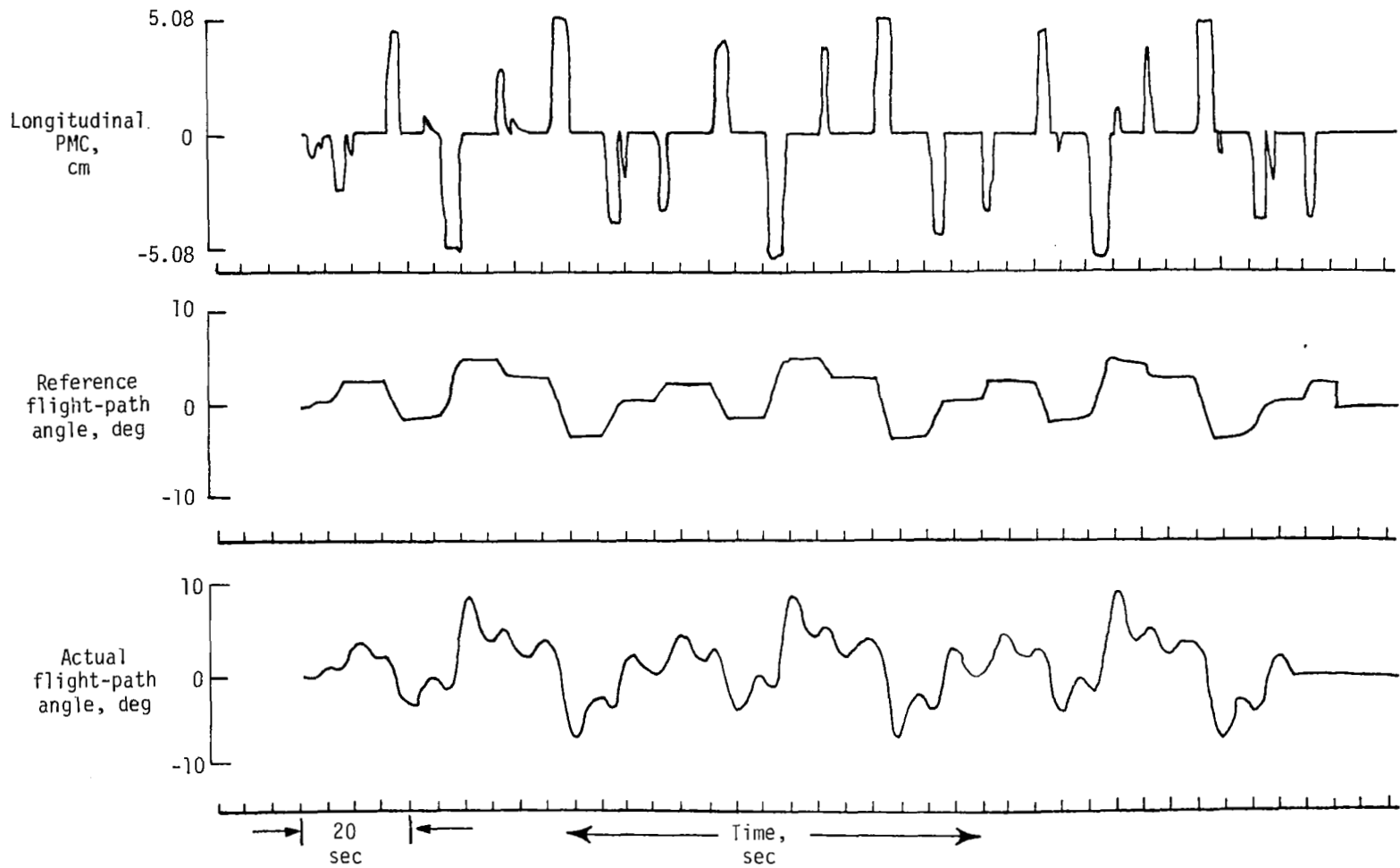


Figure 24.- Baseline control system with advance display system in calm conditions.

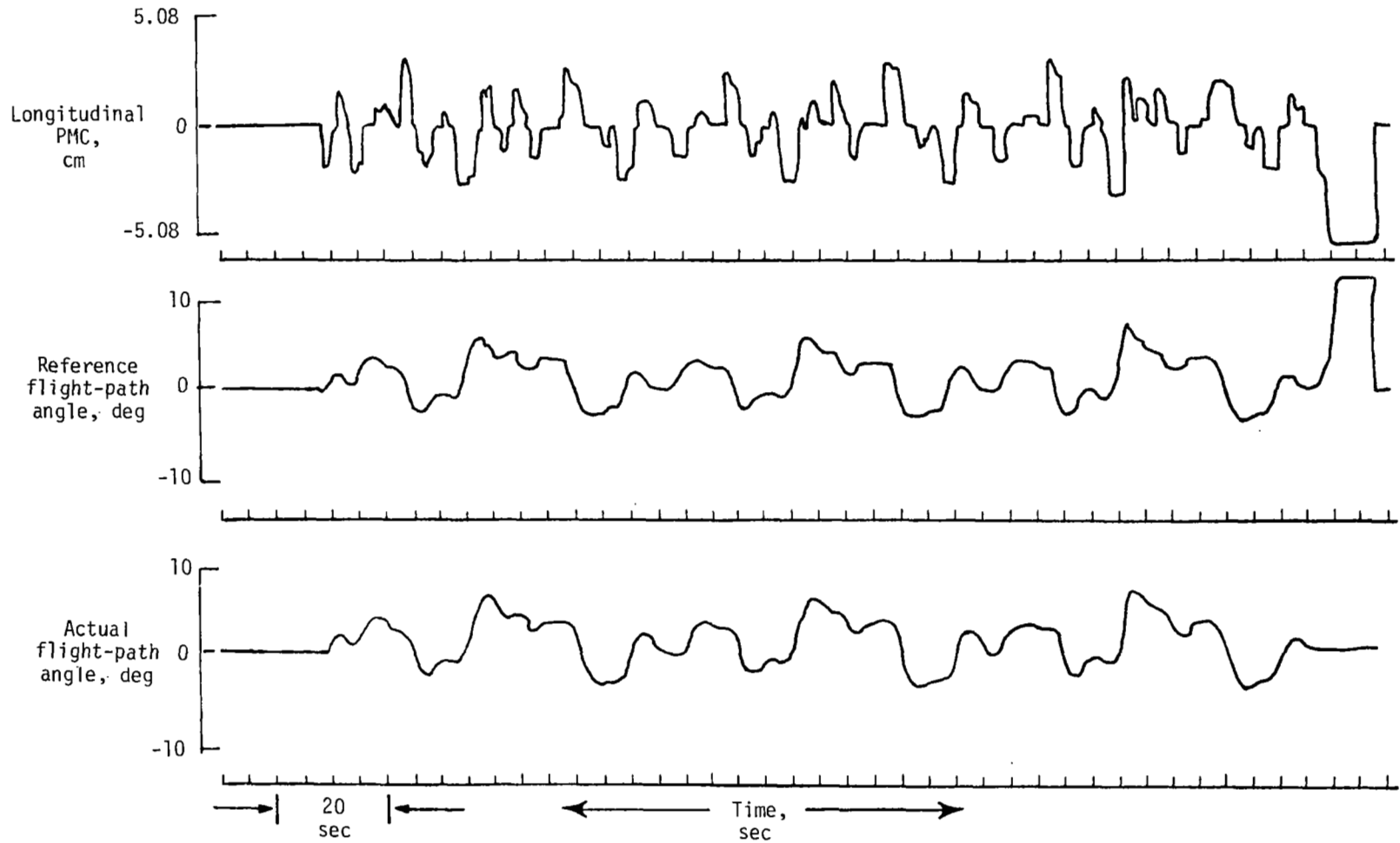


Figure 25.- Advanced control system with baseline display system in calm conditions.

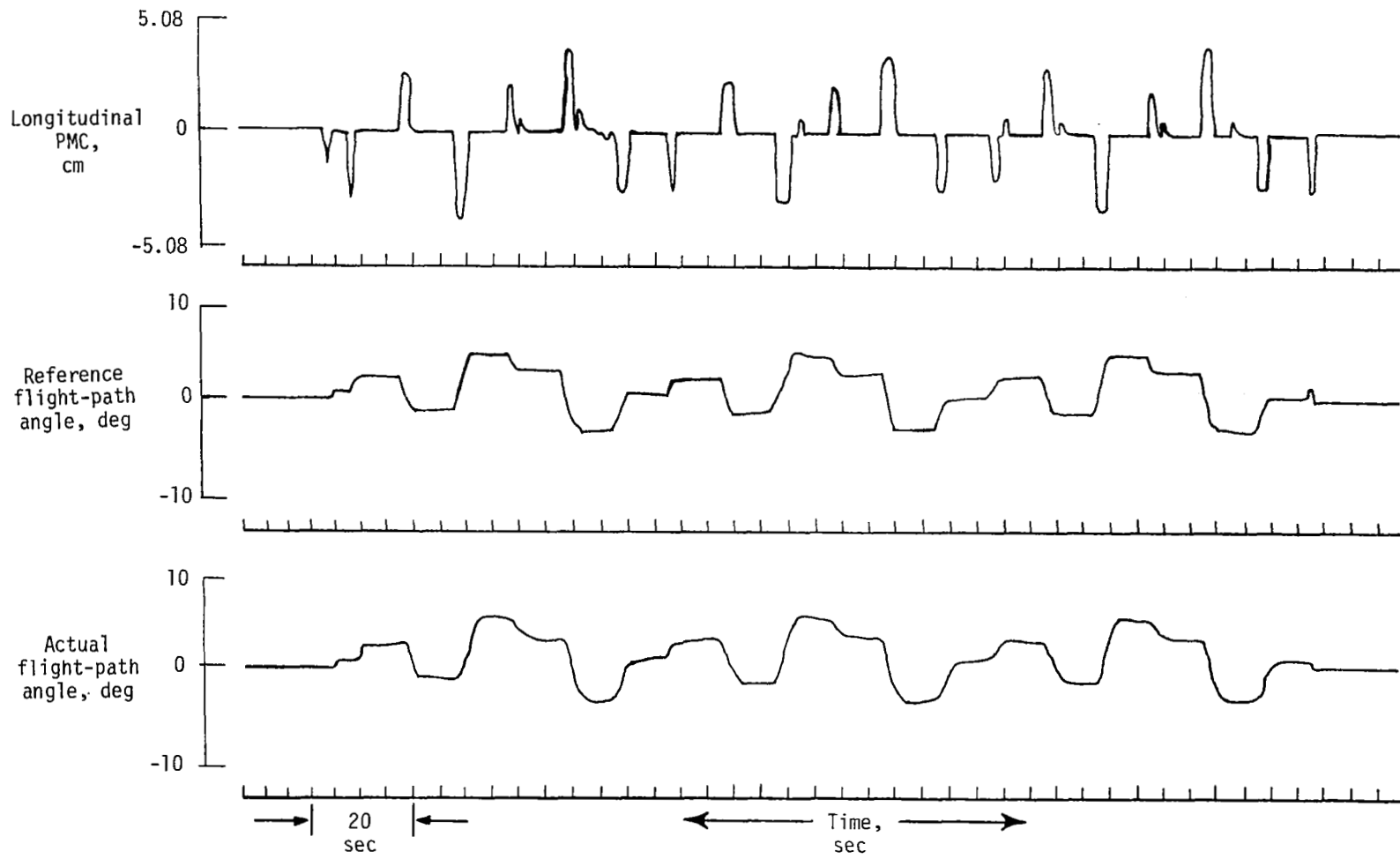


Figure 26.- Advanced system in calm conditions.

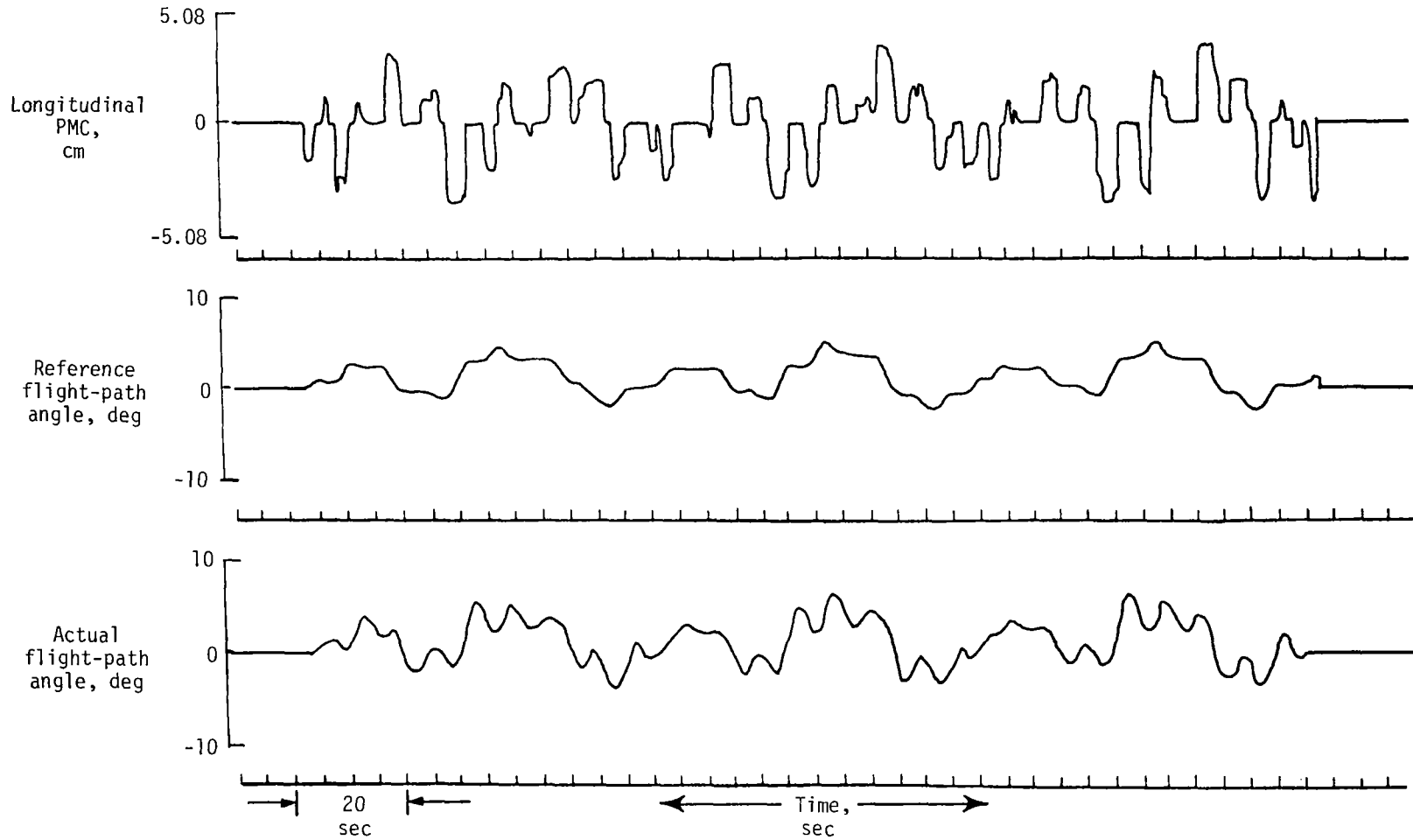


Figure 27.- Baseline system in turbulence conditions.

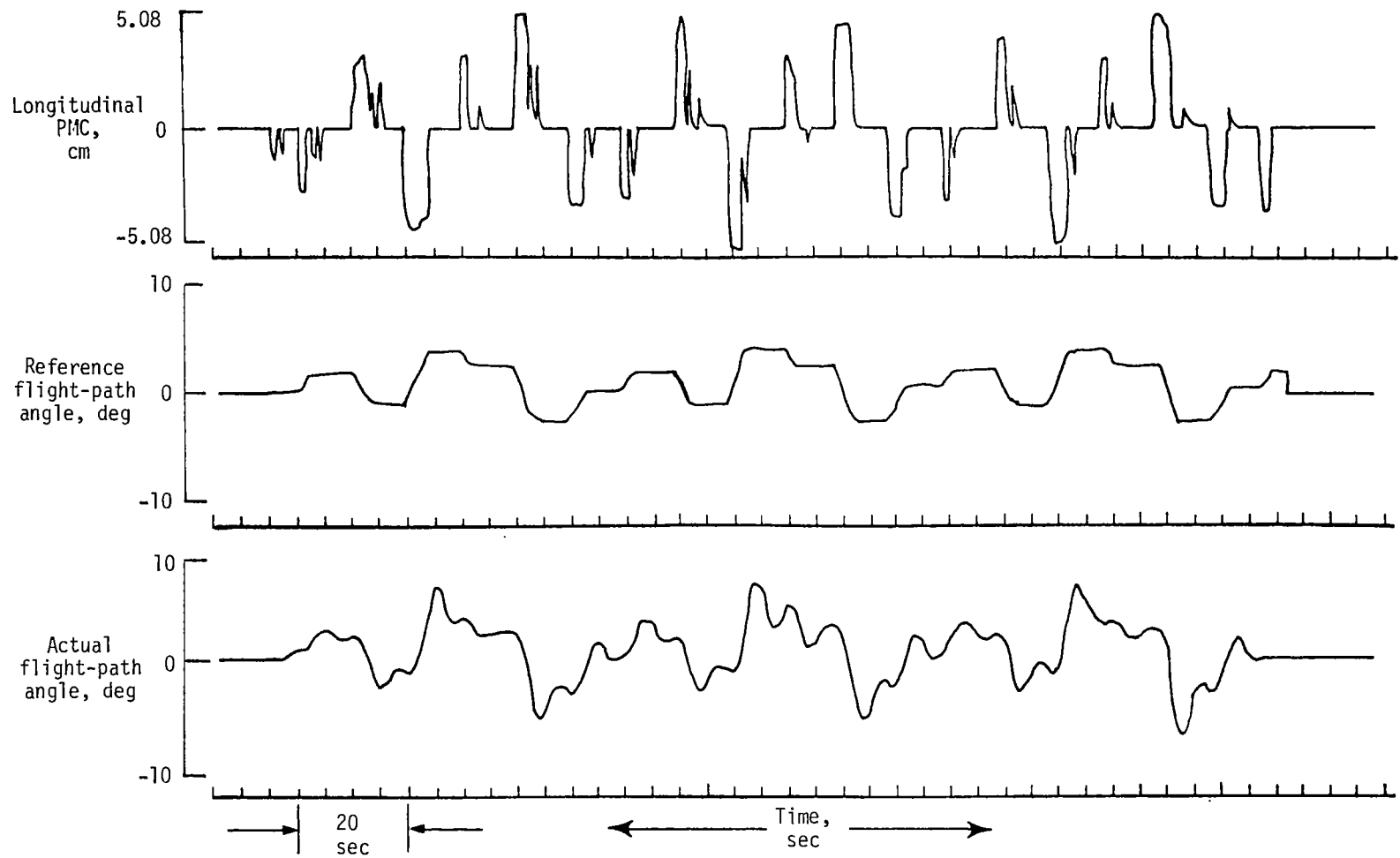


Figure 28.- Baseline control system with advanced display system in turbulence conditions.

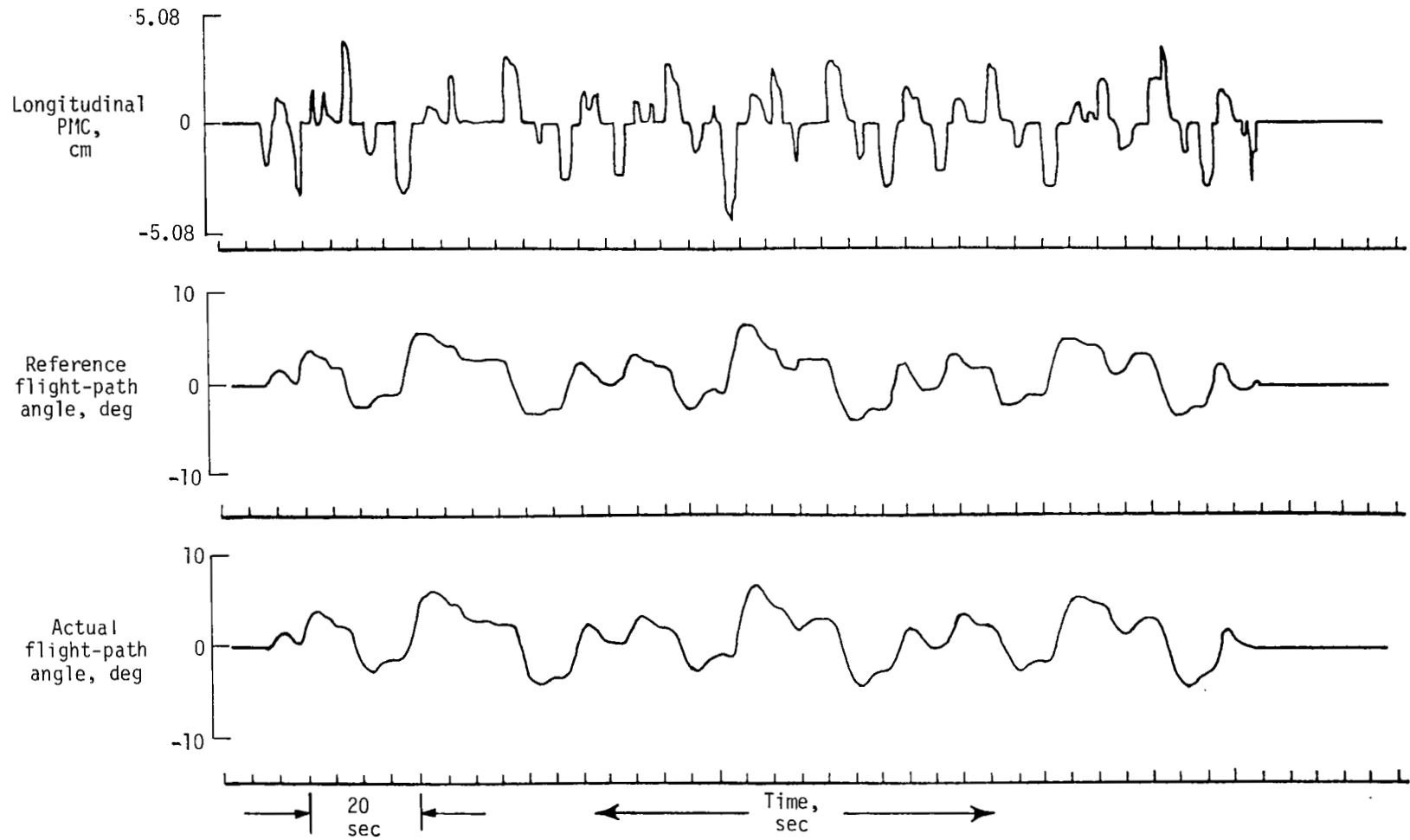


Figure 29.- Advanced control system with baseline display system in turbulence conditions.

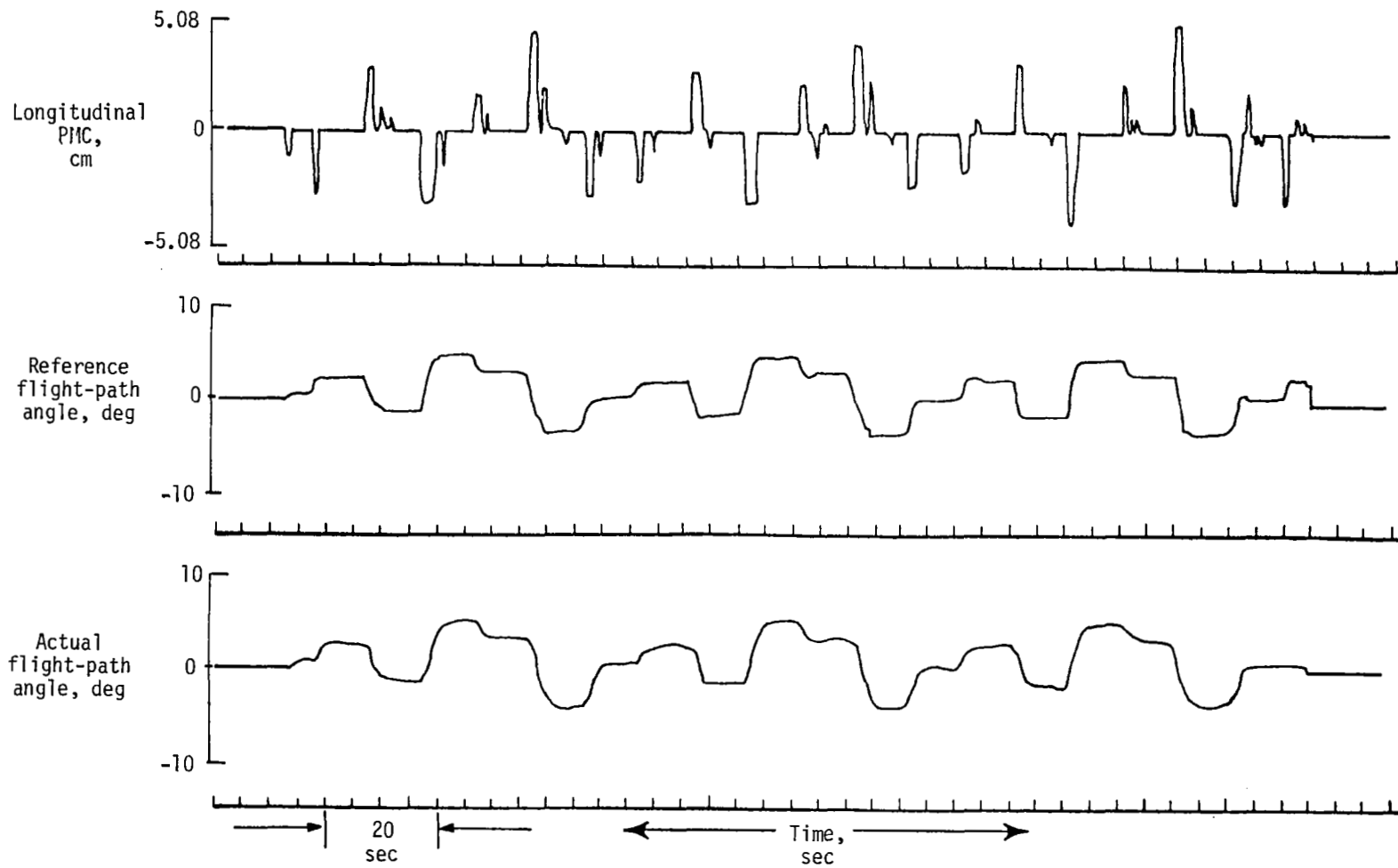


Figure 30.- Advanced system in turbulence conditions.

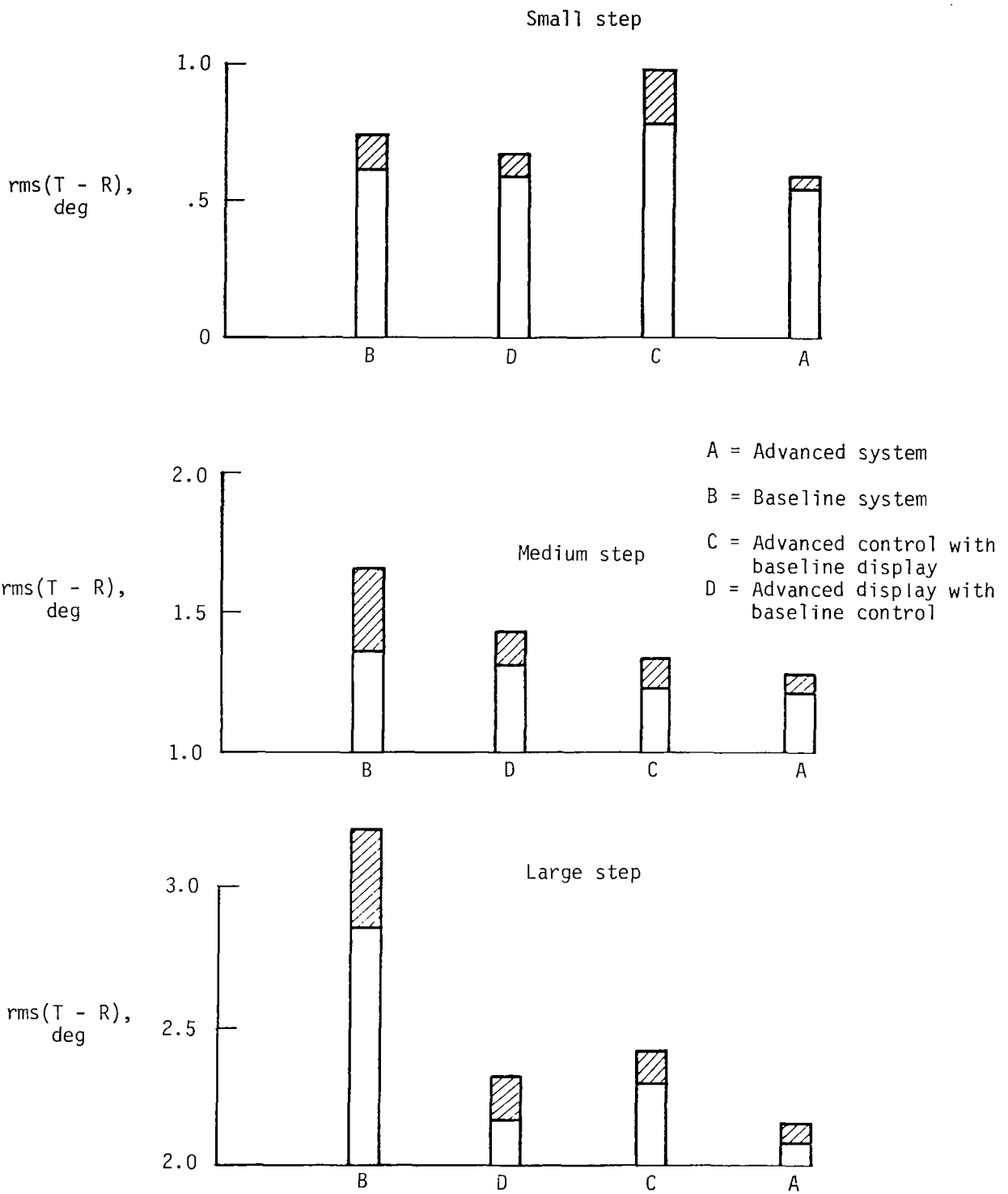


Figure 31.- Means and standard deviations for reference-line tracking task in calm conditions.

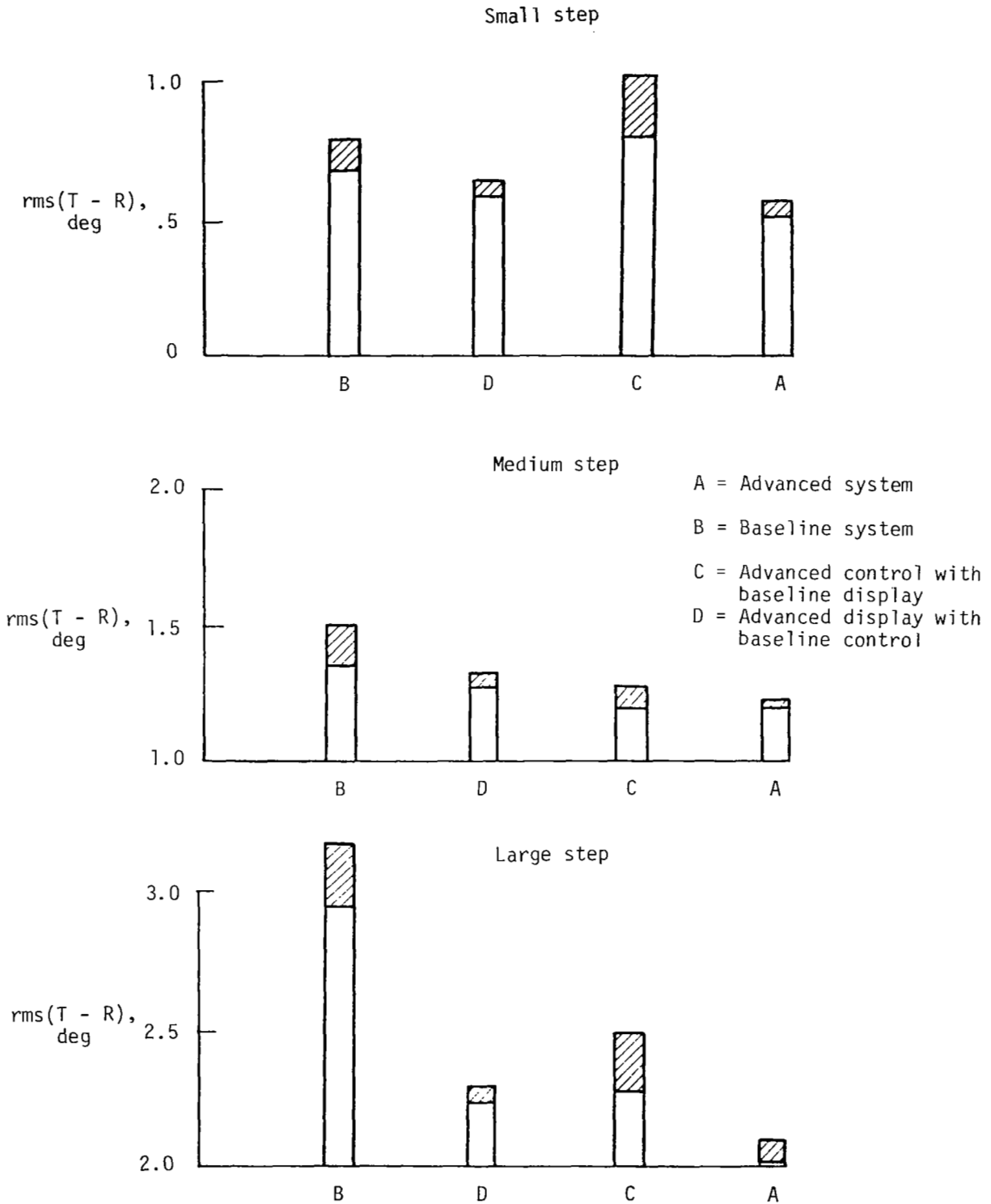


Figure 32.- Means and standard deviations for reference-line tracking task in turbulence conditions.

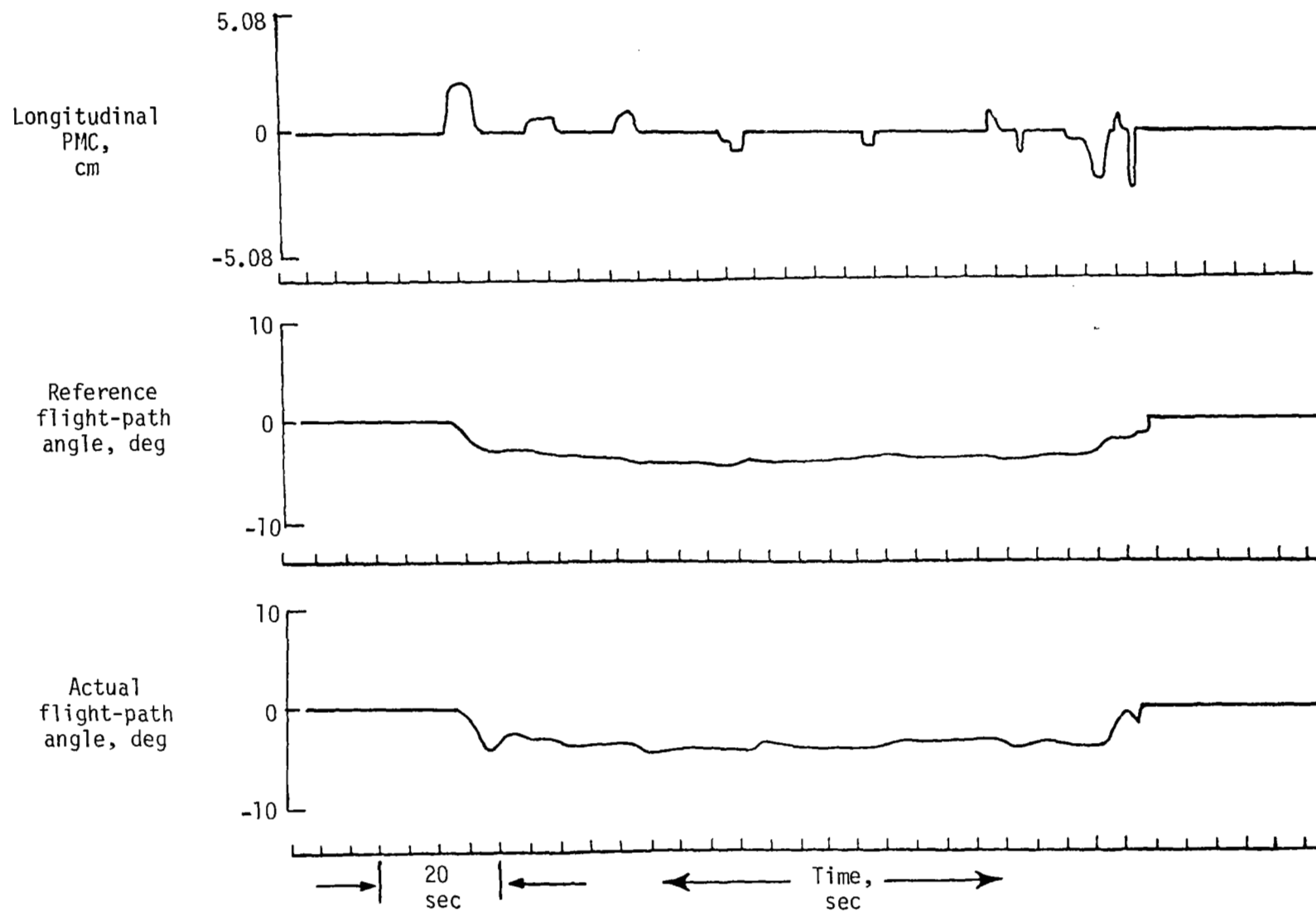


Figure 33.- Baseline system for approach task in calm conditions.

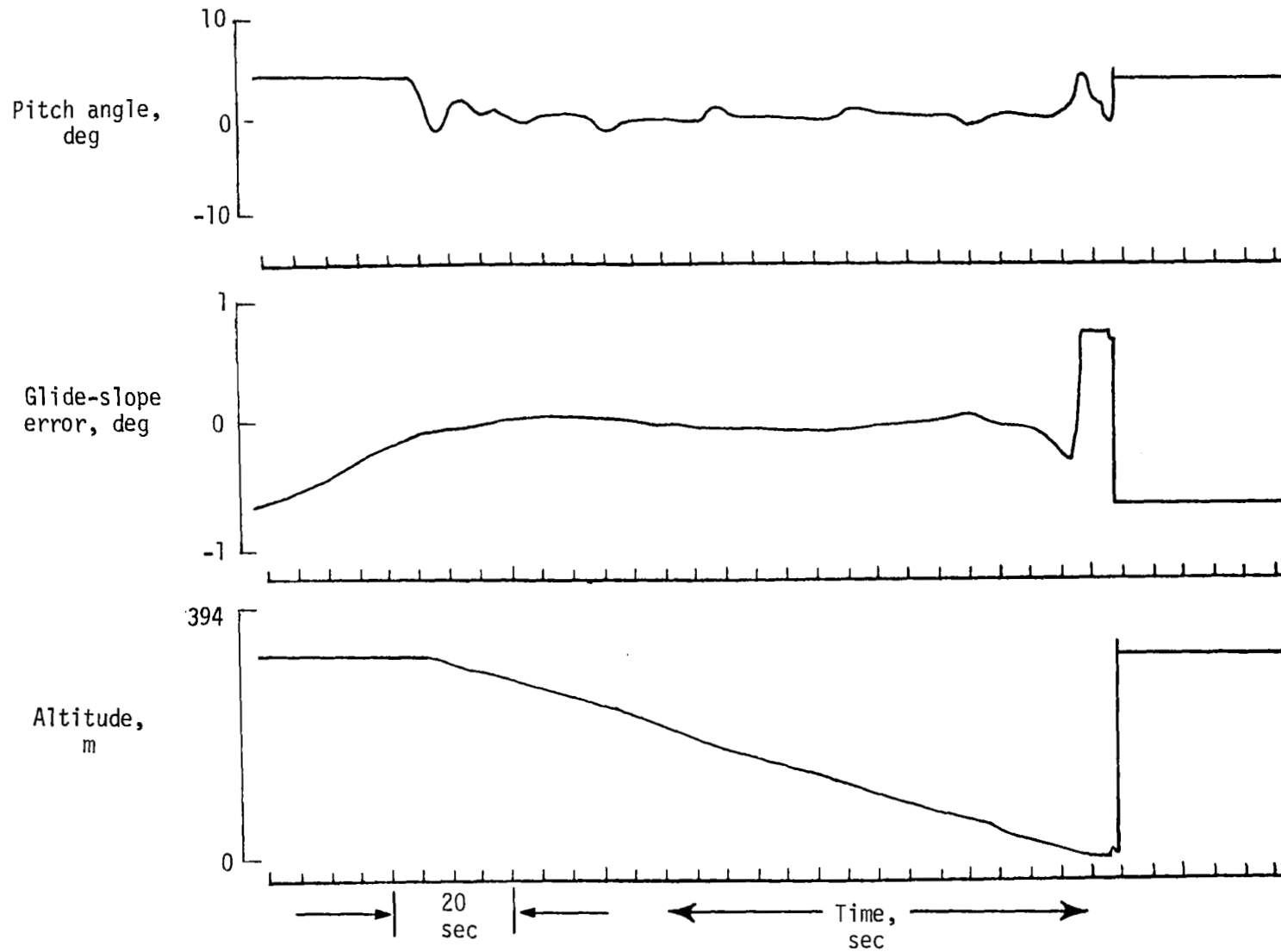


Figure 33.- Concluded.

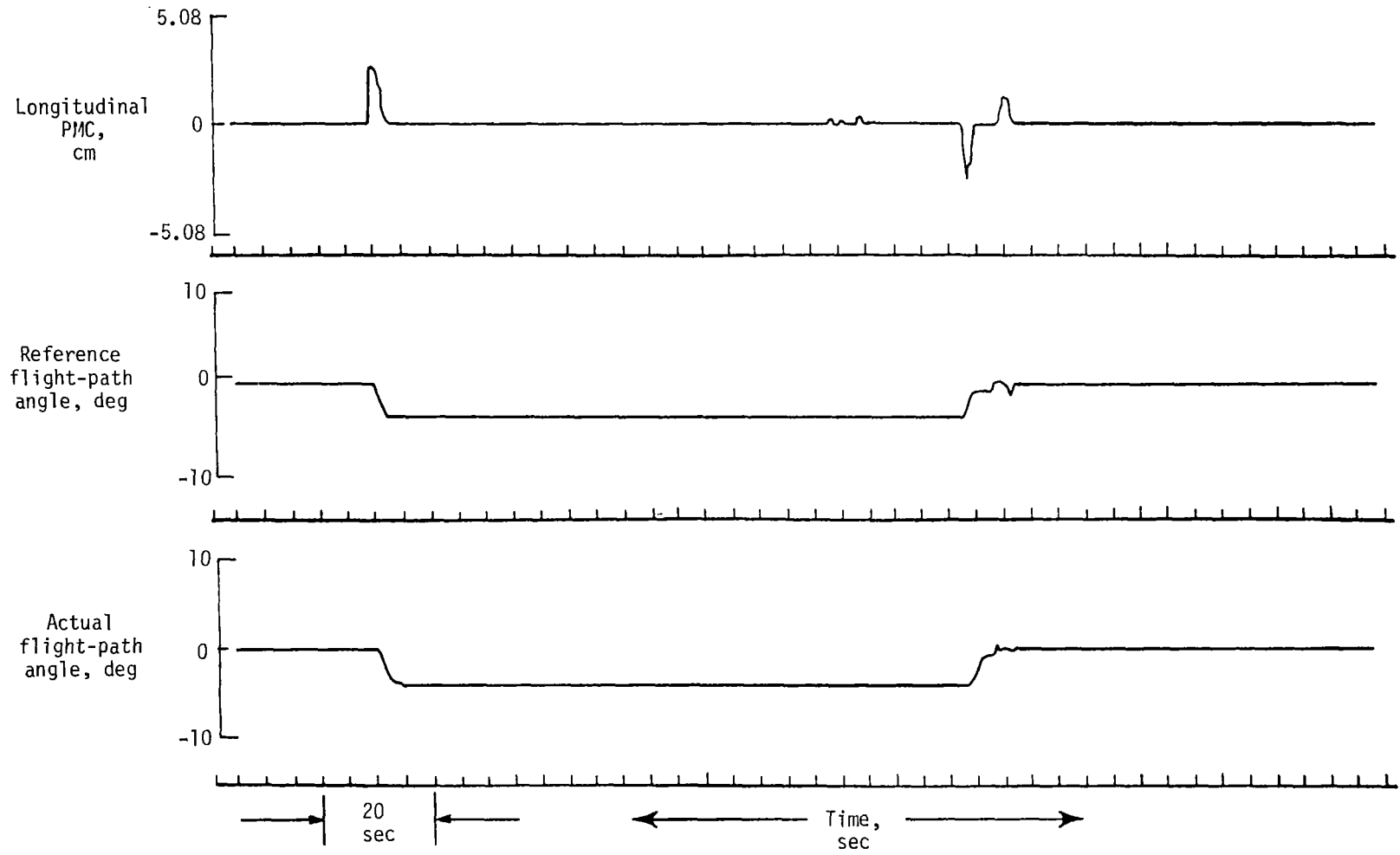


Figure 34.- Advanced system in approach task in calm conditions.

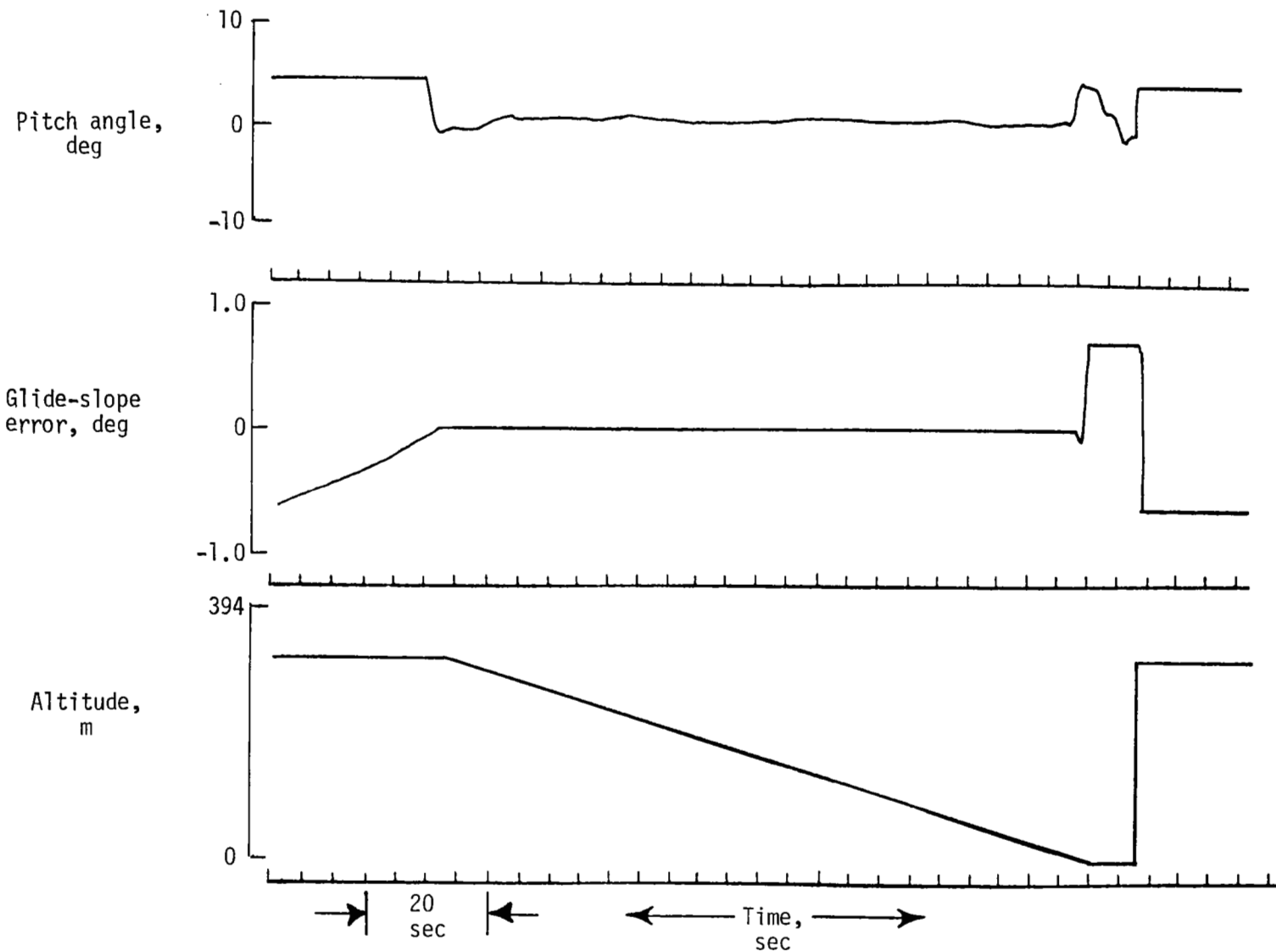


Figure 34.- Concluded.

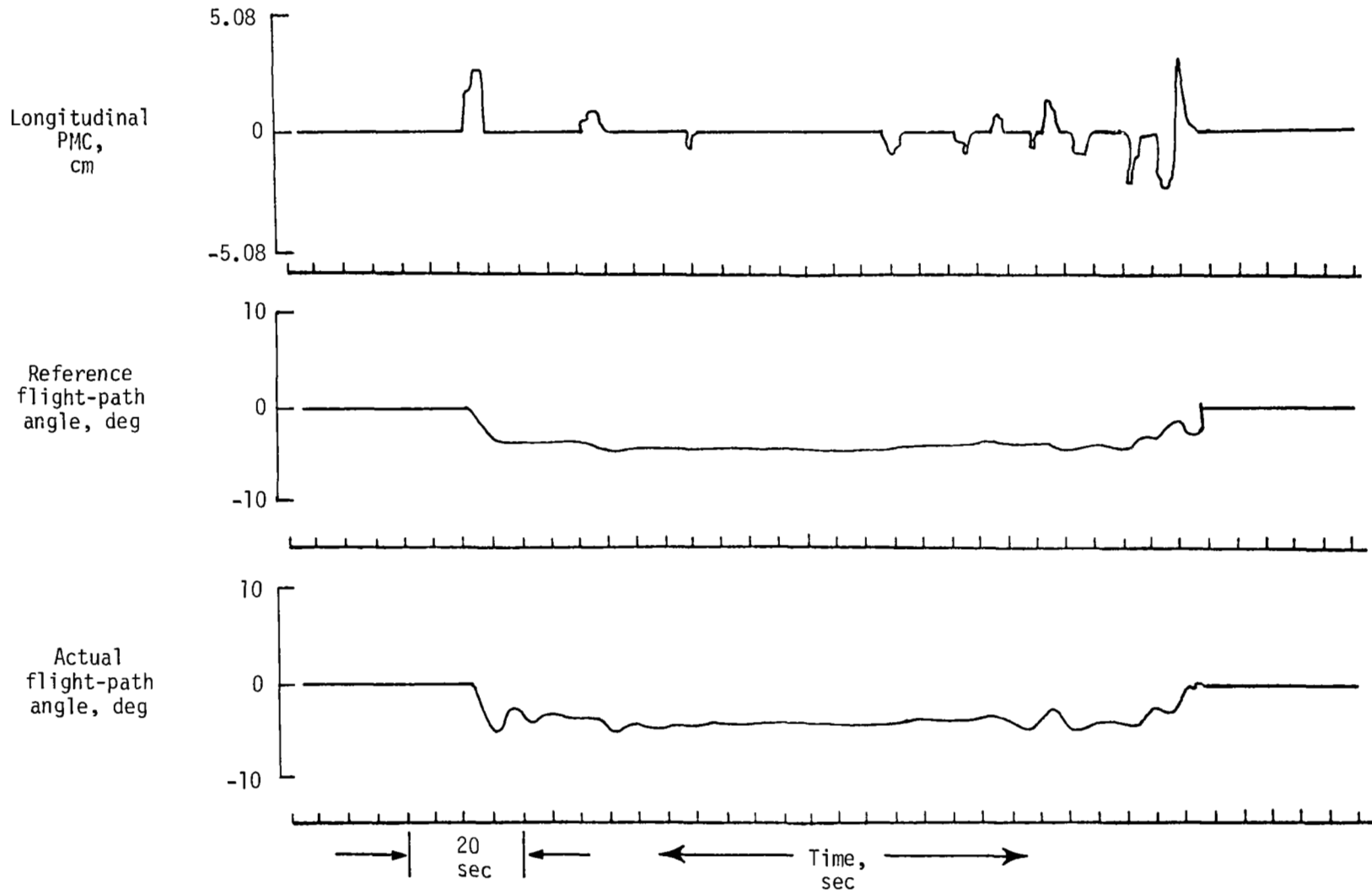


Figure 35.- Baseline system in approach task in shear conditions.

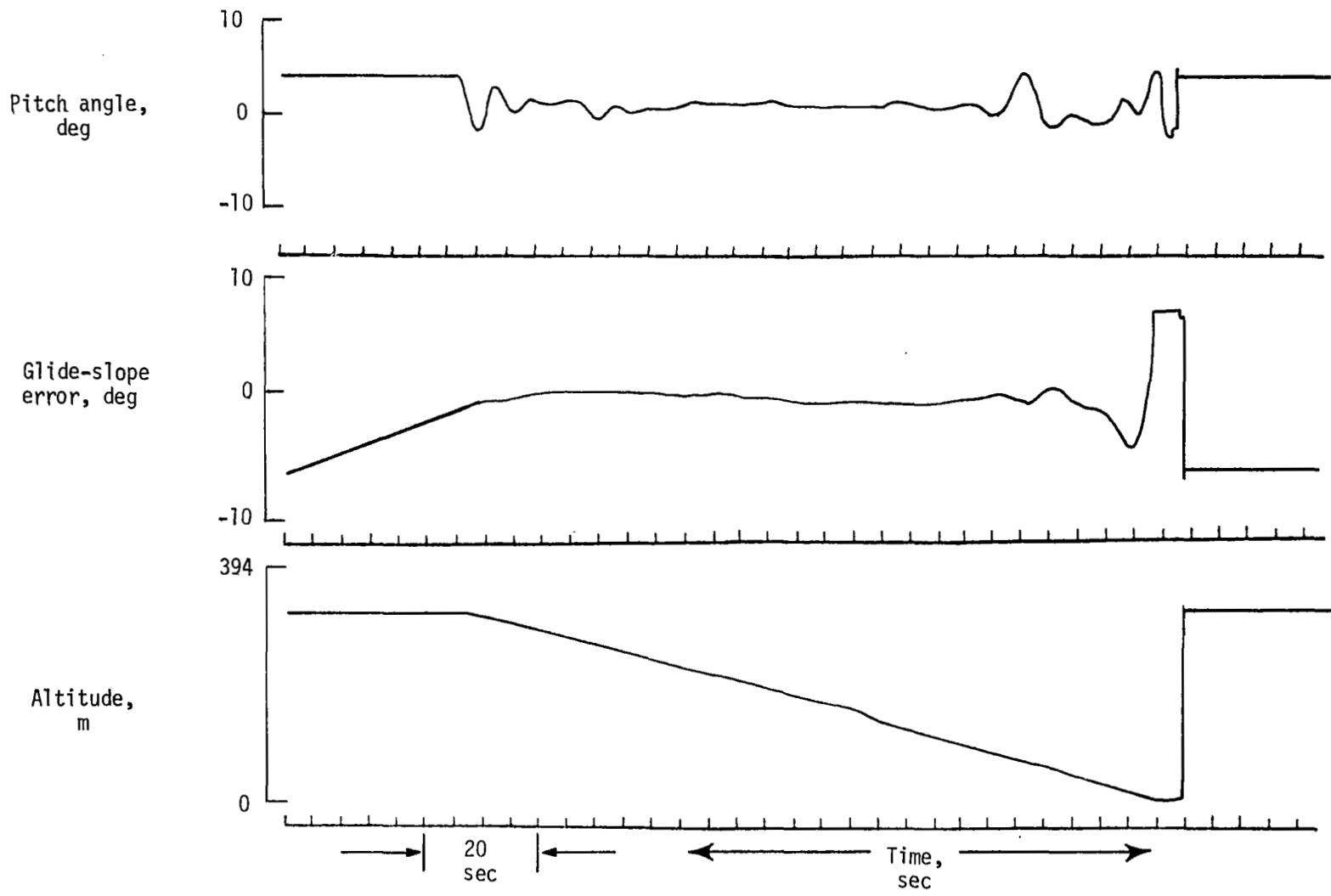


Figure 35.- Concluded.

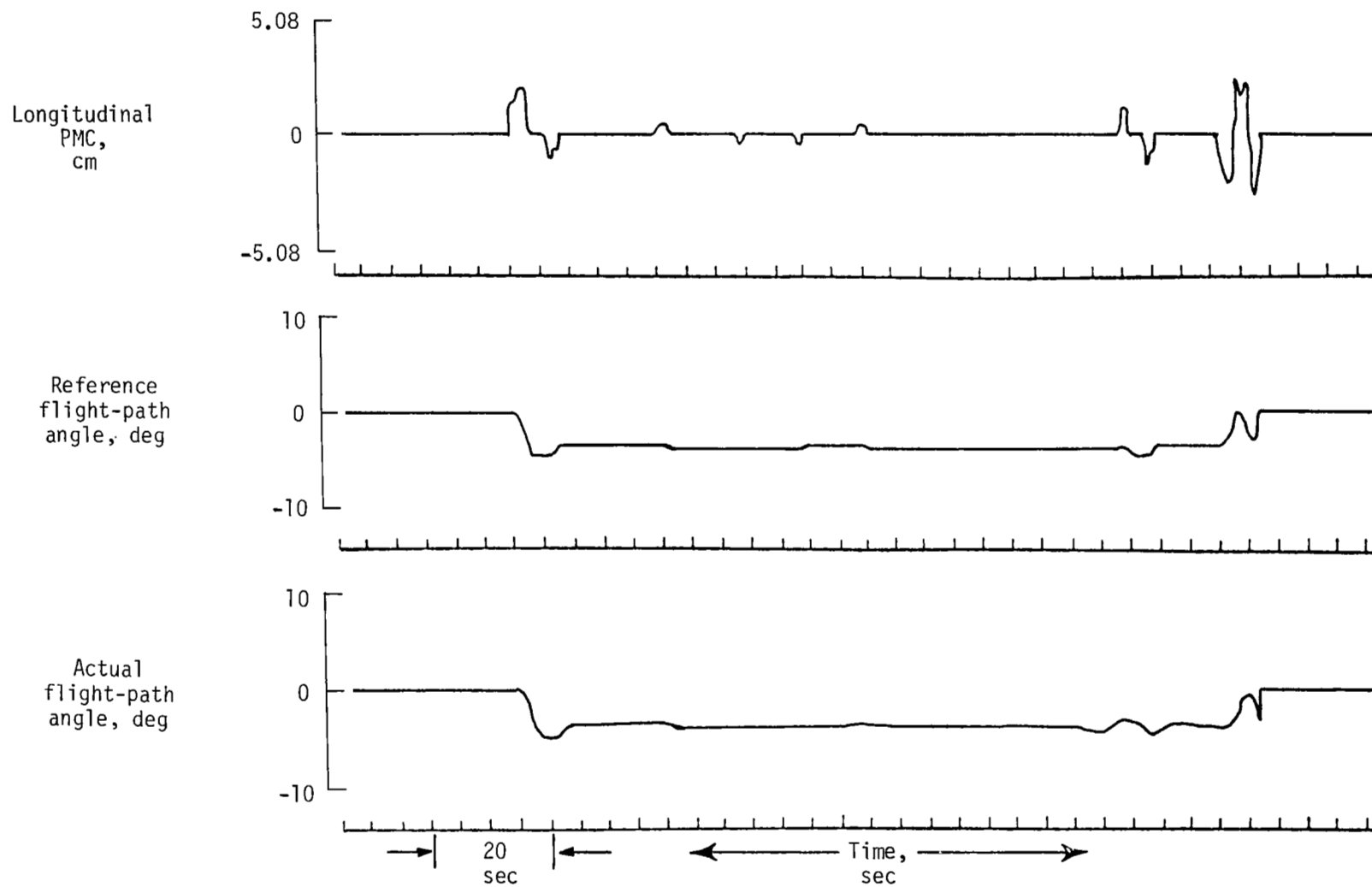


Figure 36.- Advanced control system with baseline display system in approach task in shear conditions.

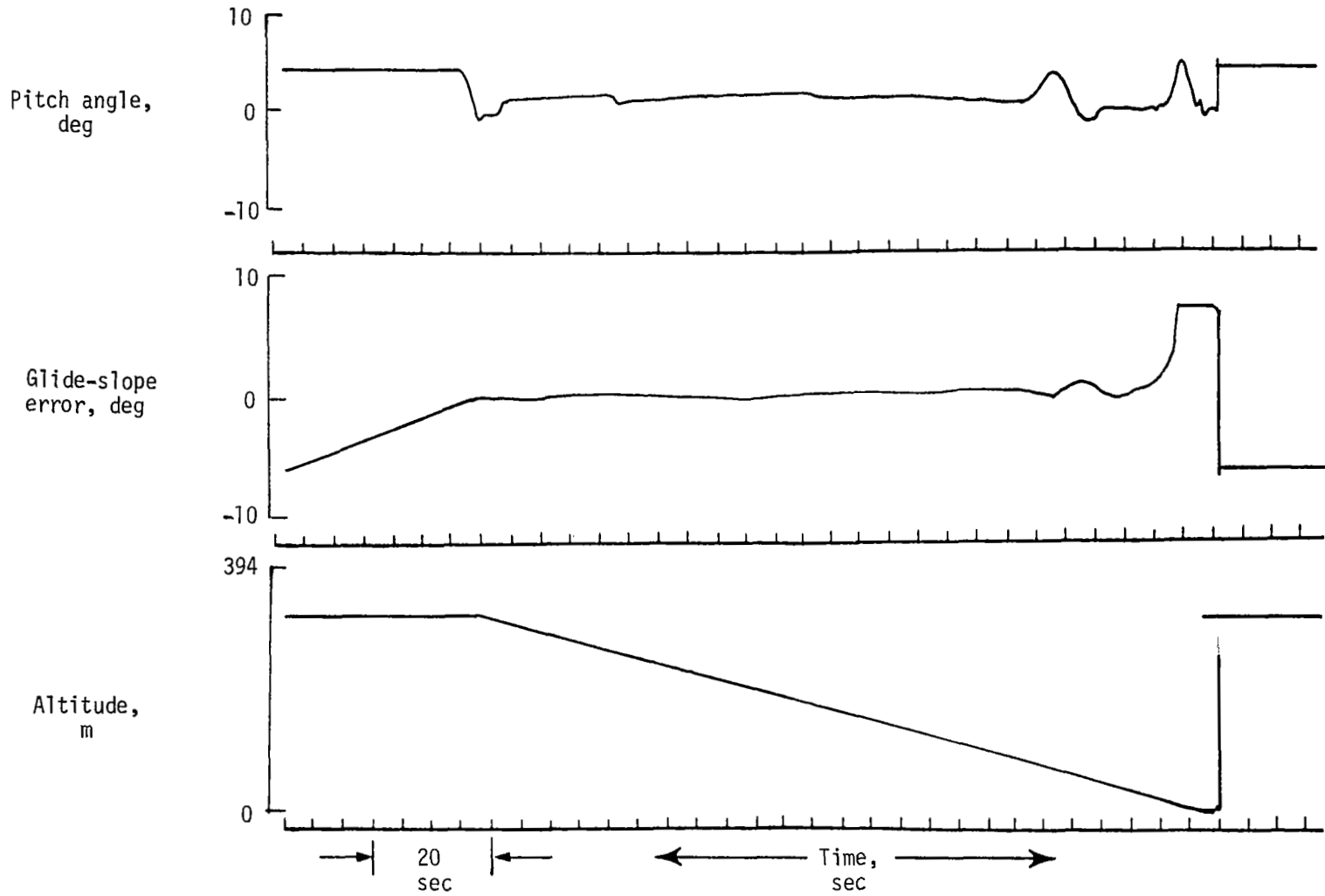


Figure 36.- Concluded.

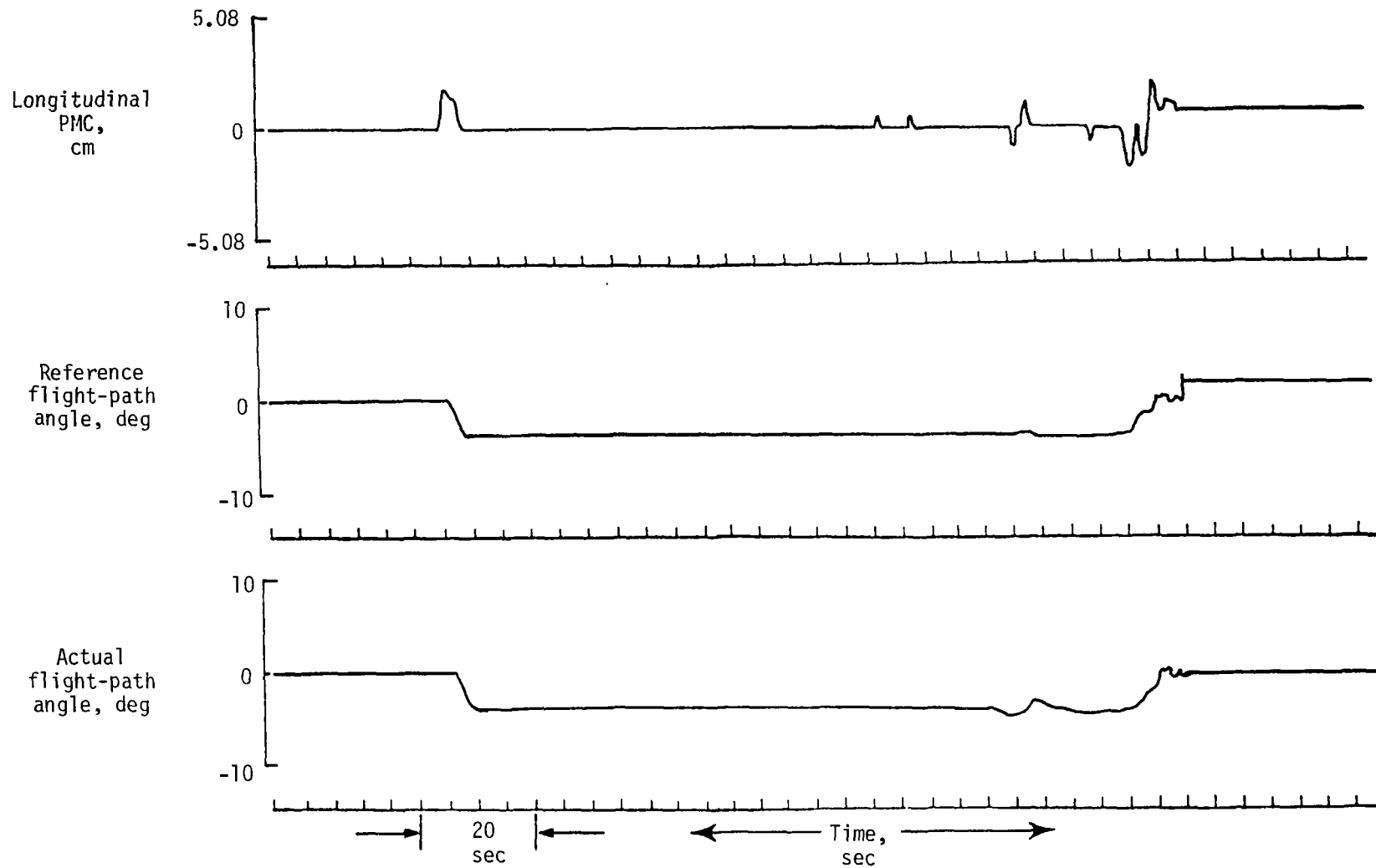


Figure 37.- Advanced system in approach task in shear conditions.

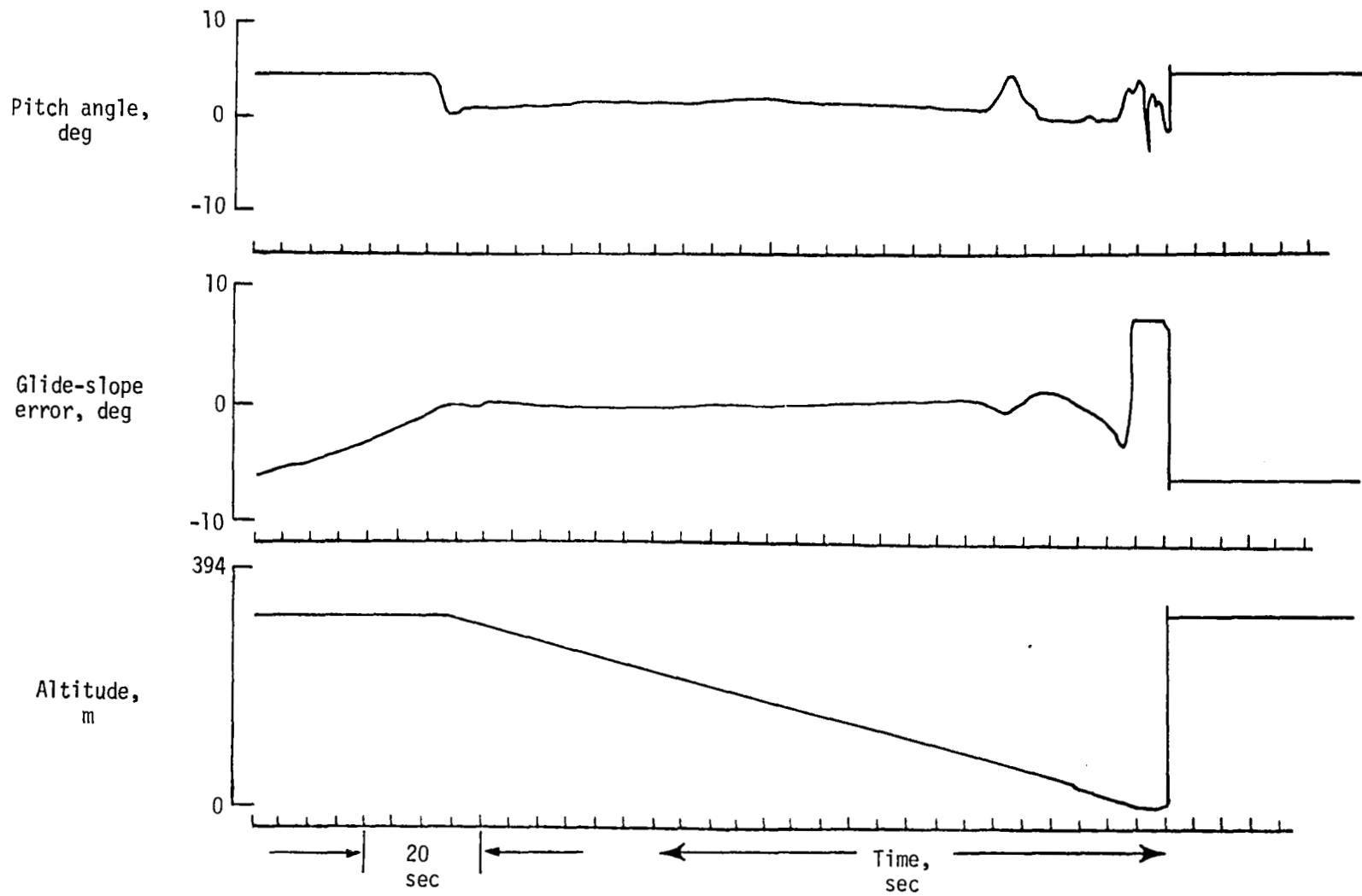


Figure 37.- Concluded.

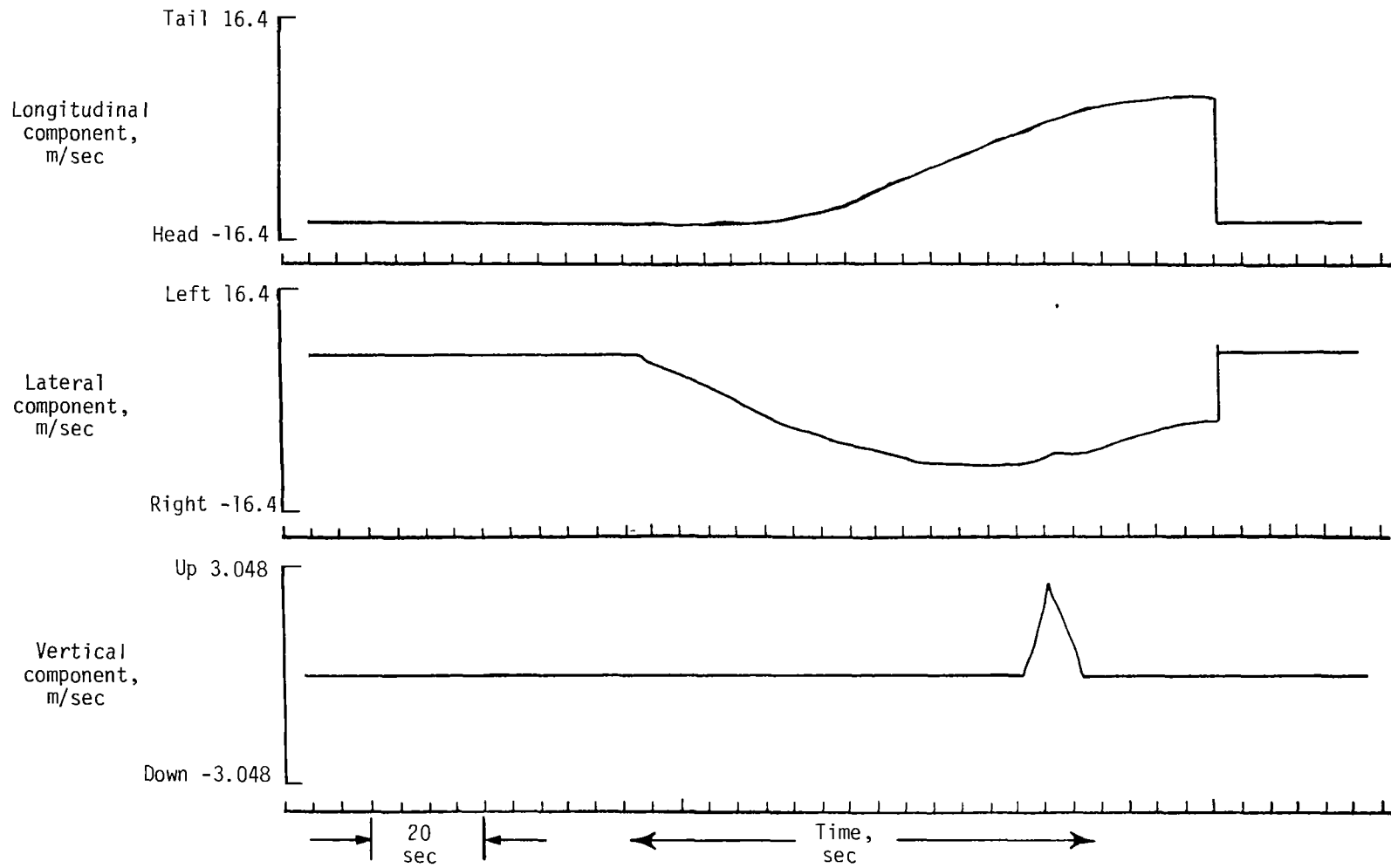


Figure 38.- Wind-shear components.

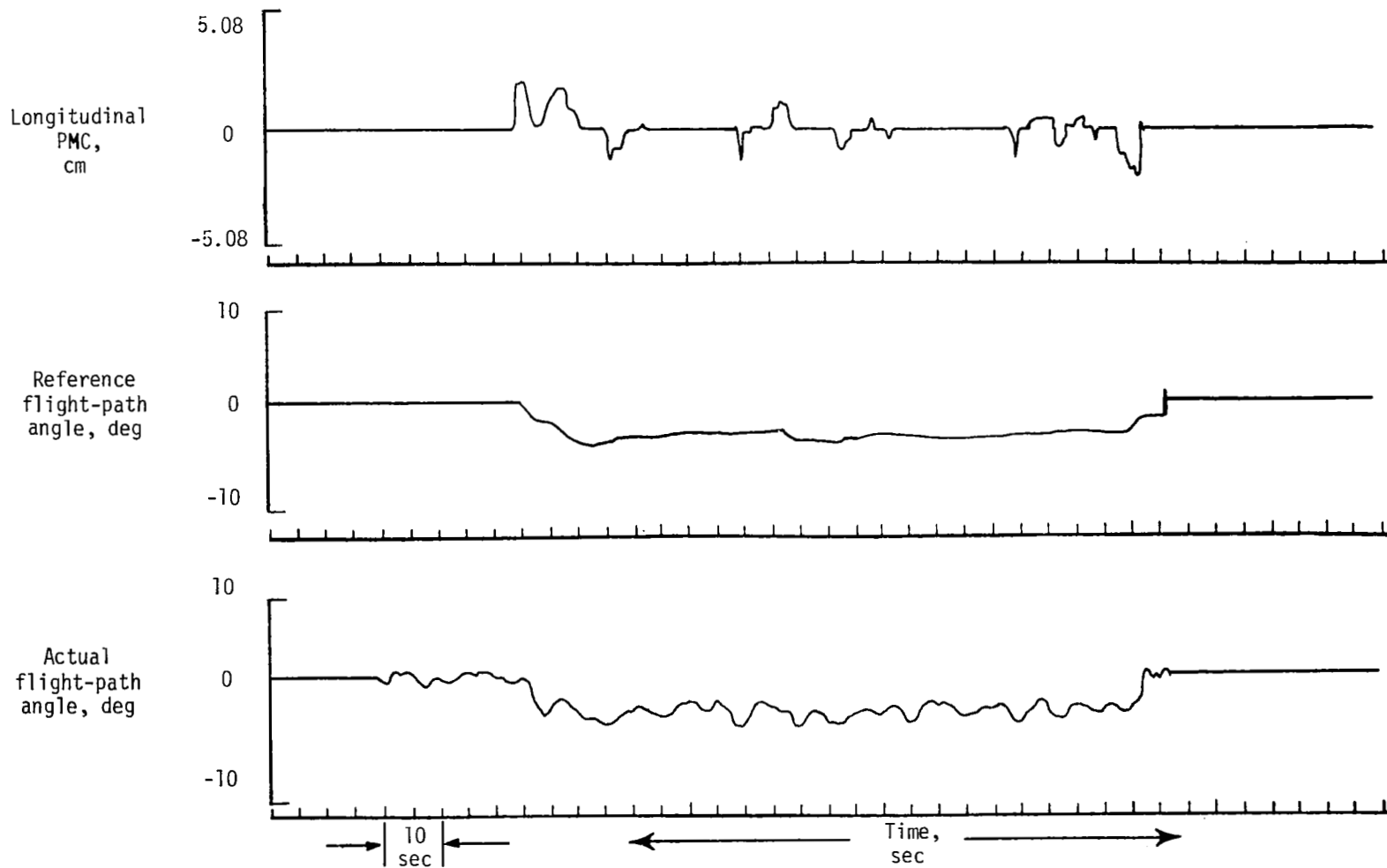


Figure 39.- Baseline system in approach task in turbulence conditions.

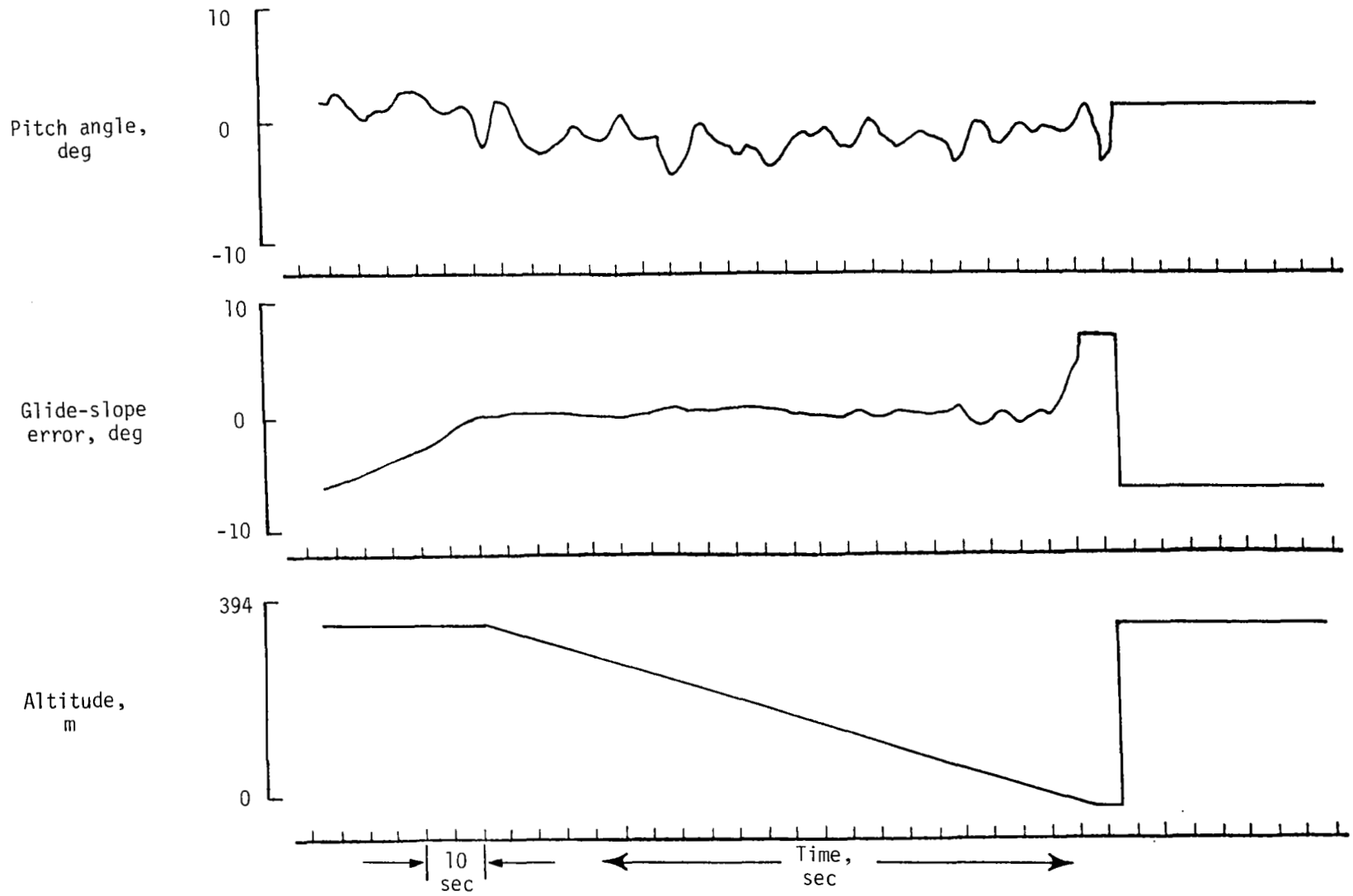


Figure 39.- Concluded.

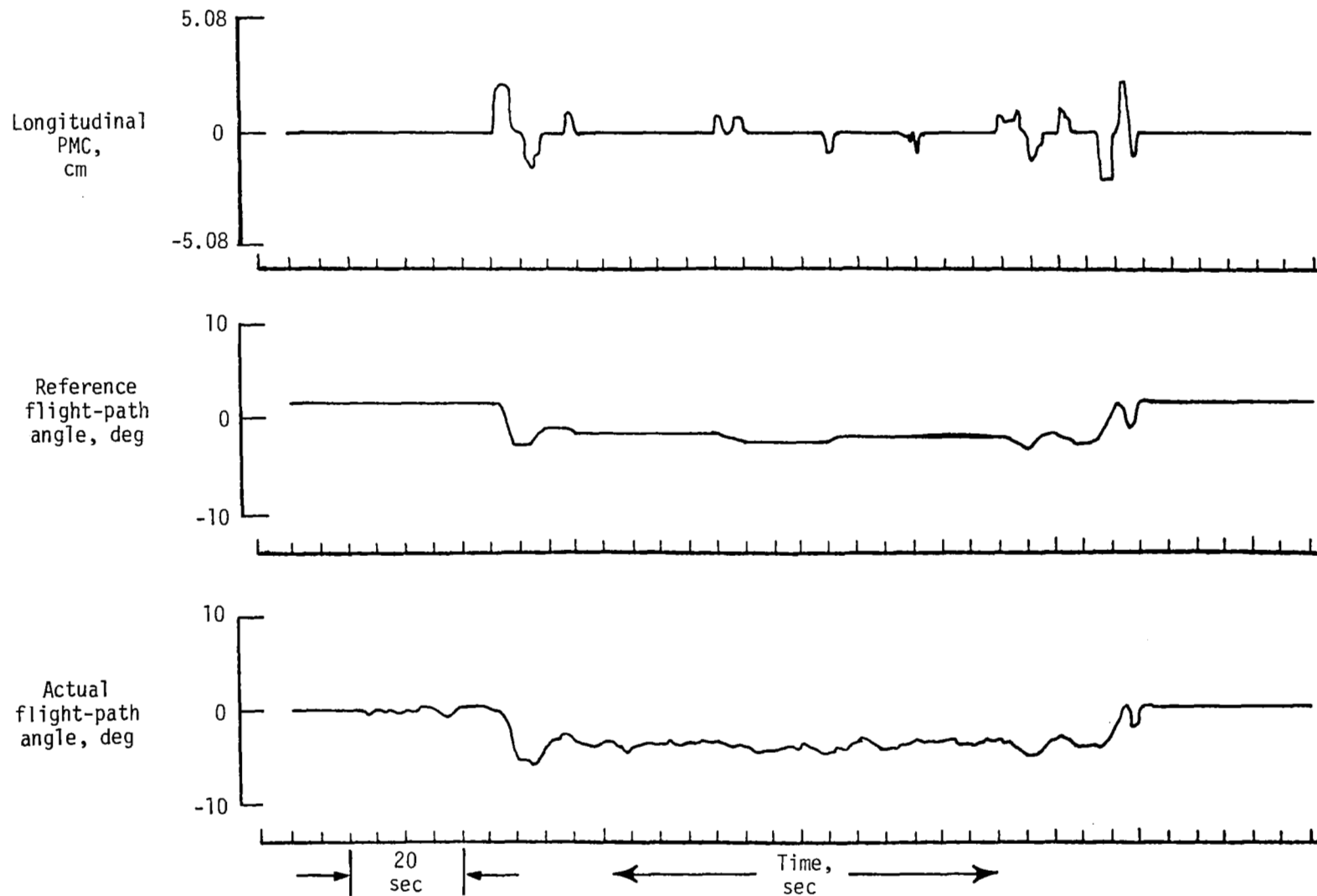


Figure 40.- Advanced control system with baseline display system in approach task in turbulence conditions.

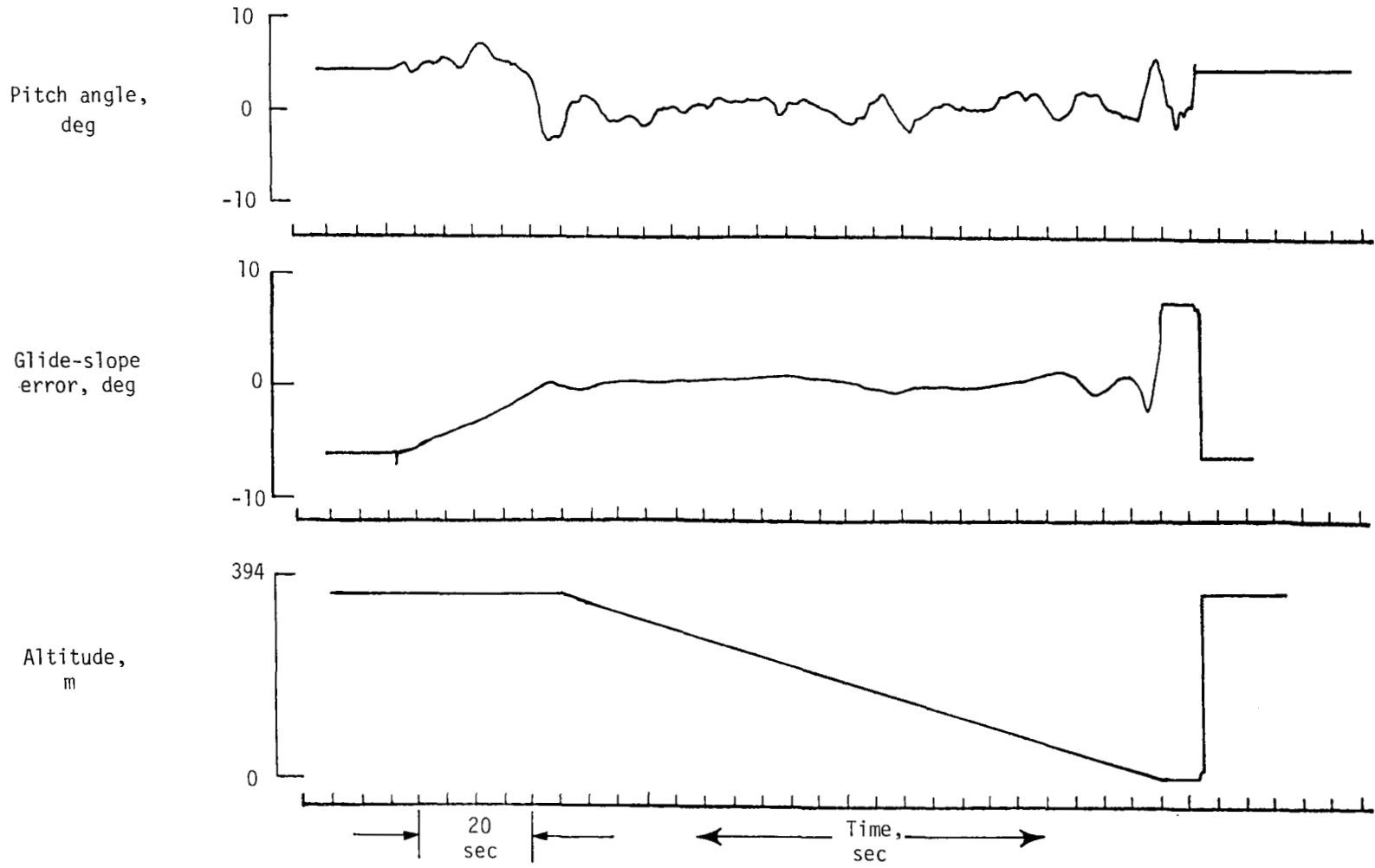


Figure 40.- Concluded.

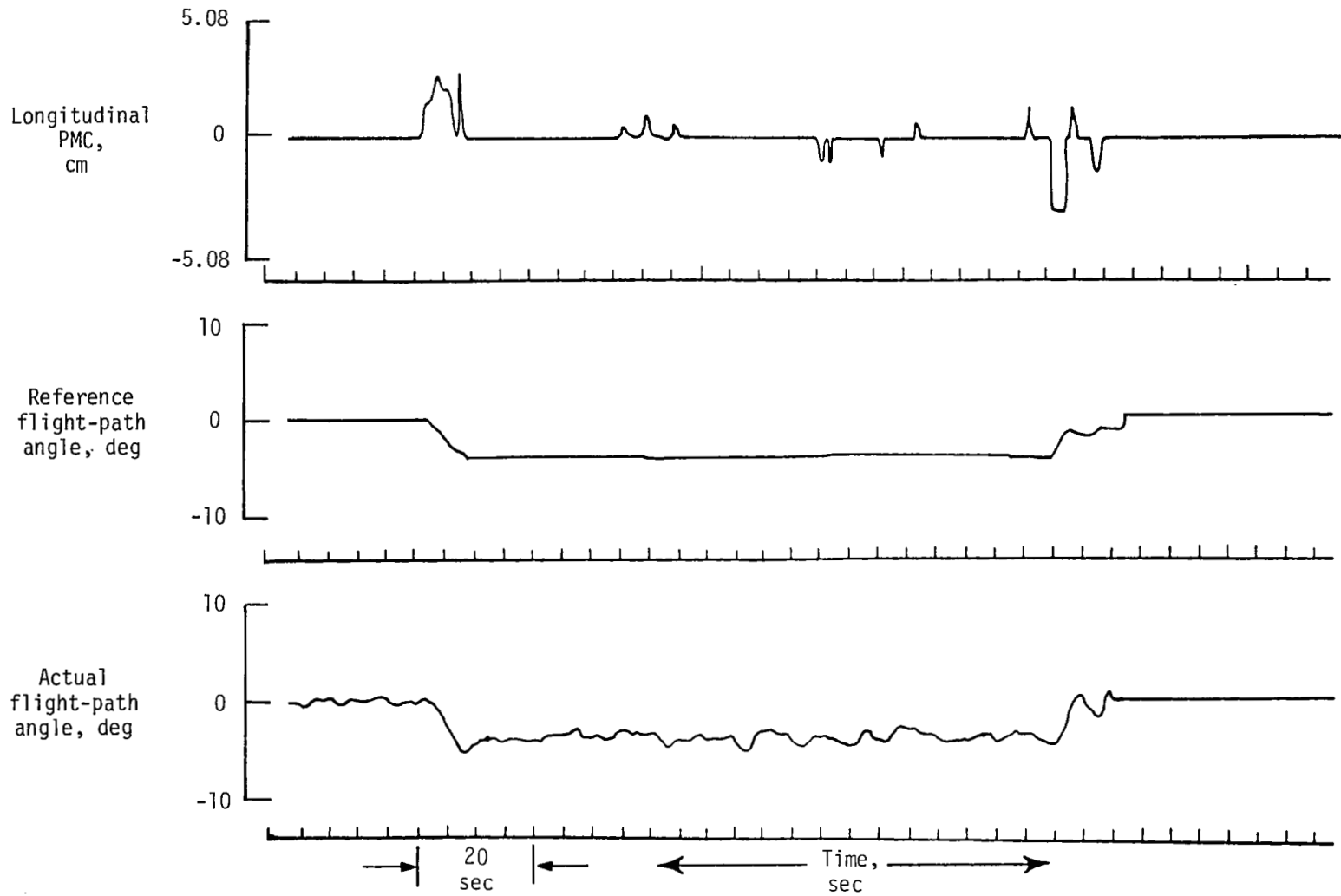


Figure 41.- Advanced display system with baseline control system in approach task in turbulence conditions.

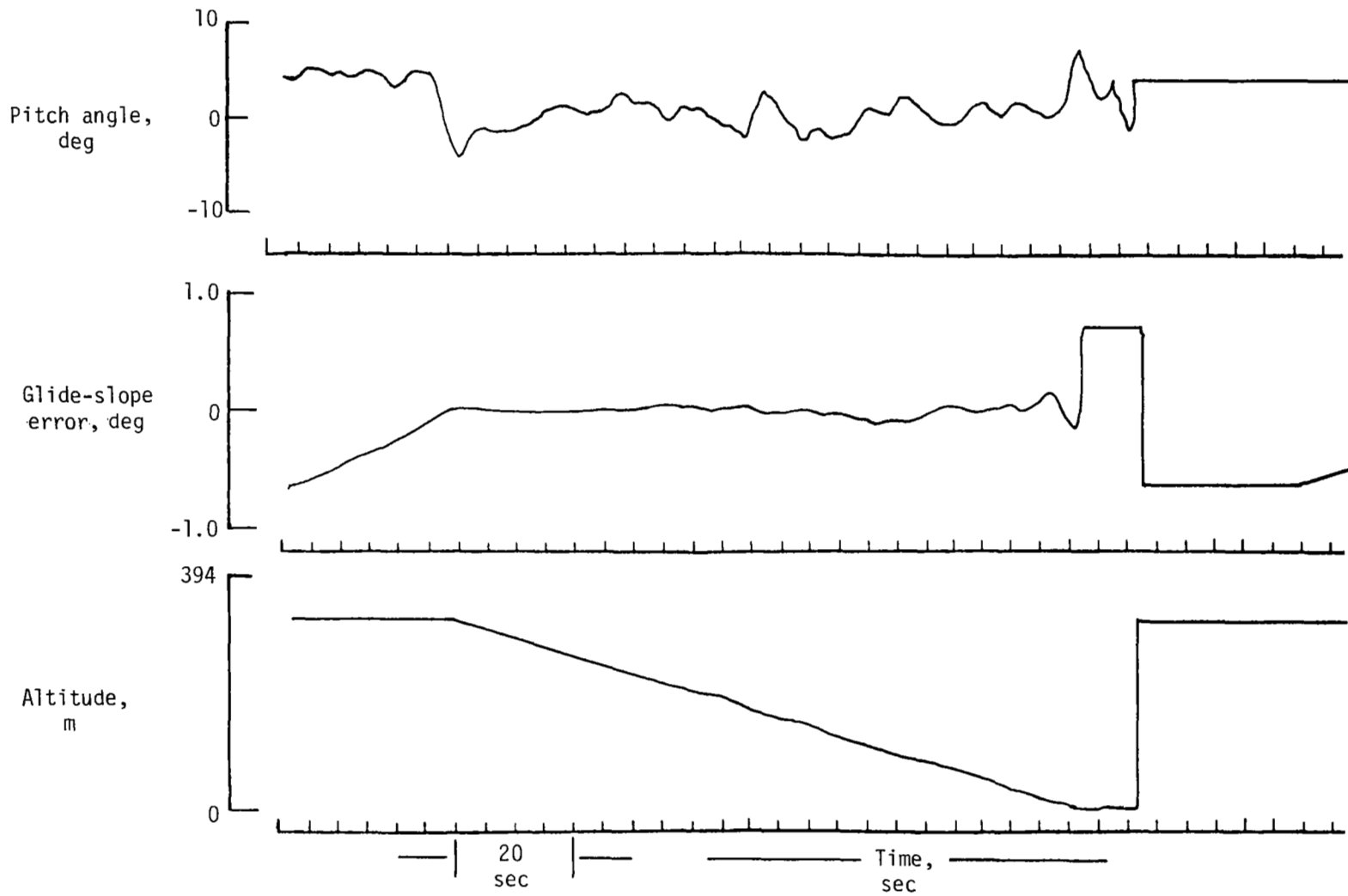


Figure 41.- Concluded.

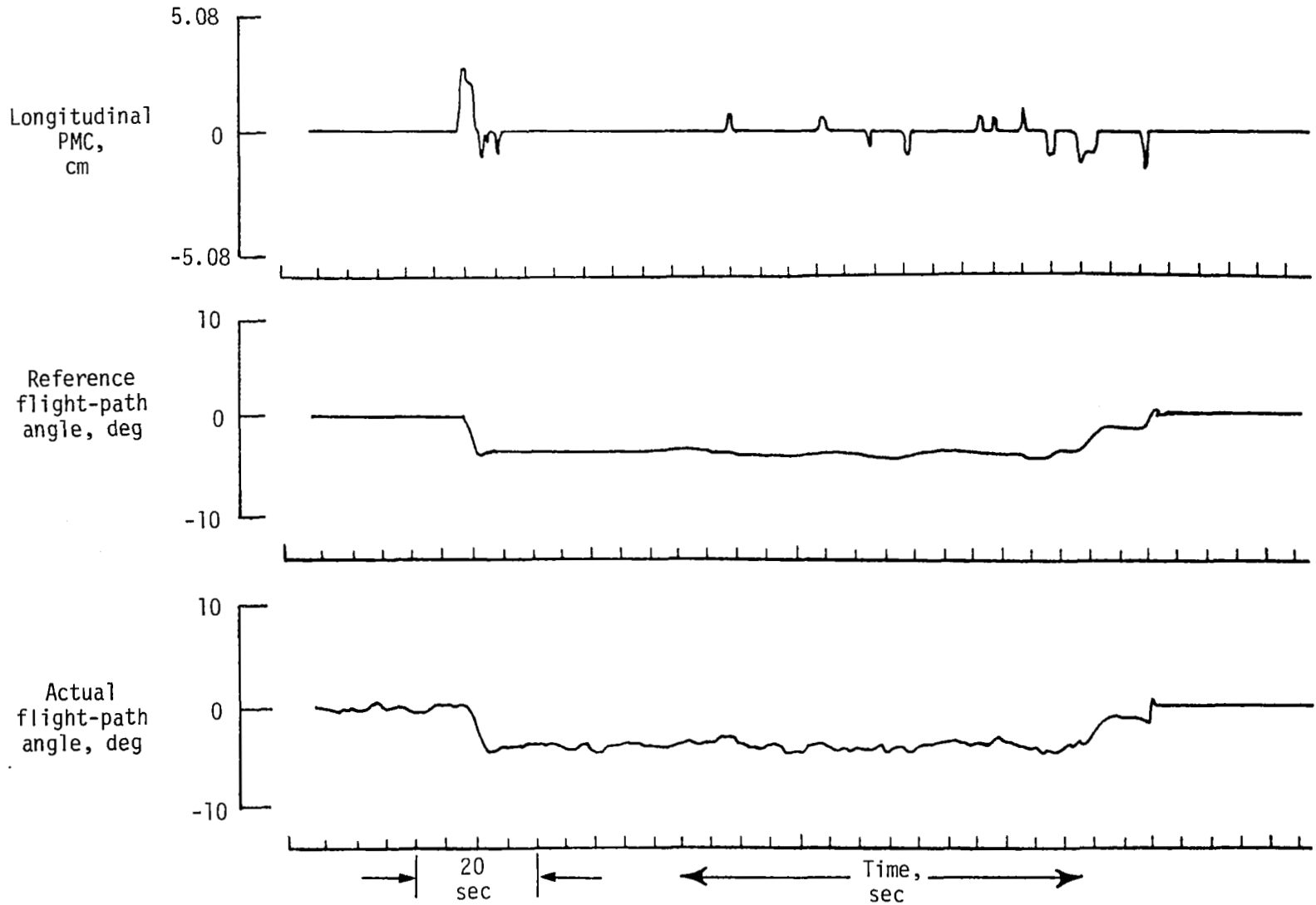


Figure 42.- Advanced system in approach task in turbulence conditions.

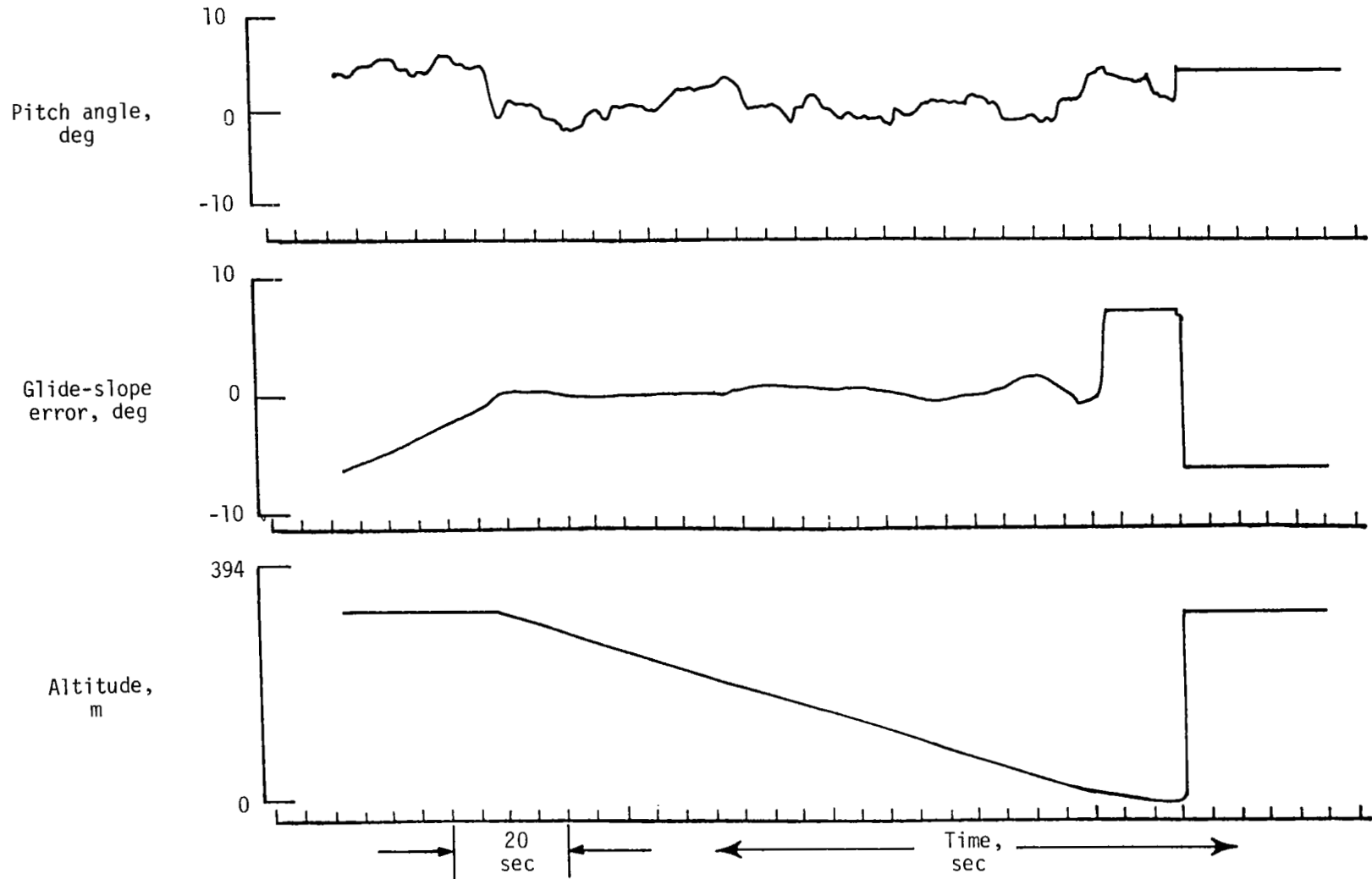


Figure 42.- Concluded.

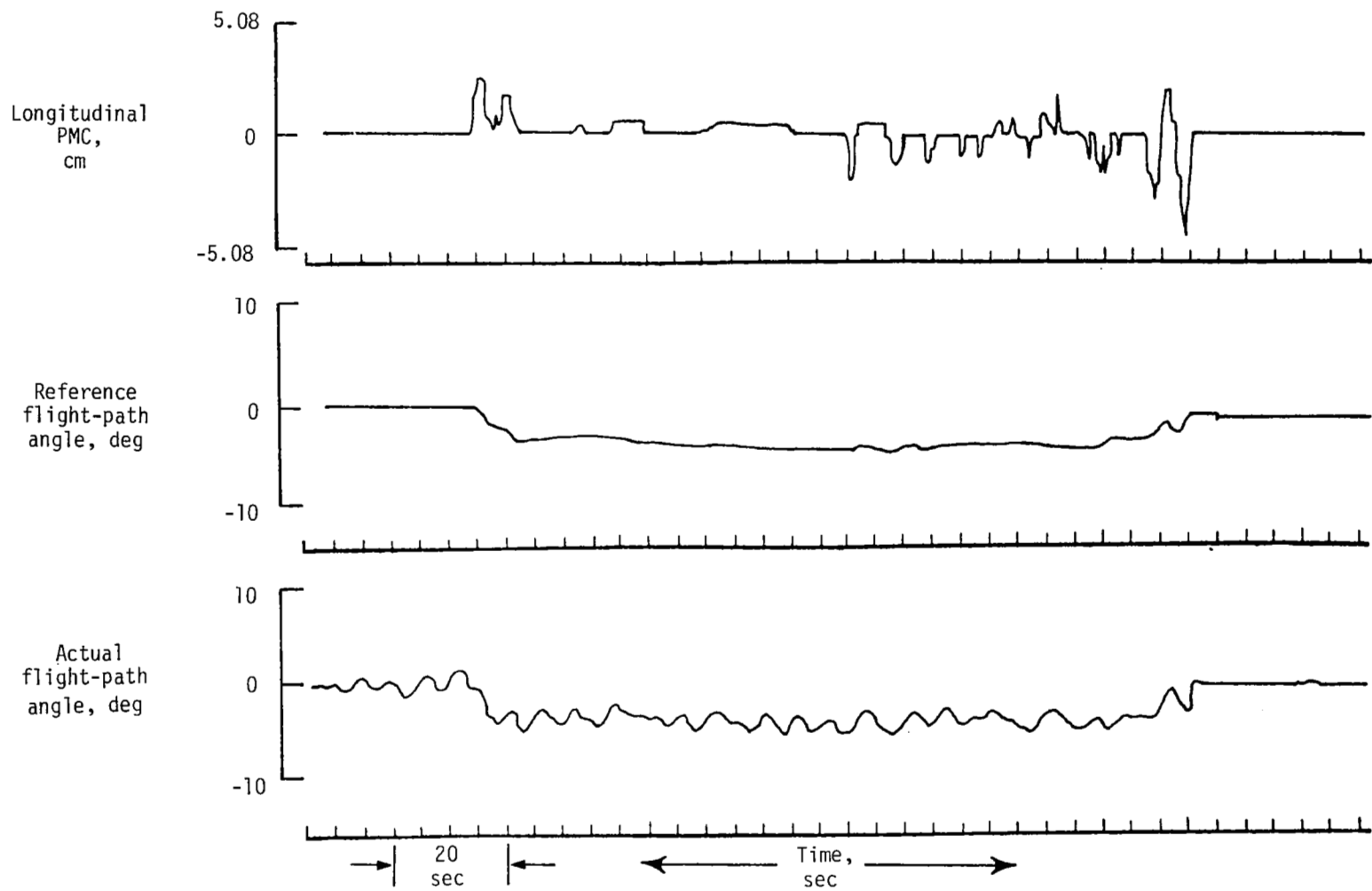


Figure 43.- Baseline system for approach task in shear and turbulence conditions.

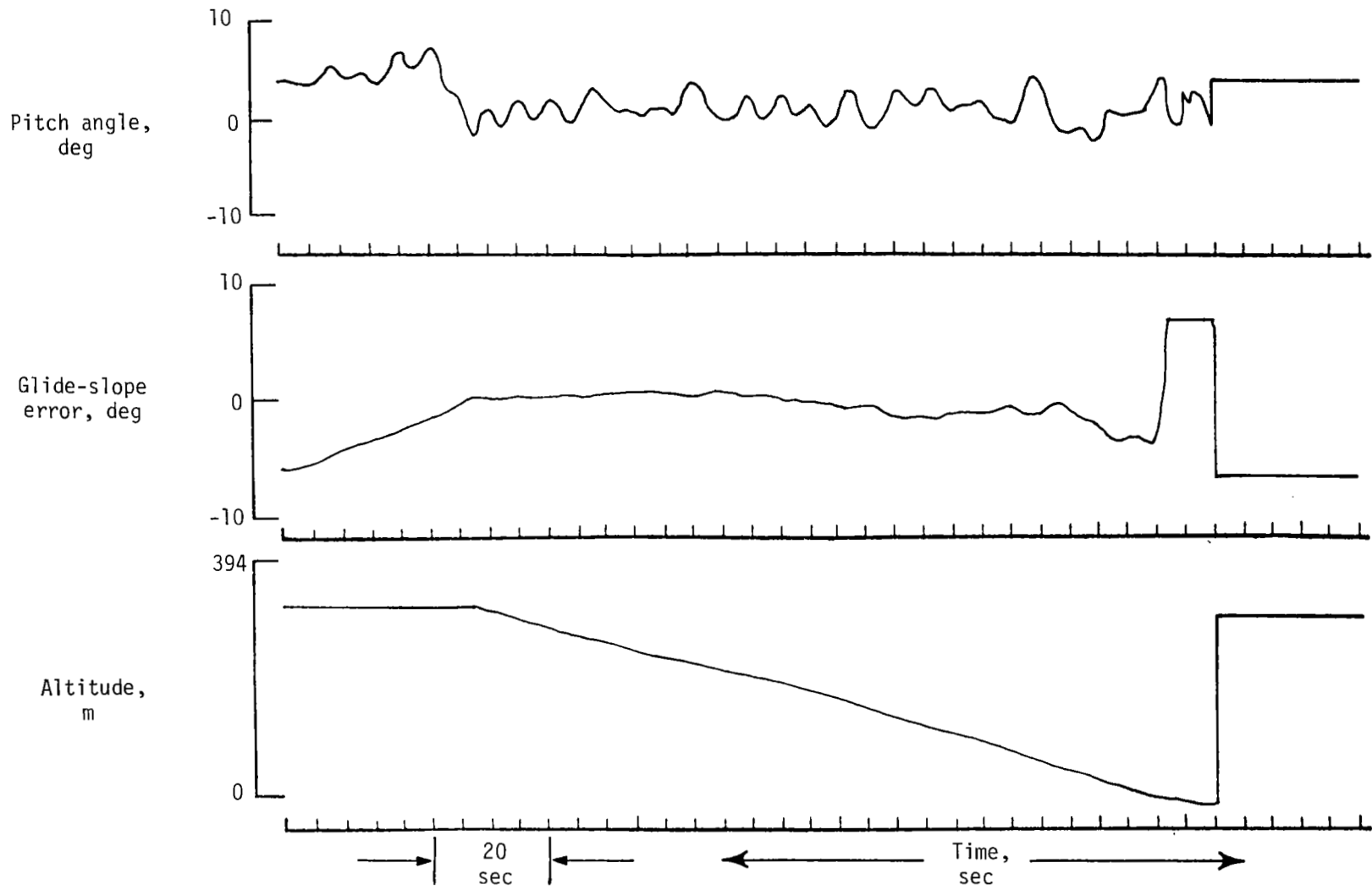


Figure 43.- Concluded.

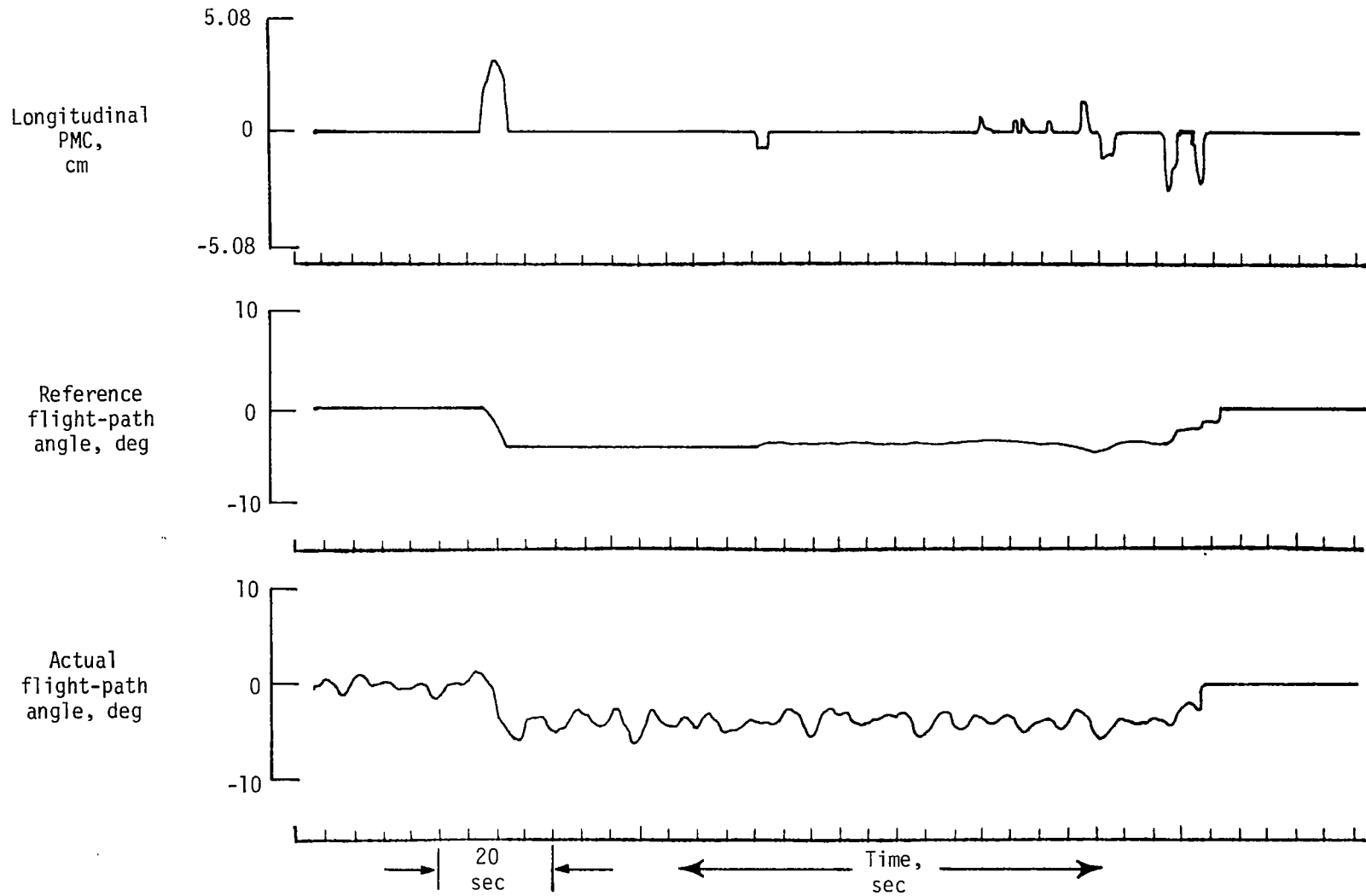


Figure 44.- Advanced display system with baseline control system for approach task in shear and turbulence conditions.

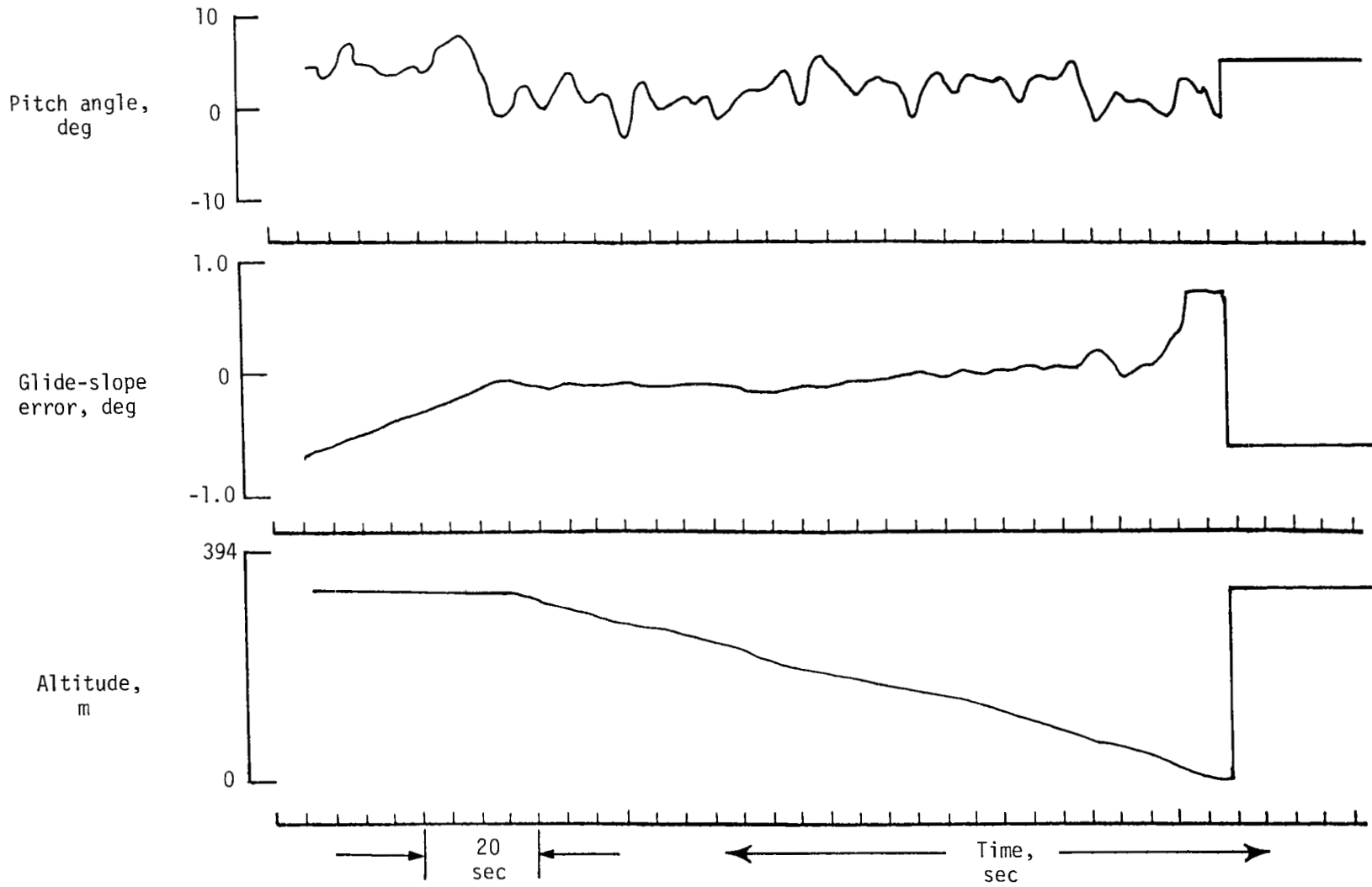


Figure 44.- Concluded.

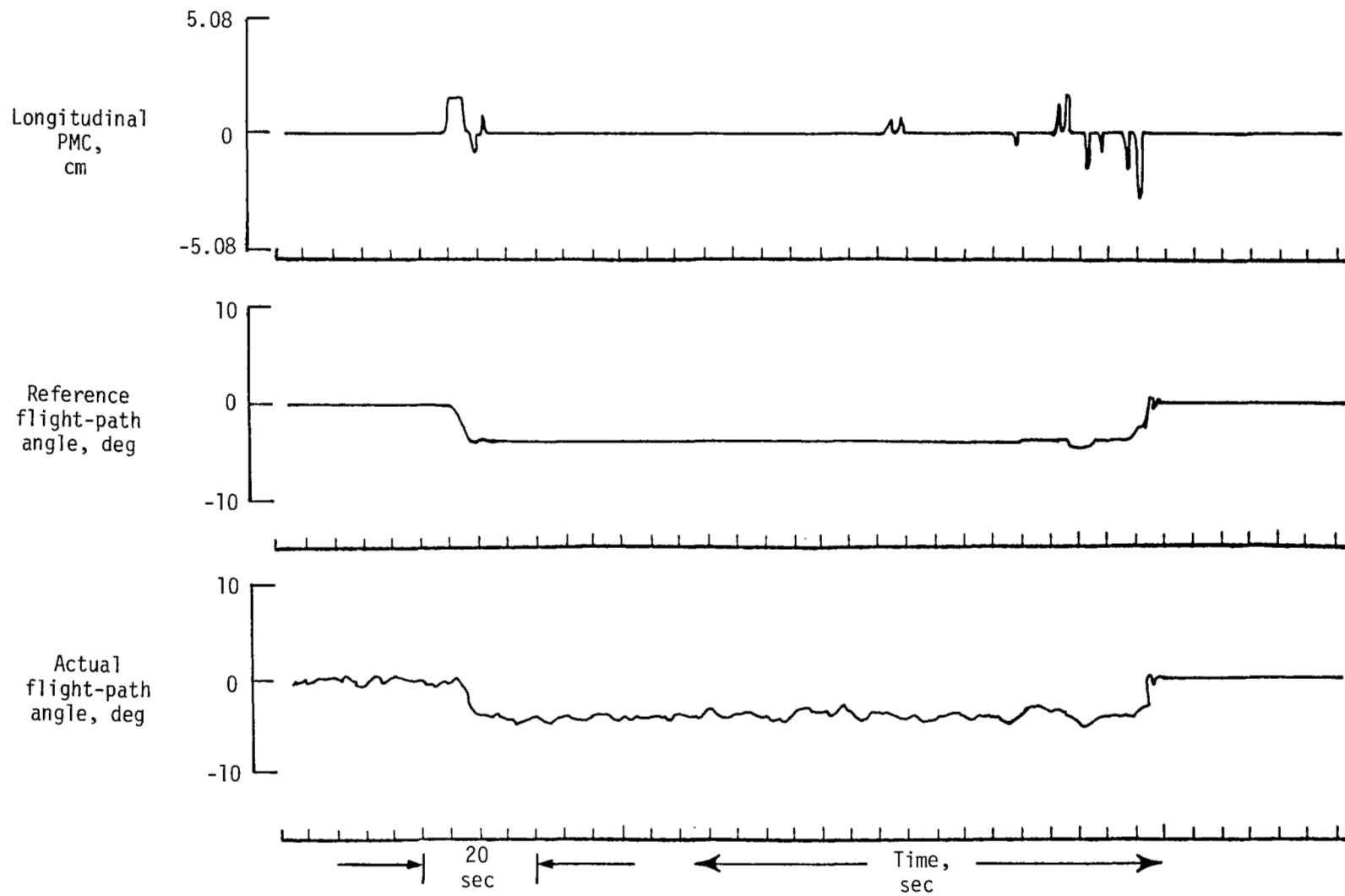


Figure 45.- Advanced system for approach task in shear and turbulence conditions.

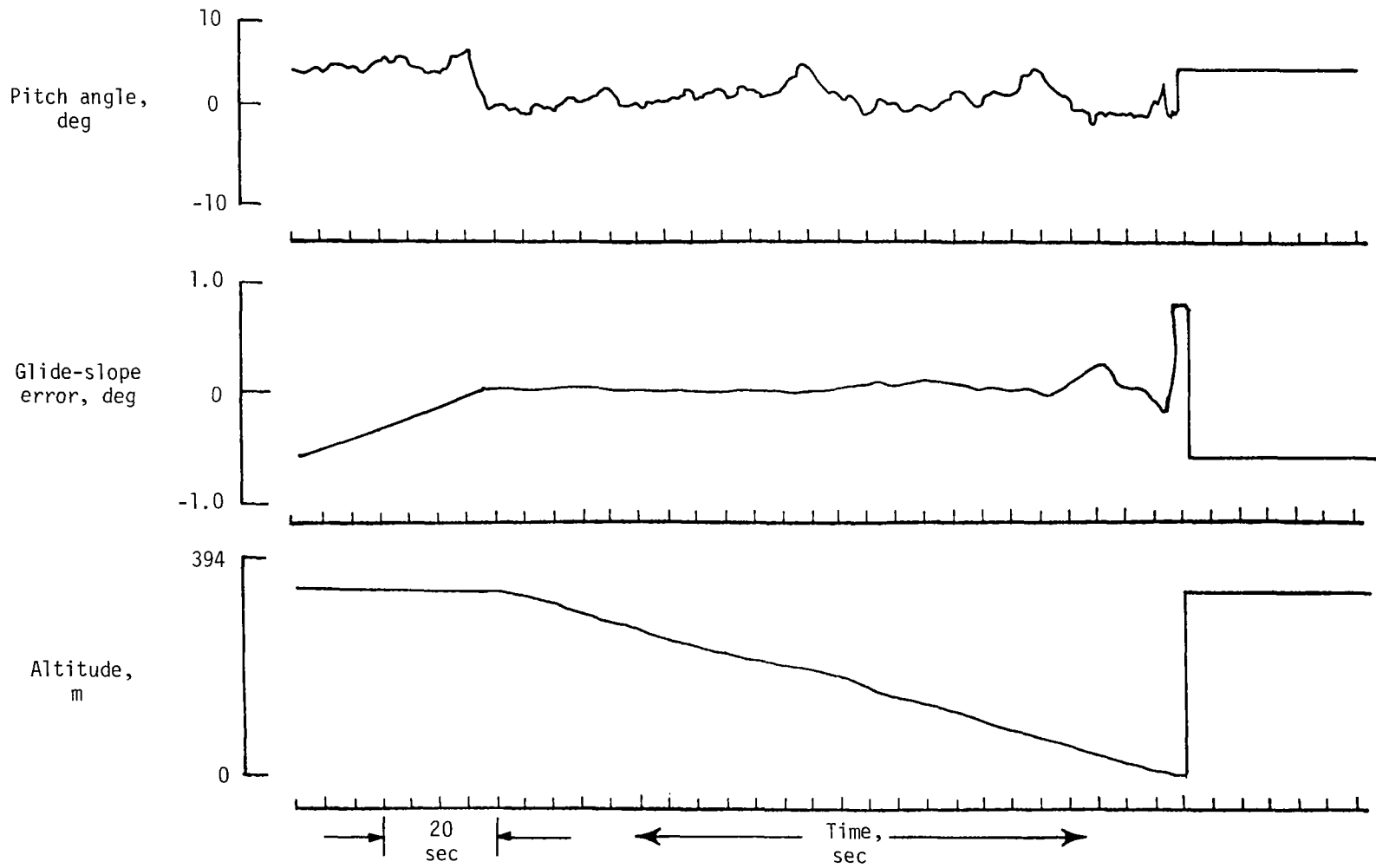


Figure 45.- Concluded.

1. Report No. NASA TP-1664	2. Government Accession No.	3. Recipient's Catalog No.	
4. Title and Subtitle SIMULATION DEVELOPMENT AND EVALUATION OF AN IMPROVED LONGITUDINAL VELOCITY-VECTOR CONTROL-WHEEL STEERING MODE AND ELECTRONIC DISPLAY FORMAT		5. Report Date August 1980	
		6. Performing Organization Code	
7. Author(s) George G. Steinmetz		8. Performing Organization Report No. L-13435	
		10. Work Unit No. 534-04-13-55	
9. Performing Organization Name and Address NASA Langley Research Center Hampton, VA 23665		11. Contract or Grant No.	
		13. Type of Report and Period Covered Technical Paper	
12. Sponsoring Agency Name and Address National Aeronautics and Space Administration Washington, DC 20546		14. Sponsoring Agency Code	
		15. Supplementary Notes	
16. Abstract  A simulation project was conducted which involved the development and testing of an improved longitudinal velocity-vector control-wheel steering mode and an improved electronic display format for an advanced avionics flight system. Guidelines for the development phase were provided by test-pilot critique summaries of the previous system. The results include performances from computer-generated step-column inputs across the full airplane speed and configuration envelope, as well as piloted performance results taken from a reference-line tracking task and an approach-to-landing task conducted under various environmental conditions. The analysis of the results for the reference-line tracking and approach-to-landing tasks indicates clearly detectable improvement in pilot-tracking accuracy with a reduction in physical workload. The original objectives of upgrading the longitudinal axis of the velocity-vector control-wheel steering mode were successfully met when measured against the test-pilot critique summaries and the original purposes outlined for this type of augment control mode.			
17. Key Words (Suggested by Author(s)) Longitudinal velocity-vector control-wheel steering mode Electronic display format Simulation Advanced avionics flight system		18. Distribution Statement Unclassified - Unlimited  Subject Category 06	
19. Security Classif. (of this report) Unclassified	20. Security Classif. (of this page) Unclassified	21. No. of Pages 94	22. Price A05